

**The interaction between A20
and the NR4A subfamily of nuclear receptors
in the pathogenesis of rheumatoid arthritis**

Vicki Wallace

Master of Science

Letterkenny Institute of Technology

Supervisors:

Dr. Joanne Gallagher

Dr. Evelyn Murphy

Submitted to Higher Education and Training Awards Council (HETAC) in fulfilment of
the requirements for the M.Sc. degree, September 2011

Declaration

I hereby declare the the work herein, submitted for the degree of Master of Science in Letterkenny Institute of Technology, is the result of my own investigation, except where reference is made to published literature. I also certify that the material submitted in this thesis has not been previously submitted for any other qualification.

Vicki Wallace 26/10/2011

Vicki Wallace

lyit | Institiúid Teicneolaíochta Leitir Ceannainn
Letterkenny Institute of Technology

Acknowledgements

I would firstly like to thank my supervisor Dr. Joanne Gallagher for giving me the opportunity to undertake a Masters degree in molecular biology and for her advice and guidance to complete it. Thank you also to my co-supervisor Dr. Evelyn Murphy for her assistance and advice. Thank you to the HEA for providing funding. Thanks to my lab colleagues Grainne Quinn and Brendan Alexander for their daily assistance and company in the lab over the course of the project. I would like to express my gratitude to Ken MacIntyre for technical support and also to Dr. Joe English for statistical advice. Thanks to the CAMBio group for use of their fluorescent microscope and qPCR instrument. Many thanks to Dr. Gerre Quinn for his help with qPCR set up. Thank you to Dr. Anne Nelson for her advice and support. A special word of thanks again to Brendan who has helped me through it all. I would finally like to thank my family for their influence and support.

lyit | Institiúid Teicneolaíochta Leitir Ceannairde
Letterkenny Institute of Technology

Abstract

Rheumatoid arthritis (RA) is a chronic, progressive inflammatory disease that affects nearly 1 % of the world's population. RA is characterized by inflammation of the synovial joints leading to joint damage which can result in deformities and loss of function. Activation of the transcription factor NF- κ B is pivotal in the pathogenesis of RA, switching on multiple proinflammatory genes. The zinc finger protein A20 inhibits induction of NF- κ B activation by a variety of stimuli including the proinflammatory cytokine TNF- α in a variety of cell types, dampening the immune response. The A20-related genes ABIN-1, ABIN-2 and Cezanne have also been shown to attenuate TNF- α -induced NF- κ B activation. The NR4A subfamily of orphan nuclear receptors comprising of NURR1, NUR77 and NOR-1 are ligand-independent transcription factors and evidence suggests that they may have a proinflammatory role in the RA synovium. Previous studies have demonstrated that overexpression of the NR4A subfamily members led to the induction of A20 gene expression, indicating the potential role of this subfamily in the regulation of A20 and A20-interacting proteins. This study investigated the potential interaction between A20 and the NR4A member NURR1 in the context of RA. Bioinformatic analysis of A20, ABIN-1, ABIN-2 and Cezanne identified the NR4A binding site (NBRE site) in the promoter region of all four genes, indicating that A20 and these A20-interacting genes may be induced by the NR4A subfamily of nuclear receptors. Transient co-transfection experiments and luciferase assays were carried out on cellular models of inflammatory arthritis (fibroblast-like synoviocytes and chondrocytes). The results indicated that A20 overexpression attenuates the induction of NBRE-luciferase activity by endogenous and overexpressed NURR1 in both synoviocyte and chondrocyte cells. Results in synoviocytes revealed a dose-dependent inhibitory effect of A20 on the transcriptional activity of NURR1. Further experiments demonstrate that in synoviocytes, A20 overexpression led to suppression of NR4A driven transactivation of the interleukin (IL)-8 promoter. In chondrocytes, A20 increased NURR1 induction of the IL-8 promoter. These results indicate that A20 may play a role in modulating the transcriptional activity of NURR1. Reverse transcription (RT)-PCR analysis of synoviocytes and chondrocytes stimulated with the proinflammatory cytokine TNF- α indicated that transcripts from A20, ABIN-1 and ABIN-2 are differentially expressed, while Cezanne is not affected by TNF- α treatment in these cellular contexts. qPCR analysis of A20 and ABIN-1 mRNA expression in chondrocytes in response to TNF- α treatment confirmed the end-point PCR results obtained for this cell type.

Abbreviations

5-ASA	5-Aminosalicylate
ABIN	A20-binding inhibitor of NFκB activation
ACPA	Antibodies to citrullinated protein antigen
ACR	American College of Rheumatology
AF	Activation function
AHD2	ABIN homology domain 2
AP-1	Activator protein-1
CAM	Cellular adhesion molecule
cDNA	Complementary deoxyribonucleic acid
CREB	Cyclic adenosine 5'-monophosphate response element-binding protein
Cys	Cysteine
DBD	DNA-binding domain
DEPC	Diethylpyrocarbonate
DNA	Deoxyribonucleic acid
dNTP	Deoxyribonucleotide triphosphate
DMARD	Disease-modifying anti-rheumatic drug
EC	Endothelial cell
EDTA	Ethylenediamine tetracetic acid
EGF	Epidermal growth factor
FADD	Fas-associated death domain
GAPDH	Glyceraldehyde 3-phosphate dehydrogenase
HEK cells	Human embryonic kidney cells
HLA	Human leukocyte antigen
HUVEC	Human umbilical vein endothelial cell
ICAM-1	Intercellular adhesion molecule-1
IgM	Immunoglobulin M
IKK	IκB kinase
IKKα	IκB kinase alpha
IKKβ	IκB kinase beta
IKKγ	IκB kinase gamma
IL	Interleukin

LB	Luria-Bertrani
LBD	Ligand-binding domain
LPS	Lipopolysaccharide
Lys	Lysine
MCP-1	Monocyte chemotactic protein-1
MHC	Major histocompatibility complex
MIP-1 α	Macrophage inflammatory protein-1 α
M-MLV	Moloney murine leukemia virus
MMP	Matrix metalloproteinase
MOPS	3-[N-Morpholino]propanesulfonic acid
mRNA	Messenger ribonucleic acid
NBRE	NGFI-B responsive element
NGFI-B	Nerve growth factor-induced clone B
NF- κ B	Nuclear factor-kappa binding protein
NOR-1	Neuron-derived orphan receptor-1
NR4A	Nuclear receptor subfamily 4A
NSAID	Non-steroidal anti-inflammatory drug
NUR77	Neuron-derived clone 77
NURR1	NUR77- related protein 1
OTU	Ovarian tumour domain
PBS	Phosphate-buffered saline
PCR	Polymerase chain reaction
PDGF	Platelet-derived growth factor
PGE ₂	Prostaglandin E ₂
qPCR	Quantitative polymerase chain reaction
RA	Rheumatoid arthritis
RANKL	Receptor activator of nuclear factor kappa B ligand
RIP1	Receptor interacting protein 1
RNA	Ribonucleic acid
RNase	Ribonuclease
rpm	Revolutions per minute
RPMI	Royal Park Memorial Institute
RT-PCR	Reverse transcription-polymerase chain reaction

SDS	Sodium dodecyl sulphate
SEM	Standard error of the mean
SMC	Smooth muscle cell
TAB1	Transforming growth factor receptor- β -activated kinase 1 binding protein 1
TAB2	Transforming growth factor receptor- β -activated kinase 1 binding protein 2
TAE	Tris acetate EDTA
TAK1	Transforming growth factor receptor- β -activated kinase 1
Tax1BP1	Tax1-binding protein 1
TE	Tris EDTA
TF	Transcription factor
TFBS	Transcription factor binding site
TLR	Toll-like receptor
TNF- α	Tumour necrosis factor-alpha
TNFR	TNF receptor
TRADD	TNF-receptor-associated death domain
TRAF2	TNF-receptor associated factor 2
TRAFB	TRAF binding domain
Treg cell	Regulatory T cell
UBD	Ubiquitin-binding domain
UV	Ultraviolet
VCAM-1	Vascular cell adhesion molecule-1
VEGF	Vascular endothelial growth factor
ZF	Zinc finger

Units

bp	Base pair
cm	Centimetre
°C	Degree Celsius
g	Gram
hr	Hour
Kb	Kilobase
Kg	Kilogram
L	Litre
µg	Microgram
µl	Microlitre
mA	Milliamp
mg	Milligram
ml	Millilitre
mM	Millimolar
min	Minute
M	Molar
ng	Nanogram
nm	Nanometre
%	Percentage
RLU	Relative light unit
s	Second
U	Unit
V	Volt
v/v	Volume per volume

Figures

- Figure 1.1 Schematic description of inflammation in the joint during RA
- Figure 1.2 Schematic representation of activation of the NF- κ B pathways by the inflammatory mediators TNF, IL-1 and LPS
- Figure 1.3 Structure of A20
- Figure 1.4 Schematic representation of the ubiquitin-editing functions of A20 which alters RIP1
- Figure 1.5 Proposed models for the mechanism by which ABIN-1 inhibits NF κ B activation
- Figure 1.6 Proposed mechanism for ABIN-2 inhibition of NF κ B
- Figure 1.7 Structures of A20 and Cezanne depicting TRAFB domains, ZF A20 and NUC
- Figure 1.8 Proposed mechanisms by which A20, ABIN-1, ABIN-2 and Cezanne inhibit TNF- α -induced NF κ B activation
- Figure 1.9 Structure of NR4A nuclear receptors binding to the NBRE sequence as a monomer
- Figure 1.10 Sites of action of biological therapies and other agents for the treatment of RA
- Figure 3.1 Schematic representation of potential consensus NBRE sites (in blue) in the promoter regions of A20 (TNFAIP3), ABIN-1 (TNIP1), ABIN-2 (TNIP2) and in two Cezanne (OTUD7B) promoters generated using Genomatix
- Figure 3.2 Potential consensus NBRE sites (blue) and NF- κ B binding sites (pink) identified in the promoter regions of A20, ABIN-1, ABIN-2 and Cezanne using Genomatix software
- Figure 3.3 Examples of promoter TF models containing the NBRE site which were identified by Frameworker as being common to the promoters of ABIN-1 and Cezanne
- Figure 4.1 RT-PCR analysis for the detection of mycoplasma in K4 IM and SW 1353 cells
- Figure 4.2 Total intact RNA isolated from K4 IM cells which were untreated, treated with vehicle or treated with TNF- α for the times indicated
- Figure 4.3 RT-PCR analysis of the housekeeping gene β -actin (234 bp) performed on RNA isolated from K4 IM cells which were untreated, treated with vehicle or treated with TNF- α for the times indicated
- Figure 4.4 RT-PCR analysis of ICAM-1 (295 bp) and VCAM-1 (350 bp) performed on RNA isolated from K4 IM cells which were untreated, treated with vehicle or treated with TNF- α for the times indicated

- Figure 4.5 RT-PCR analysis of A20 (153 bp) and ABIN-1 (168 bp) performed on RNA isolated from K4 IM cells which were untreated, treated with vehicle or treated with TNF- α for the times indicated
- Figure 4.6 RT-PCR analysis of ABIN-2 (114 bp) and Cezanne (293 bp) performed on RNA isolated from K4 IM cells which were untreated, treated with vehicle or treated with TNF- α for the times indicated
- Figure 4.7 Total intact RNA isolated from SW 1353 cells which were untreated, treated with vehicle or treated with TNF- α for the times indicated
- Figure 4.8 RT-PCR analysis of the housekeeping gene β -actin (234 bp) performed on RNA isolated from SW 1353 cells which were untreated, treated with vehicle or treated with TNF- α for the times indicated
- Figure 4.9 RT-PCR analysis of ICAM-1 (295 bp) and VCAM-1 (350 bp) performed on RNA isolated from SW 1353 cells which were untreated, treated with vehicle or treated with TNF- α for the times indicated
- Figure 4.10 RT-PCR analysis of A20 (153 bp) and ABIN-1 (168 bp) performed on RNA isolated from SW 1353 cells which were untreated, treated with vehicle or treated with TNF- α for the times indicated
- Figure 4.11 RT-PCR analysis of ABIN-2 (114 bp) and Cezanne (293 bp) performed on RNA isolated from SW 1353 cells which were untreated, treated with vehicle or treated with TNF- α for the times indicated
- Figure 4.12 Total intact RNA isolated from SW 1353 cells which were untreated or treated with TNF- α for the times indicated
- Figure 4.13 qPCR amplification curves for A20 gene expression
- Figure 4.14 qPCR analysis of A20 mRNA levels in response to TNF- α stimulation in SW 1353 chondrocyte cells
- Figure 4.15 qPCR amplification curves for ABIN-1 gene expression
- Figure 4.16 qPCR analysis of ABIN-1 mRNA levels in response to TNF- α stimulation in SW 1353 chondrocyte cells
- Figure 5.1 Restriction enzyme digests of Qiagen purified *Renilla* luciferase pRL-SV40 vector electrophoresed on 0.8 % agarose gel and visualised by staining with ethidium bromide
- Figure 5.2 Restriction enzyme digests of Qiagen purified pcDNA6/*myc*-His C plasmid electrophoresed on 0.8 % agarose gel

- Figure 5.3 Restriction enzyme digests of Qiagen purified pNBRE₃-tk-luciferase reporter construct and pCAGGS-GFP/A20 electrophoresed on 0.8 % agarose gel
- Figure 5.4 Restriction enzyme digests of Qiagen purified CMX-NURR1 plasmid electrophoresed on 0.8 % agarose gel
- Figure 5.5 Restriction enzyme digests of Qiagen purified IL-8-luciferase reporter construct and p65 expression vector electrophoresed on 0.8 % agarose gel
- Figure 5.6 K4 IM synoviocytes transfected with a GFP expression vector viewed using the Olympus 1X51 inverted fluorescent microscope with mercury lamp under 100X magnification
- Figure 5.7 SW 1353 chondrocytes transfected with a GFP expression vector viewed using the Olympus 1X51 inverted fluorescent microscope with mercury lamp under 100X magnification
- Figure 5.8 NBRE-luciferase assay results for K4 IM cells demonstrating a dose-dependant inhibitory effect of A20 on the activation of the pNBRE₃-tk-luciferase reporter construct by NURR1
- Figure 5.9 NBRE-luciferase assay results for K4 IM cell line illustrating an inhibitory effect of A20 on the activation of the pNBRE₃-tk-luciferase reporter construct
- Figure 5.10 NBRE-luciferase assay results for SW 1353 cell line illustrating the inhibitory effect of A20 on the activation of the pNBRE₃-tk-luciferase reporter construct
- Figure 5.11 IL-8-luciferase assay results for the K4 IM cell line illustrating an inhibitory effect by A20 on the transactivation of the IL-8 reporter construct by endogenous NURR1, overexpressed NURR1 and overexpressed NURR1 in combination with the NF-κB subunit p65
- Figure 5.12 IL-8-luciferase assay results for SW 1353 cells showing an enhancing effect by A20 on the transcriptional activity of endogenous NURR1, overexpressed NURR1 and overexpressed p65 subunit of NF-κB on the IL-8-luciferase reporter construct

Tables

Table 1.1	The 2010 American College of Rheumatology/European League Against Rheumatism classification criteria for rheumatoid arthritis
Table 3.1	Potential NBRE sequences identified within A20 and A20-interacting Genes using Genomatix Software
Table 3.2	Definitions of TF matrix families that have been identified in promoter models which are common to the promoters of ABIN-1 and Cezanne and which also contain the NBRE site
Table 3.3	Promoter modules identified using ModelInspector as being common to A20, ABIN-1, ABIN-2 and Cezanne promoters
Table 3.4	Promoter modules and their functions identified within A20 and A20-interacting genes using ModelInspector
Table 3.5	Promoter models identified by Frameworker as being common to A20, ABIN-1, ABIN-2 and Cezanne promoters and their p values indicating their specificity
Table 3.6	Definition of TF matrix families within promoter models identified by Frameworker as being common to A20, ABIN-1, ABIN-2 and Cezanne
Table 5.1	Composition of DNA Transfected into K4 IM cells using GeneJuice for NBRE-Luciferase Assay
Table 5.2	Composition of DNA Transfected into K4 IM cells using Turbofect for NBRE-Luciferase Assays
Table 5.3	Composition of DNA transfected into SW 1353 cells using Turbofect for NBRE-Luciferase Assays
Table 5.4	Composition of DNA transfected into K4 cells using Turbofect for IL-8-Luciferase Assays

Table of Contents

Declaration	I
Acknowledgments	II
Abstract	III
Abbreviations	IV
Units	VII
Figures	VIII
Tables	XI
.	
1. Introduction	1
1.1 Rheumatoid Arthritis	1
1.1.1 Key cells involved in RA	8
1.1.2 Key cytokines involved in RA	13
1.2 NF- κ B Activation	15
1.3 A20	18
1.4 ABIN-1	24
1.5 ABIN-2	27
1.6 Cezanne	30
1.7 NR4A Subfamily of Nuclear Orphan Receptors	34
1.7.1 Functions of NR4A receptors	36
1.7.2 Evidence of a proinflammatory role for NR4A receptors	37
1.7.3 Anti-inflammatory actions of NR4A receptors	40
1.7.4 Nuclear receptors as targets for therapeutics	41
1.8 Current Treatment for Rheumatoid Arthritis	43
1.8.1 Corticosteroids	43
1.8.2 Non-steroidal anti-inflammatory drugs (NSAIDs)	44
1.8.3 Disease-modifying anti-rheumatic drugs (DMARDs)	45
1.8.4 Biological Therapies	46
1.9 Research Objectives	51

2. Materials and Methods	53
2.1 Biological Materials	54
2.1.1 Cell Lines	54
2.1.2 Plasmids	54
2.1.3 Standard End-Point PCR Primers	55
2.1.4 Quantitative PCR Oligonucleotides	56
2.1.5 Other Biological Materials	57
2.2 Chemical Materials	57
2.2.1 Commercial Kits	58
2.3 DNA Manipulation	59
2.3.1 Bacterial Transformation	59
2.3.2 Plasmid DNA Miniprep	59
2.3.3 Plasmid Glycerol Stocks	61
2.3.4 QIAGEN Plasmid Purification	61
2.3.5 Spectrophotometric Analysis of Nucleic Acids	62
2.3.6 Restriction Enzyme Digestion of DNA	62
2.3.7 DNA Gel Electrophoresis	63
2.4 RNA Analysis	64
2.4.1 RNase-free Environment	64
2.4.2 RNA Extraction from Cultured Cells	64
2.4.3 RNA Gel Electrophoresis	65
2.4.4 Reverse-Transcription (RT)	66
2.4.5 Polymerase Chain Reaction (PCR) Primer Design	68
2.4.6 End-Point PCR Analysis	68
2.4.7 Quantitative PCR (qPCR)	70
2.5 Cell Culture Techniques	72
2.5.1 Cell Culture	72
2.5.2 Cryopreservation of Cells	73
2.5.3 Heat Inactivation of Serum	73
2.5.4 Supplementation of Media	73
2.5.5 Counting Cells	74
2.5.6 TNF- α Stimulation of Cells	74
2.5.7 Transfection of Cells using Turbofect Transfection Reagent	75

2.5.8 Transfection of Cells using GeneJuice Transfection Reagent	75
2.5.9 Luciferase Assays	76
2.5.10 Green Fluorescent Protein (GFP) Assay	76
2.5.11 Test for Mycoplasma	77
3. Bioinformatic Analysis of A20, ABIN-1, ABIN-2 and Cezanne	79
3.1 Introduction	80
3.2 Bioinformatic Analysis	80
3.3 Discussion	90
3.4 Conclusions	95
4. Analysis of Changes of Expression of Genes Functionally Related to A20 in response to TNF-α	96
4.1 Cell Lines	97
4.1.1 Mycoplasma Testing of Cells	97
4.2 Analysis of Differential Gene Expression in response to TNF- α	99
4.3 K4 IM Synoviocyte Results	101
4.3.1 Determination of the Integrity of Extracted RNA	101
4.3.2 Reverse Transcription-Polymerase Chain Reaction (RT-PCR) Results	102
4.4 SW 1353 Chondrocyte Results	106
4.4.1 Electrophoretic Analysis of Extracted RNA	106
4.4.2 RT-PCR Results	107
4.4.3 Determination of the Integrity of Extracted RNA for qPCR	111
4.4.4 Quantitative (q)PCR Results	112
4.5 Discussion	115
4.6 Conclusions	120
5. Investigating A20 as a means of Modulating the NR4A Subfamily of Nuclear Receptors	121
5.1 Introduction	122
5.2 Verification of Plasmids used for Transfection Experiments	123
5.3 Transfection Efficiencies	128

5.4 NBRE-luciferase Assays	130
5.4.1 NBRE- Luciferase Assay Results – K4 IM Synoviocytes	130
5.4.2 NBRE-Luciferase Assay Results – SW 1353 Chondrocytes	133
5.5 IL-8 Luciferase Assays	134
5.5.1 IL-8 Luciferase Assay Results – K4 IM Synoviocytes	135
5.5.2 IL-8 Luciferase Assay Results – SW 1353 Chondrocytes	137
5.6 Discussion	137
5.7 Conclusions	142
6. Summary	143
7. Bibliography	145

Chapter 1

Introduction

lyit | Institiúid Teicneolaíoch Leictir Ceánalinn
Letterkenny Institute of Technology

1. Introduction

1.1 Rheumatoid Arthritis

Rheumatoid arthritis (RA) is a chronic, autoimmune disease that results in progressive joint destruction. It affects approximately 1% of the global population and is more prevalent in females than males, by a ratio of around 3 to 1 (Deng and Lenardo 2006; Walsh 2002). Approximately 40,000 people in Ireland suffer with the disease (Arthritis Ireland 2006). The clinical symptoms are red, swollen, painful joints which become increasingly deformed, leading to loss of function. RA is characterized by chronic synovial inflammation, resulting in the destruction of cartilage and bone in the joint (Deng and Lenardo 2006). RA has a profound impact on the lives of patients. A survey carried out by Arthritis Ireland indicated that 70 % of patients with RA in Ireland are unable to work outside the home as a result of their illness. Of those who are employed, 43% are only able to work part-time (Arthritis Ireland 2006).

The etiology of RA remains unknown. RA may be defined as a complex genetic disease in which certain genes, environmental factors and random events come together, causing the disease (Lkareskog *et al.* 2009). Suggestions for environmental triggering factors include viral gene products, degraded bacterial cell wall peptidoglycans and bacterial or viral antigens (Walsh 2002). Sex hormones may be involved in the development and/or the pathogenesis of RA as it has been observed that disease activity is often reduced during pregnancy and the highest incidence of RA in women occurs at the time of menopause (Islander *et al.* 2010).

In normal joints, the fibrous joint capsule is surrounded by a thin lining of synovial tissue (the synovium), consisting of fibroblast-like and macrophage-like synoviocytes. These cells produce synovial fluid that lubricates the joint and provides nutrients to the cartilage (Davis 2003). However in RA, immune cells such as lymphocytes and macrophages infiltrate the synovium, leading to inflammation of the joint (Firestein 2003). Increased angiogenesis (growth of new blood vessels), which enables proliferation of synoviocytes, results in the delicate joint lining being transformed into a thick invasive tissue, called pannus (Firestein 2003). RA is a systemic disease and the patient may experience several major extra-articular features such as anaemia, weight loss, fatigue and fever (Walsh 2002). Rheumatoid nodules develop in approximately 25 % of RA patients, most commonly occurring at pressure points such as extensor surfaces of the forearm, but also within internal tissues such as in the lungs. Rheumatoid nodules have a

central area of necrosis surrounded by epithelioid and chronic inflammatory cells (Thinda and Tomlinson 2009). There is an increased rate of mortality in the RA population compared with the general population. This is mainly due to the development of cardiovascular disease and accelerated atherosclerosis (driven by inflammation) in many RA patients (Buch and Emery 2002). In addition, patients with RA are at a higher risk of developing lymphoma, which may be due to longstanding B-cell stimulation (Lkareskog *et al.* 2009).

Criteria for the diagnosis of RA were originally developed in the 1980s by American rheumatologists. However, new criteria for the classification of this disease, based on a greater understanding of the pathogenesis of RA, were published in September 2010 by an American College of Rheumatology (ACR) and European League Against Rheumatism (EULAR) joint working group. These criteria are given in Table 1.1 (Aletaha *et al.* 2010).

Table 1.1 The 2010 American College of Rheumatology/European League Against Rheumatism classification criteria for rheumatoid arthritis (Aletaha *et al.* 2010).

Patients should be tested who:		Score
1)	have at least 1 joint with definite clinical synovitis (swelling)	
2)	with the synovitis not better explained by another disease	
<hr/>		
Classification criteria for RA (score-based algorithm: add score of categories A-D; a score of $\geq 6/10$ is needed for classification of a patient as having definite RA)		
A. Joint involvement		
	1 large joint (shoulder, elbow, hip, knee or ankle)	0
	2-10 large joints	1
	1-3 small joints (with or without involvement of large joints)	2
	4-10 small joints (with or without involvement of large joints)	3
	>10 joints (at least 1 small joint)	5
<hr/>		
B. Serology (at least 1 test result is needed for classification)		
	Negative RF <i>and</i> negative ACPA	0
	Low-positive RF <i>or</i> low-positive ACPA	2
	High-positive RF <i>or</i> high-positive ACPA	3
<hr/>		
C. Acute-phase reactants (at least 1 test result is needed for classification)		
	Normal CRP and normal ESR	0
	Abnormal CRP or abnormal ESR	1
<hr/>		
D. Duration of symptoms		
	<6 weeks	0
	>6 weeks	1

RF = rheumatoid factor; ACPA = anti-citrullinated protein antibody; CRP = C-reactive protein; ESR = erythrocyte sedimentation rate.

Along with the physical symptoms, RA sufferers often experience psychological problems including depression, due to loss of their role in society and social isolation (Walsh 2002).

RA was first identified as an autoimmune disease when “rheumatoid factor”, a self-reactive IgM antibody, was identified and characterized in the blood of affected patients (Firestein 2003; Corper *et al.* 1997). Rheumatoid factor is present in approximately 80 % of RA patients, although a person may test positive for this antibody and not develop RA (Firestein 2003). These

antibodies are specific for antigens within connective tissues, but are mainly found in the synovium (Walsh 2002). Recently, the disease has been divided into subsets on the basis of either the presence or absence of rheumatoid factor, with different causes and severity. Increasingly however, subsets based on the presence or absence of antibodies to citrullinated protein antigen (ACPA), also known as anti-CCP (cyclic citrullinated peptide), have been used to distinguish subsets of RA (Lkareskog *et al.* 2009). This antigen is a peptide which contains the amino acid citrulline (Chou *et al.* 2007). Patients who are positive for both rheumatoid factor and ACPA display more prominent joint destruction and extra-articular manifestations than those who are negative for these factors (Lkareskog *et al.* 2009).

The first genetic susceptibility genes identified for RA were the human leukocyte antigen (HLA)-DR genes, which are located in the major histocompatibility complex (MHC). The MHC's role is to present antigens to T cells, activating an immune response. Most HLA-DR alleles have a common amino acid motif, termed the shared epitope, in the β chain of the HLA-DR molecule (Firestein 2003). The shared epitope consists of the amino acids glutamine-leucine-arginine-alanine-alanine. The fact that it resides in the MHC molecule indicates that the shared epitope may play a role in the ability of HLA-DR to bind and present certain peptides, not yet identified, that may cause the disease (Firestein 2003). In 2005, another genetic susceptibility gene was identified, PTPN22. This gene encodes Lyp, a tyrosine phosphatase that regulates signal transduction from the T-cell receptor. Additional risk alleles for the disease have recently been identified in regions containing the genes TRAF1 (C5 locus), STAT4 and OLIG3-AIP3 (Lkareskog *et al.* 2009). The gene that codes for PD-1, a molecule that regulates T cell homeostasis through apoptosis, has also been found to confer genetic susceptibility to RA. Aberrant PD-1 activity may lead to the failure of autoreactive T cells to undergo apoptosis (Lundy *et al.* 2007). It is thought that a series of variations together make up the genetic risk for RA (Lkareskog *et al.* 2009).

Cigarette smoking has been verified as an important environmental risk factor for RA. However, this is only the case with regard to the rheumatoid factor-positive or ACPA-positive subsets. Descriptive epidemiological studies have identified silica dust, mineral oils and charcoal as other potential risk factors. Moderate alcohol consumption is reported to reduce the risk and severity of the disease (Lkareskog *et al.* 2009).

The interaction between the cells and molecules involved in the pathogenesis of RA are illustrated schematically in Figure 1.1. Many cell types infiltrate the inflamed RA joint. Antigen presenting cells, such as B cells and macrophages, activate T cells, and therefore the immune response, via the MHC-T cell receptor (TCR) complex. T cell activation requires co-stimulatory signals mediated via CD28-CD80/86 receptor (Klareskog *et al.* 2009)s. B cells also produce autoantibodies which form immune complexes. Macrophages are activated by T cells and immune complexes to secrete proinflammatory cytokines. These cytokines induce the production of matrix metalloproteinases (MMPs) which break down joint cartilage. In the presence of certain cytokines, T cells develop distinct phenotypes such as T-helper 17 (Th17) which release interleukin (IL)-17, another proinflammatory cytokine, thus contributing to the inflammatory response (Klareskog *et al.* 2009). Both cell surface-bound and soluble forms of receptor activator of NF- κ B ligand (RANKL) are produced by fibroblasts, osteoblasts and T cells in response to proinflammatory cytokines. RANKL in turn activates receptor activator of NF- κ B (RANK) which is expressed on the surface of osteoclast precursors. Stimulation of RANK leads to the activation of osteoclasts which resorb bone (Klareskog *et al.* 2009).

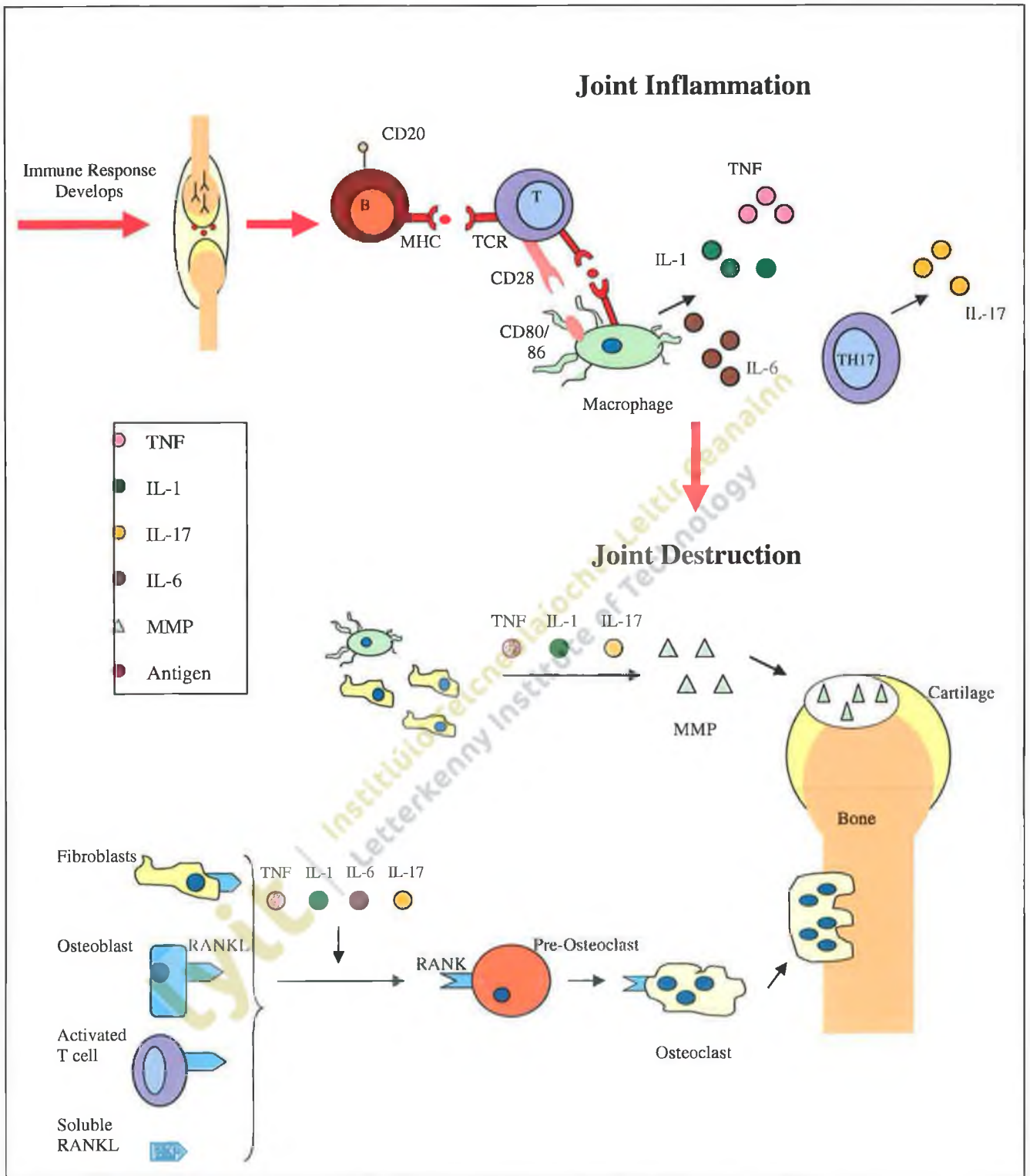


Fig. 1.1 Schematic illustration of inflammatory responses in the RA joint. The upper section illustrates joint inflammation and the lower section illustrates joint destruction (Adapted from Klareskog *et al.* 2009).

1.1.1 Key cells involved in RA

1.1.1.1 Macrophages

Macrophages are important cells in the inflamed joint of RA patients. They infiltrate the joint and accumulate in the synovial membrane and at the cartilage-pannus junction. They are antigen-presenting cells which activate T cells and, therefore, the immune response (Deng and Lenardo 2006). Macrophages themselves are activated by several factors such as interferon (IFN)- γ , produced by a subgroup of T cells known as Type 1 helper T (Th1) cells, and by direct cell-cell interaction with T cells. Activated macrophages produce a variety of proinflammatory cytokines and chemokines such as tumour necrosis factor-alpha (TNF- α), interleukin (IL)-1 β , IL-6, IL-8 and macrophage inflammatory protein-1 α (MIP-1 α). These cytokines initiate and perpetuate the inflammatory response in the joint. Macrophages also exhibit a resistance to apoptosis which may contribute to chronic inflammation (Deng and Lenardo 2006).

1.1.1.2 T cells

Helper T cells (Th), also known as CD4⁺ T cells, are one of the principal cell types found in the inflamed synovium of RA patients. These cells become activated through binding to the corresponding antigen-MHC complex on antigen presenting cells, initiating the immune response. This response involves helping B cells to divide and produce antibodies and activating phagocytes (Deng and Lenardo 2006). Effector cells such as macrophages, which are activated by Th cells, produce numerous proinflammatory cytokines and chemokines. In addition, Th cells produce RANKL (receptor activator of nuclear factor kappa B ligand) which causes considerable destruction of bone in the joint due to the activation of osteoclasts (bone resorbing cells) (Deng and Lenardo 2006; Buch and Emery 2002). Moreover, studies have demonstrated an imbalance between Th1 and Th2 cell activity within the joints of RA sufferers. The Th1 subset is characterised by the activation of cell-mediated immunity and by the synthesis of the proinflammatory factors INF- γ and IL-2. In contrast, Th2 cells stimulate humoral immunity and synthesize the anti-inflammatory cytokine IL-4 (Islander *et al.* 2010).

1.1.1.3 B cells

B cells, as key elements of the immune system, are also involved in the aberrant inflammatory response in RA. Activated B cells produce the autoantibody rheumatoid factor and antibodies to citrullinated protein antigen (ACPA), which may be initiators of RA by forming immune

complexes. Immune complexes activate complement in the innate immune response and recruit inflammatory cells to the joint (Deng and Lenardo 2006). B cells can also act as antigen-presenting cells, activating T cells (Klareskog *et al* 2009). In addition, B cells can produce cytokines and chemokines, promoting angiogenesis, synovial proliferation and the infiltration of leukocytes into the inflamed joint (Silverman and Carson 2003).

1.1.1.4 Endothelial cells

Endothelial cells (ECs) are crucial cells in the pathogenesis of RA. These cells line the inner surface of blood vessels, forming the endothelium. It is through the endothelium that leukocytes and proinflammatory mediators migrate into the synovial tissue of inflamed joints. ECs become activated by these inflammatory stimuli and are themselves stimulated to produce several proinflammatory mediators such as cytokines and cellular adhesion molecules (CAMs), contributing to the inflammatory response (Szekanecz and Koch 2000). Indeed, the first sign of abnormality within synovial tissues of RA patients is thought to be endothelial cell activation or injury. This is detected by the increased expression of activation markers such as class II MHC antigens, leukocyte adhesion molecules and metalloproteinases by ECs (Wilder *et al.* 1990). Angiogenesis within the synovium begins in the very early stages of RA and this facilitates the growth of invasive pannus tissue. ECs, along with fibroblast-like synoviocytes, produce vascular endothelial growth factor (VEGF) and angiopoietin-2, which promote angiogenesis and the proliferation of ECs (Pratt *et al.* 2009).

Several CAMs mediate the migration of leukocytes through the endothelium, into the inflamed synovium. These primarily belong to three families of CAMs - the integrin, selectin and immunoglobulin families (Szekanecz and Koch 2000). There are four steps involved in the adhesion of leukocytes to endothelial cells and migration through the endothelium. Firstly, E-, P- and L-selectins and their receptors mediate relatively weak adhesion (termed rolling) between leukocytes and ECs. This is followed by leukocyte activation through the interaction of chemokine receptors on leukocytes and proteoglycans on ECs. Firm adhesion then occurs mainly due to $\alpha_4\beta_1$ integrin-vascular cell adhesion molecule (VCAM)-1 and $\alpha_L\beta_2$ integrin-intercellular adhesion molecule (ICAM)-1 interactions (Szekanecz and Koch 2000). The final step of transendothelial migration (known as diapedesis) occurs when the firmly-attached leukocytes edge across the endothelial surface due to cyclic alteration of integrin receptor avidity and then pass through the vascular endothelium at an intercellular junction, between the endothelial cells

(Carlos and Harlan 1994). This results in the infiltration of inflammatory cells into the synovium, leading to joint degradation in RA (Szekanecz and Koch 2000).

E- and P-selectin CAMs are found on ECs and their expression is also induced by inflammatory cytokines. E-selectin is highly expressed in RA synovial tissue and is responsible for the adhesion of neutrophils, along with eosinophils and monocytes, to the endothelium. P-selectin mediates rapid adhesion of neutrophils and monocytes to endothelial cells and is also expressed on ECs from RA synovial tissue (Szekanecz and Koch 2000). ECs express the integrins β_1 and β_3 , which allow endothelial adhesion to extracellular matrix (ECM) components, such as various types of collagen, fibronectin and fibrinogen, and can also mediate cell-cell interactions by binding to the immunoglobulin family of CAMs, such as during firm adhesion of leukocytes to endothelial cells (Szekanecz and Koch 2000). ICAM-1 and VCAM-1 are expressed constitutively by ECs at basal levels but their expression is distinctly increased by stimulation with cytokines such as TNF α . ICAM-1 is a ligand for β_2 integrins, while VCAM-1 is a ligand for the $\alpha_4\beta_1$ and $\alpha_4\beta_7$ integrins. ICAM-1 and VCAM-1 are both expressed by ECs from the inflamed synovium of RA patients. The endothelial adhesion molecules mentioned here are among the most important CAMs involved in endothelial-leukocyte adhesion and leukocyte migration into the RA synovium (Szekanecz and Koch 2000).

1.1.1.5 Fibroblast-like synoviocytes

Fibroblast-like synoviocytes (also called synovial fibroblasts) are crucial cells in the pathology of RA (Karouzakis *et al.* 2006). These cells form part of the synovium, the thin lining of the joint, and produce synovial fluid (Davis 2003). Proliferation of fibroblast-like synoviocytes, which also exhibit resistance to apoptosis, leads to synovial hyperplasia, a major hallmark of RA (Müller-Ladner *et al.* 2000). Synoviocytes exhibit increased expression of transcription factors and growth factors which are markers of proliferation. Activated synoviocytes in the RA joint become aggressive and invasive and are likened to metastatic cancer cells (Karouzakis *et al.* 2006).

Synoviocytes express toll-like receptors (TLRs) on their surface and, along with responding to pathogenic stimuli, these receptors may also be activated by endogenous ligands, including hyaluronan fragments and high-mobility-group box 1 protein (HMGB-1), which may be found in healthy synovial tissue (Pratt *et al.* 2009). These cells are also activated by numerous

proinflammatory cytokines such as TNF- α , IL-1 and IL-6 (Karouzakis *et al.* 2006). As a result, synoviocytes produce chemokines including granulocyte chemotactic protein (GCP)-2, which are important for the recruitment and retention of leukocytes in the inflamed synovium (Pratt *et al.* 2009). They also express cytokines themselves, heightening the inflammatory response. Synoviocytes secrete various types of matrix metalloproteinases (MMPs), including MMP-1, MMP-3 and MMP-13, along with cathepsins B, K and L, all of which degrade ECM and cartilage in the joint. The destructive properties of synoviocytes are partly due to their ability to adhere to cartilage through the production of adhesion molecules. Synoviocytes, along with T cells, produce RANKL which regulates the differentiation of osteoclasts. They also secrete high levels of prostaglandin E₂ (PGE₂), another important mediator of inflammation (Karouzakis *et al.* 2006).

The aggressive behaviour of fibroblast-like synoviocytes in the RA synovium may be due, in part, to dysregulation of the transcription factors activator protein (AP)-1 and nuclear factor-kappa binding protein (NF- κ B), along with the tumour suppressor gene, p53. Chronic inflammation induces expression of p53, which is a cell-cycle regulatory gene. However, mutations in this gene have been found in synoviocytes from patients with established RA (Davis 2003). Synoviocytes exhibit resistance to both Fas- and TNF- α -induced apoptosis, the main cell death pathways. This may be due to the downregulation of apoptotic signaling molecules such as the tumour suppressor genes p16 and PTEN (phosphatase and tensin homolog) in RA synoviocytes (Davis 2003).

As a result of these features, activated synoviocytes play a central role in the complex network of cell interactions which maintain chronic inflammation and joint erosion in RA (Karouzakis *et al.* 2006).

1.1.1.6 Chondrocytes

Cartilage covers the two opposing bone surfaces in the joint and acts as a shock absorber, as well as allowing the bones to move with minimum friction. Chondrocytes make up the cells within cartilage, synthesising cartilage matrix components such as collagen and proteoglycans. The cartilage matrix is an avascular environment and chondrocytes depend on diffusion of nutrients and metabolites from the cartilage surface or nearby bone. These cells have the ability to survive due to the intracellular expression of survival factors such as hypoxia-inducible factor (HIF)-1 α .

These stimulate the production of glucose transporter proteins (GLUTs), angiogenic factors including VEGF and genes related to cartilage anabolism (Otero and Goldring 2007).

Proinflammatory cytokines and degraded matrix components activate chondrocytes, inducing the production of MMPs such as MMP-1, MMP-2 and MMP-13. These proteolytic enzymes break down collagen and proteoglycans which make up cartilage and these degraded components are then released into the joint where they maintain and heighten inflammation by contributing to cellular activation (Rannou *et al.* 2006). Chondrocytes can produce proinflammatory cytokines themselves, including TNF- α , IL-1 and IL-6, driving the immune response. In addition, they may express toll-like receptor-1 (TLR-1), TLR-2 and TLR-4. Toll-like receptors are important in innate immunity and inflammation. When activated, TLR-2 increases the synthesis of MMPs and other proinflammatory factors such as nitric oxide and VEGF which drive the inflammatory responses in the RA joint (Otero and Goldring 2007).

Activated chondrocytes also produce several chemokines including monocyte chemoattractant protein (MCP)-1, MCP-4, macrophage inflammatory protein (MIP)-1 α and MIP-1 β . Furthermore, chondrocytes can secrete receptors for a number of these chemokines. Many adhesion molecules which are necessary for the binding and interaction of cells in the inflamed synovium are also produced in cartilage. These include ICAM-1 and VCAM-1 (Otero and Goldring 2007).

Some studies have found that antibodies against particular cartilage antigens, for example collagen type II, may be present in RA joints and these antigen-antibody complexes may initiate the inflammatory response in this disease (Rannou *et al.* 2006).

1.1.1.7 Osteoblasts and Osteoclasts

Osteoblasts are the cells responsible for the formation and maintenance of bone architecture. They synthesize type I collagen and numerous non-collagen proteins including osteocalcin, osteopontin and bone sialoprotein. These proteins regulate bone turnover and bone mineral deposition (Neve *et al.* 2010). Bone remodelling constantly takes place, which is a process requiring osteoclasts, as well as, osteoblasts. Osteoclasts are cells derived from mononuclear monocyte/macrophages that co-ordinate with osteoblasts in bone remodelling. Osteoclasts normally become activated and resorb bone, before undergoing apoptosis (Neve *et al.* 2010).

Osteoblasts migrate to the site and secrete bone matrix proteins, filling the cavity left by the osteoclasts. The ECM then becomes mineralized. In RA, there is an increase in bone resorption by osteoclasts. RANKL binds to its receptor RANK on the surface of osteoclast precursors, inducing differentiation, activation and survival of osteoclasts (Neve *et al.* 2010). RANKL is produced by activated T cells, macrophages, synoviocytes and osteoblasts (Deng and Lenardo 2006; Neve *et al.* 2010). High levels of RANK, RANKL and mature osteoclasts are found in the diseased joints of patients with inflammatory arthritis (Deng and Lenardo 2006). Furthermore, it is thought that TNF- α inhibits the differentiation and function of osteoblast cells in the RA joint (Neve *et al.* 2010). Therefore, there is an increase in osteoclast activity and a reduced level of osteoblast activity contributing to RA.

1.1.2 Key cytokines involved in RA

1.1.2.1 TNF- α

TNF- α is one of the main cytokines found in the joint of RA patients and is a key inflammatory mediator. It stimulates the activation of NF- κ B, a transcription factor which is a crucial driver of the inflammatory response, inducing the expression of numerous proinflammatory mediators (Deng and Lenardo 2006). NF- κ B induces TNF- α itself, among many other inflammatory cytokines (Kast 2005). TNF- α is synthesized by most cells of the body, macrophages being one of the primary sources. It initiates the signal transduction cascade leading to NF- κ B activation through binding to one of its receptors, TNF-receptor 1 (TNF-R1) or TNF-receptor 2 (TNFR-2). Studies have shown that injection of TNF- α into the joint can directly induce arthritis and TNF- α knockout mice are resistant to developing arthritis. This cytokine, along with RANKL, stimulates the differentiation of osteoclasts which resorb bone, leading to bone erosion. Anti-TNF- α agents such as Etanercept and Infliximab are now widely used for the treatment of RA (Deng and Lenardo 2006). However, while 50-70 % of patients treated respond positively, the remaining patients do not demonstrate any improvement (Atzeni *et al.* 2009).

1.1.2.2 IL-1

IL-1 is another important cytokine involved in chronic inflammation and RA. It is produced mainly by macrophages (Deng and Lenardo 2006). Different genes encode IL-1 α and IL-1 β , but both cytokines bind to the same receptors. IL-1 β has been identified in the serum of patients with active RA and this cytokine plays a central role in joint damage, activating synovial fibroblasts

and chondrocytes to express metalloproteinases and PGE₂. IL-1 causes a decline in the synthesis of cartilage components and an increase in bone resorption (Piecny and Anderson 2001). It also induces the activation of T cells and enhances infiltration of lymphocytes, neutrophils and monocytes into inflamed tissues (Deng and Lenardo 2006).

1.1.2.3 IL-6

Elevated levels of IL-6 are found in the serum and synovial fluid of RA patients and this cytokine plays an important role in both systemic and local RA symptoms. IL-6 is involved in inducing the acute-phase inflammatory response. Acute-phase proteins stimulate the immune system by complement activation and cytokine induction (Cronstein 2007). C-reactive protein (CRP) and serum amyloid A are acute-phase proteins which have been implicated in RA. Other systemic symptoms involving IL-6 include fever and anaemia due to expression of the iron regulatory peptide, hepcidin, which interferes with iron absorption. IL-6 contributes to local RA symptoms through stimulating synoviocyte proliferation and activating endothelial cells, leading to the production of adhesion molecules and the recruitment of leukocytes to inflamed areas. IL-6 also leads to the expression of MMPs, resulting in joint destruction (Cronstein 2007).

1.1.2.4 IL-17

IL-17, produced by a subset of T cells named Th17 cells, is a potent inflammatory cytokine, inducing a milieu of effector molecules produced by cells in the inflamed joint. These include TNF- α and IL-1 (with which it can work in synergy), RANKL, VEGF, PGE₂ and MMPs. IL-17 induces the degradation of cartilage by chondrocytes. The cytokines induced by IL-17 can upregulate the production of IL-17 itself, forming a positive feedback loop that perpetuates the disease (Lundy *et al.* 2007).

1.1.2.6 IL-8

IL-8 is a chemokine which is found in higher levels in the synovial fluid and serum of RA patients. It acts as a neutrophil chemoattractant, drawing polymorphonuclear neutrophils into the inflamed joint, contributing to pain and inflammation. IL-8 is also a pro-angiogenic factor, inducing the formation of new blood vessels within the synovium and thus facilitating the further infiltration of proinflammatory mediators and cells into the joint. IL-8 is produced by synoviocytes, chondrocytes, synovial stromal cells and subchondral bone marrow stromal cells. TNF- α and IL-1 both induce the synthesis of IL-8 (Slavic *et al.* 2005).

1.2 NF- κ B Activation

The transcription factor NF- κ B is a key regulator of the inflammatory response in many diseases, including RA. In total, more than 150 genes have been identified as being induced by activated NF- κ B (Makarov 2001). This transcription factor controls the expression of genes required for normal cell processes such as cell growth, differentiation and survival. However, uncontrolled NF- κ B activity is associated with chronic inflammation, inducing the transcription of at least 27 different proinflammatory factors including cytokines, chemokines, proteins involved in antigen presentation and adhesion molecules. These factors form a self-perpetuating cycle of chronic inflammation and joint destruction (Yamamoto and Gaynor 2001). NF- κ B is also responsible for inducing the expression of antiapoptotic genes such as members of the IAP (inhibitor of apoptosis) family, TNF-receptor associated factor (TRAF)1 and TRAF2 which would contribute to hyperplasia within the joint (Makarov 2001; Schoemaker *et al.* 2002).

Five different NF- κ B (or Rel family) subunits have been identified: NF- κ B1 (p50 derived from its inactive precursor, p105), NF- κ B2 (p52 derived from p100), RelA (p65), RelB and c-Rel. These subunits form homodimers or heterodimers and are sequestered in the cytoplasm by the inhibitory protein, I κ B. When this inhibitory protein is phosphorylated, the active NF- κ B dimer moves to the nucleus, where it binds to the κ B binding sequence, 5'-GGRNYYYCC-3' (R is an unspecified purine; Y is an unspecified pyrimidine; N is any nucleotide). Studies have found a correlation between high levels of the NF- κ B1 subunit in synovial tissue and joints with the greatest amount of destruction (Srivastava and Ramana 2008).

The activation of NF- κ B may be stimulated by numerous extracellular stimuli, including TNF- α , IL-1, lipopolysaccharide (LPS), platelet-derived growth factor (PDGF), oxidative stress and viral products (Miyagkov *et al.* 1998). There are three types of NF- κ B activation pathways. The first is activated by proinflammatory cytokines or infection and is termed the classical or canonical pathway category. The classical signal transduction cascade leads to activation of the I κ B kinase (IKK) complex and degradation of the NF- κ B inhibitory protein, I κ B. This pathway depends primarily on the IKK β subunit of the IKK complex and principally targets p50:RelA and p50:c-Rel heterodimers. The classical pathway is necessary for the innate immune response and for control of apoptosis. The alternative or non-canonical NF- κ B pathway plays an important role in adaptive immunity and in the development of secondary lymphoid organs (Lee *et al.* 2007). This

pathway is stimulated by specific members of the TNF cytokine family, such as lymphotoxin β or CD40 ligand, via activation of the IKK α subunit of the IKK complex. This leads to the processing of p100 precursor proteins and activation of p52:RelB heterodimers. The third type of pathway is known as atypical since it induces I κ B degradation independently of the IKK complex. It is stimulated by UV which causes damage to DNA (Lee *et al.* 2007).

The TNF- α -induced NF- κ B pathway is perhaps the most widely studied NF- κ B activation pathway, followed by IL-1- and LPS-induced activation (see Fig.1.2). These are termed classical NF- κ B activation pathways. TNF- α binds to its receptor, TNF receptor 1 (TNF-R1 or p55) or TNF-R2 (p75) and initiates the signaling cascade. TRAF2 and receptor interacting protein (RIP)-1 are recruited to the receptor by binding to an adaptor protein, TRADD (TNF-receptor-associated death domain) (Beyaert *et al.* 2000). The anti-apoptotic proteins cIAP1 and cIAP2 also bind, forming a receptor-associated complex (Harhaj and Dixit 2011). Fas-associated death domain (FADD) may be recruited to TRADD, leading to activation of the caspase cascade and apoptosis (Beyaert *et al.* 2000). It is thought that baculoviral IAP repeat containing (cIAP)1 and cIAP2 act as direct ubiquitin ligases for the polyubiquitination (the addition of ubiquitin chains) of RIP1. This leads to recruitment of the transforming growth factor receptor- β -activated kinase (TAK)1 complex, made up of TAK1 and the regulatory subunits TAK1 binding protein (TAB)1 and TAB2. Activation of TAK1 results in phosphorylation of the IKK β subunit of the IKK complex and activation of this complex (Harhaj and Dixit 2011). The IKK complex consists of two catalytic subunits, IKK α and IKK β , and a regulatory subunit, IKK γ , also known as NEMO (NF- κ B essential modulator). The NF- κ B inhibitory protein, I κ B, binds the nuclear localization sequence of NF- κ B, retaining it in the cytoplasm (Hayden and Ghosh 2004). However, when activated, the IKK complex phosphorylates I κ B, leading to its ubiquitination and its subsequent proteolytic degradation by the proteasome. This leaves NF- κ B free to translocate into the nucleus and induce the expression of target genes (Srivastava and Ramana 2008).

IL-1 and bacterial LPS bind to their receptors, the IL-1 receptor/IL1-RAcP complex and TLR4 respectively, followed by the recruitment of MyD88, an adapter protein, IL-1 receptor associated kinase (IRAK)1, IRAK4 and TRAF6, forming a receptor-associated complex. TRAF6 is then activated and polyubiquitinated, resulting in the recruitment of the TAB1-TAB2-TAK1 complex where the pathway converges with the TNF- α activation pathway (Beyaert *et al.* 2000; Harhaj and Dixit 2011).

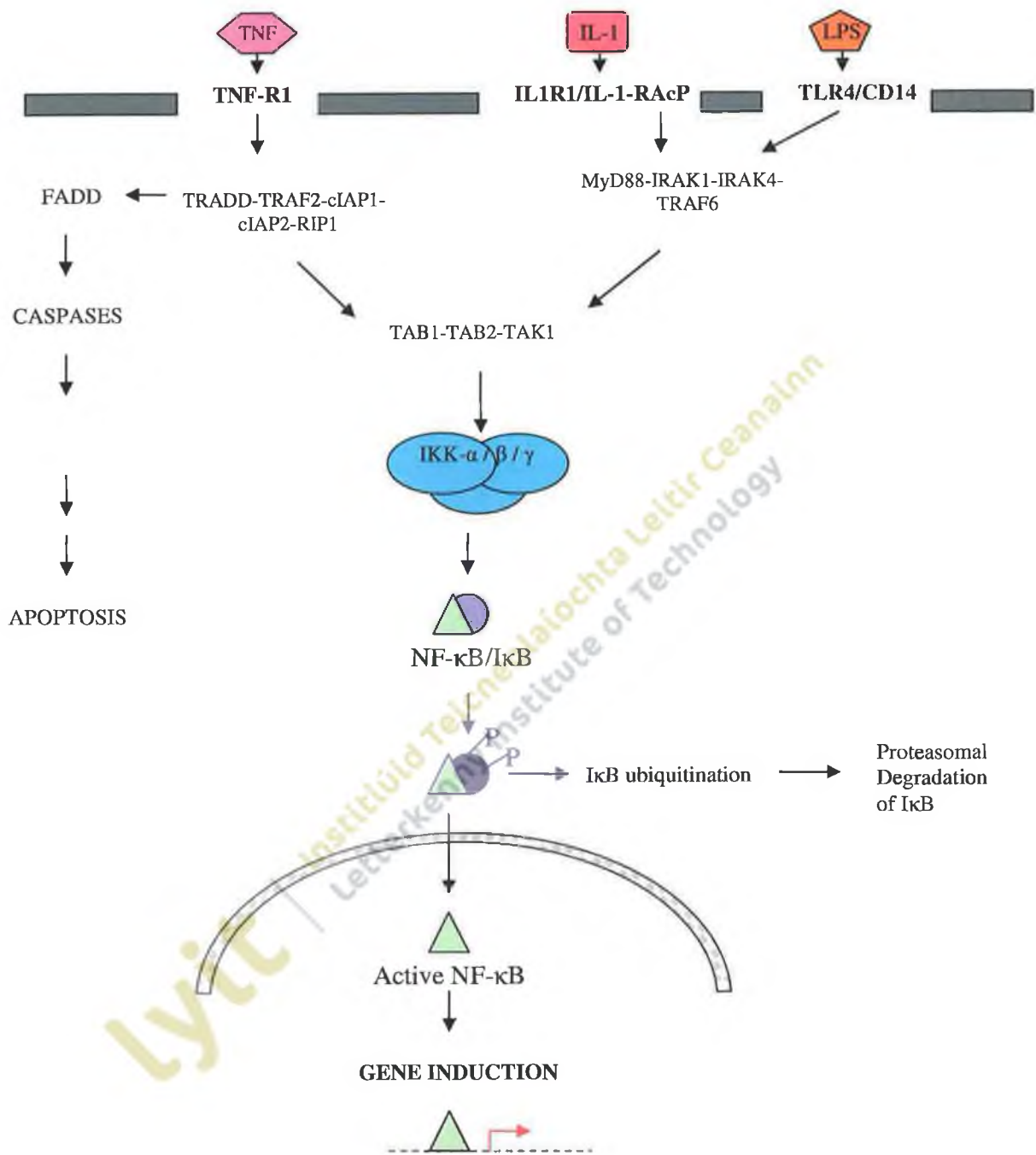


Fig.1.2 Schematic representation of activation of the NF- κ B pathways by the inflammatory mediators TNF, IL-1 and LPS (Adapted from Beyaert *et al.* 2000; Harhaj and Dixit 2011).

NF- κ B is a crucial element in the body's response to pathogens and stress. It initiates the transcription of receptors for immune recognition of invaders, antigen presentation proteins, cytokines, chemokines, receptors for neutrophil adhesion and migration, as well as apoptotic and cell cycle control genes (Yamamoto and Gaynor 2001). Consequently, inhibition of NF- κ B activation as a means of therapy for inflammatory diseases can lead to serious implications, primarily infection, however malignancy and congestive heart failure have also been linked to NF- κ B inhibition (Lin *et al.* 2008). Maintenance of appropriate levels of NF- κ B activity is therefore necessary for normal cellular processes but suppression of prolonged NF- κ B activation or inhibition by certain stimuli may be beneficial in treating autoimmune diseases (Yamamoto and Gaynor 2001).

1.3 A20

A20 (also known as tumour necrosis factor alpha-induced protein 3, TNFAIP3) was first discovered as a TNF- α -induced early response gene in primary human umbilical vein endothelial cells (Dixit *et al.* 1990). This gene is induced in many cell types and by a wide variety of stimuli, including TNF- α , IL-1, CD40 (a B cell surface receptor), LPS and the Epstein-Barr virus oncoprotein latent membrane protein (LMP)1, a member of the TNF receptor superfamily (Fries *et al.* 1996). These factors stimulate the activation of NF- κ B and it is through this transcription factor that A20 gene expression is induced (Beyaert *et al.* 2000). A20 is a cytoplasmic protein that consists of 790 amino acids and is 90kDa in size. The structure of A20 is shown in Fig. 1.3. The C-terminal end contains seven zinc fingers, six of which consist of a Cys-X4-Cys-X11-Cys-X2-Cys motif and one consisting of a Cys-X2-Cys-X11-Cys-X2-Cys motif. The N-terminal region of A20 consists of an ovarian tumour (OTU) domain (Beyaert *et al.* 2000; Heyninck and Beyaert 2005). It is thought that A20 may be an important protein in several cell types. A20 expression has essential roles in the function of the lymphoid system and may be involved in the development of skin epidermis and hair follicles, although not in the maintenance of normal skin architecture (Beyaert *et al.* 2000).

Several studies have shown that A20 is a potent inhibitor of NF- κ B activation, through a negative feedback mechanism, in some cell types. NF- κ B induces the expression of A20, which then has the ability to suppress the activation of this transcription factor (Jaattela *et al.* 1996). Studies suggest that A20 may down-regulate the activation of NF- κ B by diverse stimuli (Song *et al.* 1996). Inhibition of NF- κ B often renders cells sensitive to TNF- α -induced apoptosis. However, A20 has also been shown to prevent TNF- α -mediated apoptosis in certain cell types, such as primary endothelial cells (Zetoune *et al.* 2001). A20-deficient mice, generated by gene targeting, developed severe multi-organ inflammation and died prematurely. Severe inflammation and tissue damage were present in the liver, kidneys, intestines, joints and bone marrow of these 3- to 6-week old mice. Thickened epidermal and dermal layers of skin were observed. In addition, higher numbers of activated lymphocytes, granulocytes and macrophages were found in the spleens and livers of these mice. Furthermore, mice injected with low doses of TNF- α died within 2 hours (Lee *et al.* 2000). Cells without A20 cannot regulate TNF- α -induced NF- κ B activation and are more susceptible to TNF- α -induced apoptosis (Lee *et al.* 2000). It has been suggested that A20 plays a protective role since its expression by endothelial cells enhances the survival of transplanted organs and prevents the development of transplant arteriosclerosis (Hancock *et al.* 1998).

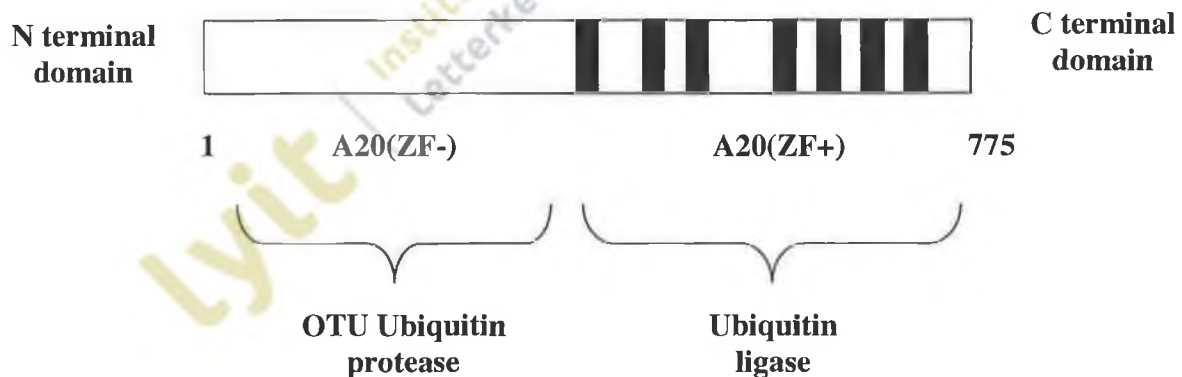


Fig. 1.3 Structure of A20 showing the N terminal ovarian tumour (OTU) domain with ubiquitin protease activity and the C terminal zinc finger domain with ubiquitin ligase activity for the regulation of NF- κ B activation (adapted from Beyaert *et al.* 2000; Evans 2005).

Constitutive expression of A20 has been observed in thymocytes, resting peripheral T cells, the endothelial cell line EaHy and in the differentiated monocyte cell line THP-1. In most cells however, A20 expression is induced, that is, only expressed in stimulated cells (Beyaert *et al.* 2000; Ning and Pagano 2010).

Studies have shown that A20 can interact with different components within NF- κ B activation pathways (such as TRAF2 and IKK γ) and also with proteins termed A20-binding inhibitor of NF- κ B activation (ABIN)-1 and ABIN-2. A study by Song *et al.* in 1996 demonstrated that A20 interacts with the TRAF1/TRAF2 complex which associates with the cytoplasmic domain of TNF receptors. This interaction is through binding of the N-terminal region of A20 with the C-terminal TRAF domain of TRAF1 and TRAF2. They also demonstrated that inhibition of NF- κ B is mediated through the C-terminal zinc finger domain of A20. They proposed that A20 consists of two functionally distinct domains; the N-terminal domain which functions to recruit A20 to the TRAF1/TRAF2 complex and the C-terminal domain which displays the NF- κ B inhibitory activity (Song *et al.* 1996). The N-terminal region of A20 has also been shown to bind to TRAF6, which is involved in both IL-1 and LPS activation of NF- κ B (Heyninck and Beyaert 1999). The C-terminal zinc finger domain of A20 has been shown to bind to IKK γ which is thought to transfer the upstream activator signal to the catalytic subunits, IKK α and IKK β . This may be significant in the inhibitory effects of A20 on NF- κ B activation by halting activation of the IKK complex, thereby terminating the NF- κ B activation pathway (Beyaert *et al.* 2000). However, while a study by Zetoune *et al.* (2001) also demonstrated that A20 binds and interacts with the IKK complex, in their experiments they found that A20 bound to the IKK α component rather than IKK γ , but actually inhibits the IKK β component of the complex, thus disabling the NF- κ B pathway. They suggested that the studies showing A20 bound to IKK γ were, in fact, showing A20 hybridized to endogenous IKK α , which was still bound to IKK γ (Zetoune *et al.* 2001).

Recently, studies have illustrated that A20 exhibits dual ubiquitin-editing functions in the inhibition of NF- κ B. Ubiquitin is a small conserved polypeptide that can be attached covalently to a lysine residue of the target protein by ubiquitin ligase. Several ubiquitin molecules may attach to the initial ubiquitin on the substrate, forming polyubiquitin chains (Heyninck and Beyaert 2005). Ubiquitin contains seven lysine residues and polyubiquitin chains are primarily linked through Lys⁴⁸ or Lys⁶³. Lys⁴⁸-linked polyubiquitination (sometimes termed K⁴⁸

polyubiquitination) usually targets proteins for degradation by proteasomal enzymes. Whereas Lys⁶³-linked polyubiquitination (sometimes termed K⁶³ polyubiquitination) regulates protein kinase activity and protein trafficking. De-ubiquitinating enzymes, which are cysteine hydrolases, have the ability to reverse ubiquitination by cleaving polyubiquitin chains. Ubiquitination plays an integral part of the TNF- α -induced NF- κ B activation pathway. The NF- κ B-inhibitory protein, I κ B, is targeted for degradation by the ligation of ubiquitin, enabling the active NF- κ B to translocate to the nucleus. In addition, when the TNF- α receptor is activated, TNF-R1, TRAF2, RIP1, IKK λ and IKK β are also ubiquitinated (Heyninck and Beyaert 2005). A ubiquitinated form of RIP1 is recruited to the TNF-R1 complex following activation by TNF- α . A20 has been shown to modify the ubiquitination profile of RIP1, as shown in Fig. 1.4. This occurs in two steps: firstly, de-ubiquitination of its Lys⁶³-linked ubiquitin chains mediated by A20's N-terminal domain, followed by Lys⁴⁸-linked polyubiquitination of RIP, mediated by A20's C-terminal domain. This marks RIP1 for degradation, preventing IKK activation and halting the NF- κ B activation cascade (Heyninck and Beyaert 2005; Harhaj and Dixit 2011). A20 has also been shown to de-ubiquitinate TRAF6 in LPS-induced NF- κ B activation in the same manner in which it acts on RIP1, in addition to de-ubiquitinating IKK γ , suggesting that the ubiquitin-modifying properties of A20 may act at different levels within the NF- κ B activation pathway (Willaert *et al.* 2006; Harhaj and Dixit 2011).

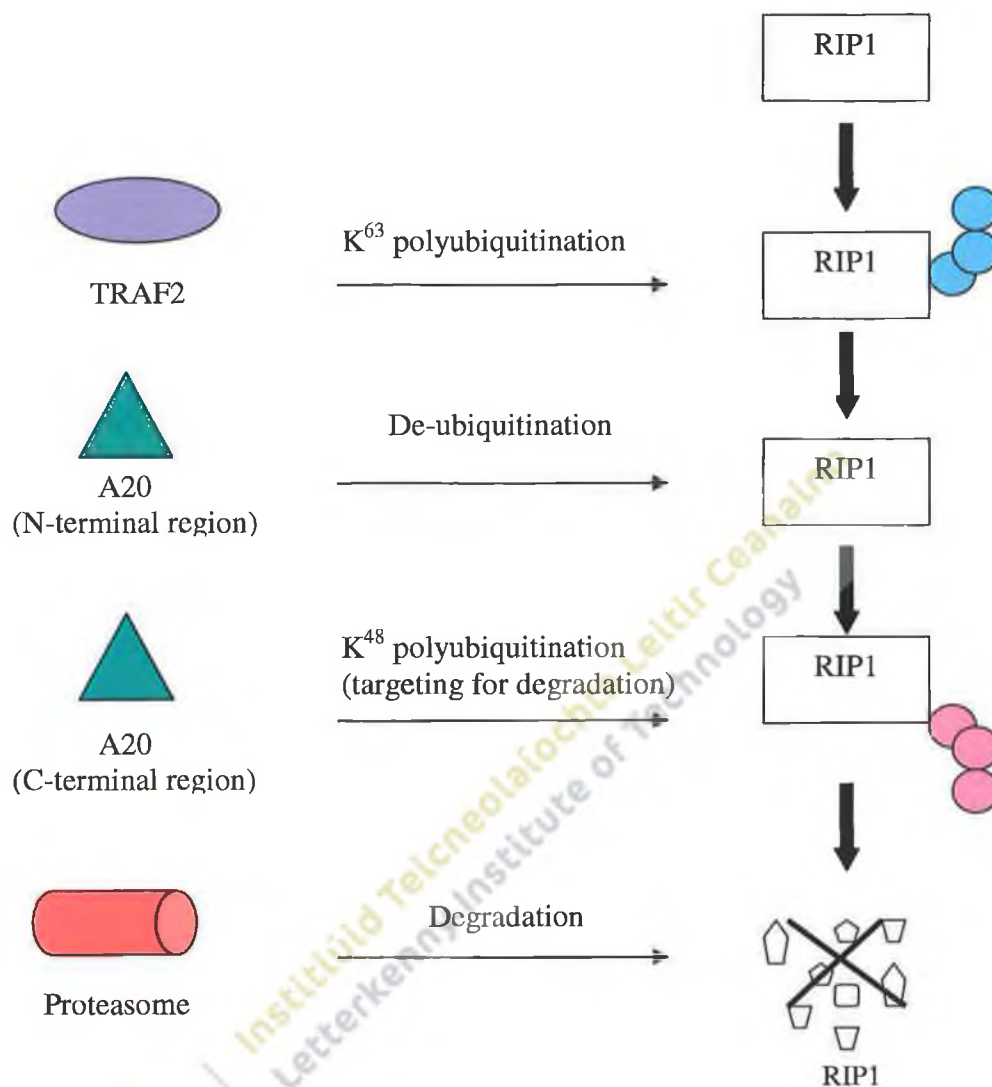


Fig 1.4 Schematic representation of the ubiquitin-editing functions of A20 which alters RIP1. This is a possible mechanism for NF- κ B inhibition by A20.

Recent studies have revealed that A20 is regulated by Tax1-binding protein 1 (TAX1BP1). This protein is necessary for A20 de-ubiquitination of RIP1 and inhibition of TNF- α -, IL-1- and LPS-induced activation of NF- κ B. In addition, it has been discovered that A20 forms a complex with TAX1BP1 (Shembade *et al.* 2007). This complex, termed the A20 ubiquitin-editing complex, also contains the proteins ring finger protein (RNF)11 and the E3 ligase Itch, both of which have been shown to be essential for A20 to down-regulate NF- κ B signaling pathways in mouse fibroblasts (Shembade *et al.* 2009). This ubiquitin-editing complex may also contain other proteins including ABIN-1 (Harhaj and Dixit 2011). It is thought that TAX1BP1 may act as an

adaptor protein, bringing A20 into contact with RIP1 and TRAF6 (Harhaj and Dixit 2011). However, the function of TAX1BP1 in aiding A20 in the inhibition of inflammation may be tissue specific since TAX1BP1-knocked down mice only developed inflammatory cardiac valvulitis (Iha *et al.* 2008) compared to A20-deficient mice which suffered widespread inflammation (Lee *et al.* 2000).

TNF- α has been shown to induce apoptosis by binding to TNFR1, followed by recruitment of the death domain signaling adaptors TRADD and RIP1 to the TNF receptor. TRADD and RIP1 then associate with TRAF2 and FADD (FAS-associated death domain protein), leading to the activation of caspase 8 and apoptosis. However, in Jurkat T cells, it has been found that A20 inhibits TNF- α -induced apoptosis by preventing the recruitment of TRADD and RIP1 to TNFR1, thereby blocking the TNF- α -induced apoptosis signaling pathway. In addition, this would impair the NF- κ B activation pathway since these molecules form an essential part of the NF- κ B signaling cascade also, although this has not been proven (He and Ting 2002). This could explain how A20 has the ability to inhibit NF- κ B activation, whilst not rendering the cell susceptible to TNF- α -induced apoptosis.

Furthermore, it has been observed that overexpression of the IKK-activating kinase, NF- κ B-inducing kinase (NIK), overrides the inhibition properties of A20, indicating that A20 may restrict the accessibility of the IKK complex to its activating kinases. Studies involving the overexpression of A20 have also shown that it can inhibit the phosphorylation of I κ B in response to TNF- α (Beyaert *et al.* 2000). These may represent additional mechanisms by which A20 exerts its inhibitory functions. A20 is also able to inhibit the activation of proinflammatory transcription factors activator protein (AP)-1, interferon regulatory factor (IRF)3 and IRF7 (O'Reilly and Moynagh 2003; Ning and Pagano 2010). A20 has been shown to regulate IRF7 ubiquitination and, therefore, its activation (Ning and Pagano 2010).

Genome-wide association studies of RA have led to a hypothesis that polymorphisms in the A20 gene and in the 6q23 chromosome region may be associated with an increased risk of developing the disease. Indeed, initial studies appear to be consistent with this hypothesis (Dieguez-Gonzalez *et al.* 2009). In addition, polymorphisms in A20 and the 6q23 region have previously been demonstrated to be associated with systemic lupus erythematosus. These studies indicate that A20 has a role in autoimmune diseases and may be critical in regulating such diseases, since

a defective A20 gene may not have the ability to suppress the activation of NF- κ B and AP1, leading to uncontrolled inflammatory signals (Dieguez-Gonzalez *et al.* 2009).

1.4 ABIN-1

Yeast-two hybrid screening with A20 demonstrated binding of the C terminal domain of A20 with two novel proteins, termed A20-binding inhibitor of NF- κ B activation (ABIN)-1, also known as human immunodeficiency virus Nef-associated factor 1 (Naf-1), and ABIN-2. Upon overexpression, these proteins have the ability to inhibit the activation of NF- κ B and it is thought that the inhibitory effects of A20 may be mediated by these proteins. ABIN-1 can down-regulate NF- κ B activation in response to TNF- α and IL-1 (Heyninck *et al.* 2003). ABIN-1 has been shown to be a TNF- α responsive gene in primary synoviocytes and elevated levels of ABIN-1 have been found in tissue from patients with inflammatory arthritis (Gallagher *et al.* 2003).

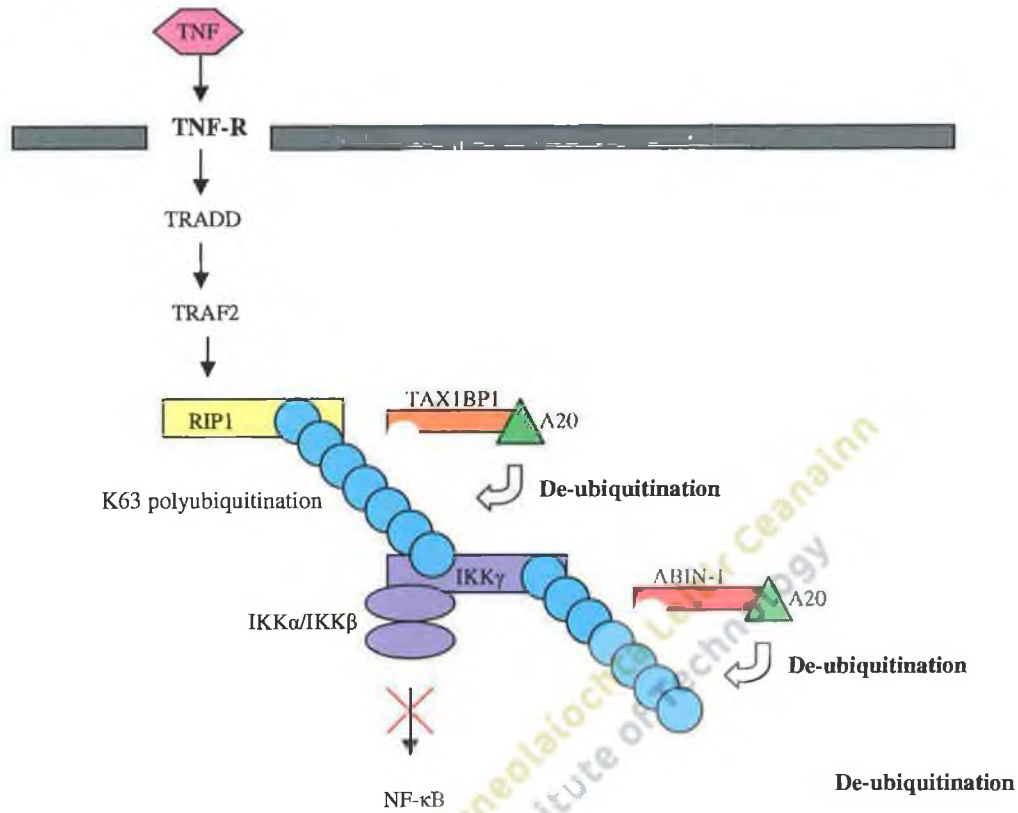
The ABIN-1 gene has two alternatively spliced isoforms, Naf-1 α and Naf-1 β , differing only in their C-terminal amino acids. Naf-1 α is approximately 2800 nucleotides in length with an open reading frame consisting of 1941 nucleotides, which encodes a 72kDa protein. Naf-1 β is approximately 2600 base pairs (bp) long and has an open reading frame of 1781 bp, encoding a 68kDa protein. Both proteins contain a leucine zipper structure consisting of an amphipathic helix with four consecutive repeats of a leucine, followed by six random amino acid residues (Beyaert *et al.* 2000).

A study showing that A20 carries out de-ubiquitination of IKK γ as a means of inhibiting NF- κ B, also provided evidence that ABIN-1 and A20 co-operate at the level of IKK γ to hinder the activation of this transcription factor. They demonstrated that there was a reduction in A20's ability to de-ubiquitinate IKK γ when the ABIN-1 gene was silenced. Conversely, there was a reduction in ABIN-1's ability to modulate NF- κ B when A20 was silenced. They proposed that ABIN-1 functionally connects A20 and IKK γ , where A20 can then alter the ubiquitination profile of IKK γ , negatively regulating the activation of NF- κ B (Mauro *et al.* 2006; Harhaj and Dixit 2011). Further evidence in support of this hypothesis was provided when a ubiquitin-binding domain (UBD) was identified within ABIN-1 with which it can then interact with IKK γ . In addition, TAX1BP1 also contains a UBD and was shown to recruit A20 to RIP1, where it can

carry out its ubiquitin-editing functions (Verstrepen *et al.* 2009). Figure 1.5A illustrates this model of NF- κ B inhibition. ABIN-1 may form part of the A20 ubiquitin-editing complex, along with TAX1BP1 and others (Harhaj and Dixit 2011). There may be some functional redundancy exhibited by these A20-adaptor proteins and their functions may be cell-specific (Verstrepen *et al.* 2009).

ABIN-1 and ABIN-2 have been shown to contain a short homologous region termed the ABIN homology domain 2 (AHD2) in the C-terminal domain. This region is also present in the regulatory subunit IKK γ . Furthermore, the UBD of ABIN-1 was found to overlap with this AHD2 region. Studies on AHD2 in ABIN-1 have suggested that ABIN-1 could compete with IKK γ for an upstream activator or compete with another ubiquitin-binding protein for binding to polyubiquitinated IKK γ , thereby disrupting the NF- κ B activation cascade (Fig. 1.5B). Site-specific mutagenesis of the AHD2 domain illustrated its importance in the inhibition of NF- κ B, since without this region, ABIN-1 could no longer impede its activation. However, attenuation of NF- κ B by A20 was unaffected by the mutagenesis of ABIN-1, indicating that A20 may not require binding to ABIN-1 for its inhibiting function. This may be due to functional redundancy of ABIN-1 with other proteins such as ABIN-2 (Heyninck *et al.* 2003; Verstrepen *et al.* 2009).

(A) Adaptor model



(B) Competition model

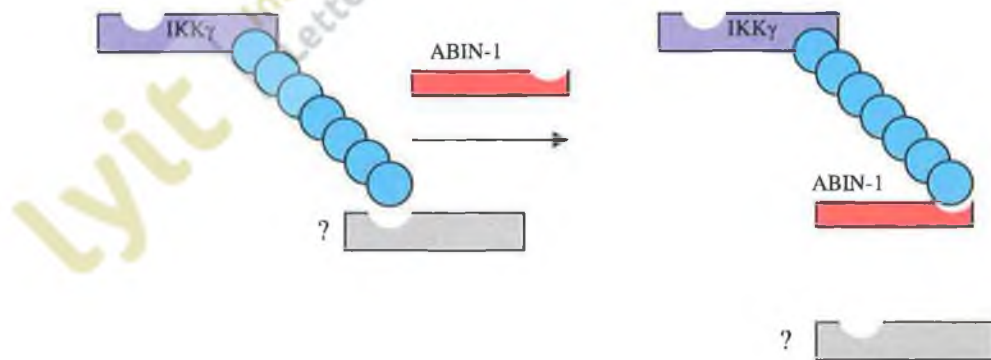


Fig 1.5 Proposed models for the mechanism by which ABIN-1 inhibits NF- κ B activation.

(A) Adaptor model: ABIN-1 and TAX1BP1 recruit A20 to K⁶³ polyubiquitinated RIP1 or IKK γ where A20 can alter the ubiquitin profile of these proteins. (B) Competition model: ABIN-1 competes with another ubiquitin-binding protein for binding to IKK γ , preventing its activation (Adapted from Verstrepn *et al.* 2009).

It has been demonstrated that A20 inhibits the immune response to viral infection. A recent study has revealed that ABIN-1 forms a complex with A20 and TAX1BP1 via its UBD to inhibit antiviral signaling. Recruitment of ABIN-1 was necessary for inhibition of IFN- β by A20 and TAX1BP1 in response to viral infection (Gao *et al.* 2011).

Overexpression of ABIN-1 in epidermal growth factor (EGF) receptor overexpressing tumour cell lines inhibits constitutive and EGF-induced NF- κ B activation, resulting in a decrease in tumour cell proliferation (Verstrepen *et al.* 2009). Furthermore, studies have shown that ABIN-1 can bind to the p100 and p105 NF- κ B subunits. However, the significance of this binding has not yet been established (Verstrepen *et al.* 2009).

ABIN-1, in addition to A20, has anti-apoptotic properties. ABIN-1 deficient mice die during embryogenesis due to fetal liver apoptosis and anemia. The fact that A20 deficient mice do not appear to have any defects during embryonic development, but die after birth with cachexia and severe inflammation (Lee *et al.* 2000), reveals an important A20-independent role of ABIN-1 during fetal development. ABIN-1 suppresses TNF- α -induced apoptosis by preventing the recruitment of caspase-8 to FADD and halting the signaling cascade (Verstrepen *et al.* 2009).

1.5 ABIN-2

ABIN-2 (also known as FLIP1 or TNIP2, TNFAIP3-interacting protein 2) is a cytosolic protein which has been found to inhibit TNF- α -, IL-1- and tetradecanoylphorbol acetate (TPA)-induced NF- κ B activation. Murine ABIN-2 mRNA is ubiquitously expressed in all tissues, with maximum expression in the kidneys. This mRNA translates into a 50kDa protein, displaying 76 % homology with the human ABIN-2 protein. Complete murine ABIN-2 cDNA consists of 1967 nucleotides, with an open reading frame of 1290 bp (Van Huffel *et al.* 2001). The human ABIN-2 gene is found on chromosome 4p16.3 and has six exons (Verstrepen *et al.* 2009). The human protein is made up of 429 amino acids and has a molecular weight of 47 kDa (Liu *et al.* 2003). Chien *et al.* (2003) discovered that, in both yeast and mammalian cells, ABIN-2 has the ability to enter the nucleus and may act as a transcriptional co-activator. In mammalian cells, this transactivating activity is only carried out by the C-terminal fragment. The N-terminal region of ABIN-2 acts as a regulatory domain, retaining it in the cytoplasm (Chien *et al.* 2003). A study by

Papoutsopoulou *et al.* (2006) demonstrated that ABIN-2 is necessary for the positive regulation of the Erk MAP kinase pathway in the innate immune response by stabilizing the TPL-2 MEK kinase, which activates this pathway.

Liu *et al.* (2004) proposed a mechanism by which ABIN-2 regulates NF- κ B activation and apoptosis, similar to that described for ABIN-1 (see Fig. 1.6). In a previous study, they demonstrated that ABIN-2 binds to IKK λ specifically, and forms a stable complex. They went on to show that ABIN-2 and RIP1 share a similar region of approximately 50 amino acids and termed this region the core motif for binding (CMB). RIP1 is a vital element involved in the TNF- α -induced NF- κ B activation cascade, as described previously, and it has been shown that RIP1 associates with IKK λ in RIP1-induced NF- κ B activation. In the absence of ABIN-2, RIP1 binds to IKK λ , activating NF- κ B which induces the expression of anti-apoptotic genes. Liu *et al.* (2004) demonstrated that ABIN-2 competes with RIP1 for binding with IKK λ , thus preventing activation of the IKK complex which is required for the phosphorylation of I κ B, leading to termination of the NF- κ B pathway. Furthermore, they illustrated that the cells in which ABIN-2 down-regulated NF- κ B underwent apoptosis in response to RIP1 (Liu *et al.* 2004).

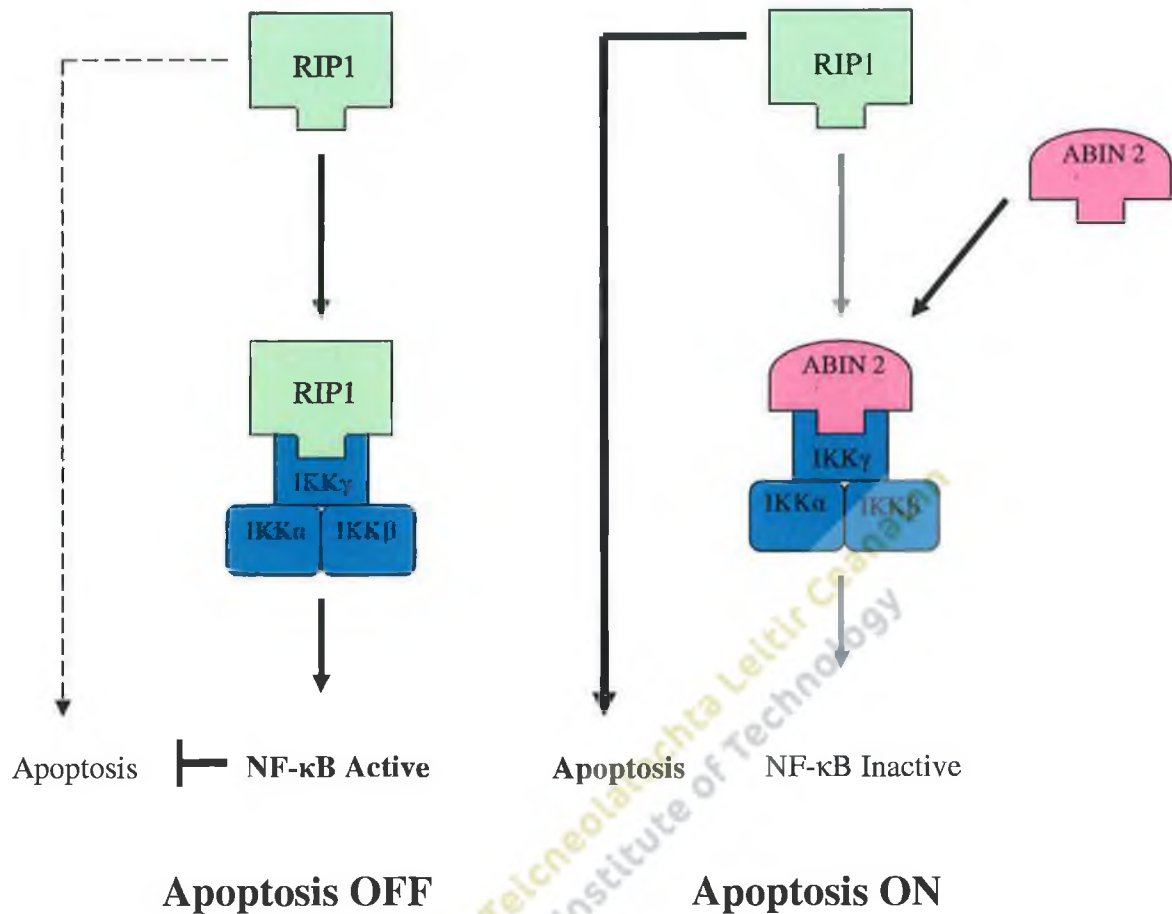


Fig. 1.6 Proposed mechanism for ABIN-2 inhibition of NF- κ B, which then sensitizes the cell to RIP1-induced apoptosis (Adapted from Liu *et al.* 2004).

ABIN-2 deficient mice do not exhibit any differences in NF- κ B signaling, but ABIN-1 may be compensating for the loss of ABIN-2 activity (Verstrepen *et al.* 2009).

An additional A20-binding protein with the capacity to inhibit NF- κ B was discovered in 2007 and was termed ABIN-3 (also known as LIND, *Listeria* INDuced, since it was found to be induced by *Listeria* infection in human mononuclear phagocytes). ABIN-3 shares sequence homology to ABIN-1 and ABIN-2, although it relates more closely to ABIN-1. Experiments demonstrated that ABIN-3 attenuates the LPS-induced NF- κ B activation pathway at a level downstream of TRAF6 but upstream of IKK β . Furthermore, it was also established that ABIN-3 does not compete with ABIN-1 or ABIN-2 for A20-binding (Wullaert *et al.* 2007).

1.6 Cezanne

Cezanne (cellular zinc finger anti-NF- κ B) was first discovered in 2004 and exhibits sequence similarity with the N-terminal region of A20. The structure of Cezanne is given in Fig. 1.7 below. Amino acids 160-416 of Cezanne display 39 % homology with A20. This region was termed TRAFB (TRAF binding), since it corresponds to the TRAF binding domain of A20. A putative nuclear localization signal is located within amino acids 497-513. Cezanne also has one A20-like zinc finger in the C-terminal end. Sequence alignment of A20 and Cezanne identified conserved hydrophobic and basic residues which indicate that both have similar structural features (Evans *et al.* 2001).

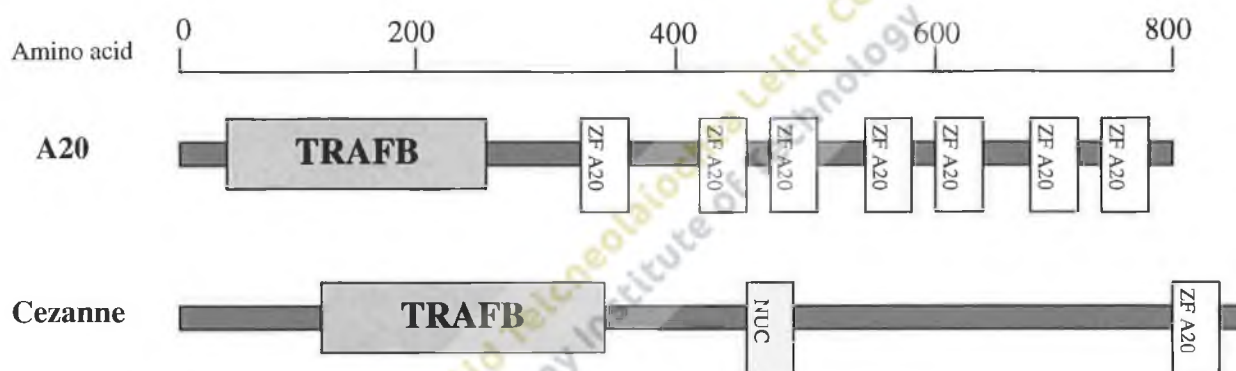


Fig. 1.7 Structures of A20 and Cezanne depicting TRAFB domains, ZF A20 (A20-like zinc finger) and NUC (putative nuclear localization sequence) (adapted from Evans *et al.* 2001).

Cezanne transcripts are expressed in a wide variety of murine and human tissues, particularly in the kidney, heart and fetal liver of both species (Evans *et al.* 2001). A study in 2008 demonstrated that in human embryonic kidney epithelial (HEK 293) cells, Cezanne is induced in response to TNF- α , suggesting that Cezanne may be involved in regulating cellular responses to inflammatory signals (Enesa *et al.* 2008).

Studies using green fluorescent protein (GFP) fusion proteins in live cells revealed that A20 was positioned in the cytoplasm of HEK 293 and fibroblast (NIH3T3) cell lines. In endothelial (EaHy) cells, A20 was observed in the nucleus in addition to the cytoplasm. Cezanne was found scattered throughout the cytoplasm of epithelial and fibroblast cells and not detected within the

nucleus of these cells. In a proportion of cases, Cezanne was detected in the nucleus of endothelial cells, suggesting that the putative nuclear localization sequence within Cezanne is functional but under stringent control (Evans *et al.* 2001).

The similarity of Cezanne to A20 prompted the analysis of Cezanne's ability to inhibit NF- κ B activation. This was tested in HEK 293 and EaHy cells. The EaHy cells produce low constant levels of A20 and Cezanne, whereas in HEK 293 cells, these proteins are induced. In both cell types, Cezanne was able to down-regulate TNF- α -induced NF- κ B activation in a dose-dependant manner. However, compared to A20, Cezanne was less efficient in inhibiting this transcription factor. Expression of the C-terminal, zinc-finger domain of Cezanne, unlike A20, was unable to inhibit NF- κ B on its own. The full length protein was required. IL-1 α -induced NF- κ B activation was also shown to be down-regulated by Cezanne, with similar efficiency as the inhibition of TNF- α stimulated NF- κ B activation (Evans *et al.* 2001).

A more recent study has demonstrated that Cezanne inhibits TNF- α -induced NF- κ B activation at the level of the IKK complex or upstream from it. This study also found that Cezanne possesses de-ubiquitinating activity and that this activity is necessary for the suppression of NF- κ B (Enesa *et al.* 2008). Furthermore, it has been demonstrated that Cezanne is recruited to the TNFR and it suppresses RIP1 ubiquitination, thus down-regulating activation of the IKK complex and inhibiting NF- κ B (Enesa *et al.* 2008; Harhaj and Dixit 2011).

A20 has been shown to interact with a TRAF1/TRAF2 complex and with TRAF6 in NF- κ B activation pathways induced by TNF- α and IL-1, respectively. Tests were carried out on Cezanne to determine whether it could bind to TRAF6, since it contains the same TRAF binding domain (TRAFB) as A20. Indeed, it was found that Cezanne co-immunoprecipitated with TRAF6 in HEK 293 cells and was not immunoprecipitated without TRAF6. This indicates that Cezanne binds specifically to TRAF6, although this binding is weaker in comparison to A20. It is thought that binding to TRAF molecules recruits A20 and Cezanne to the NF- κ B signaling cascade where they can inhibit the process. This would explain why the C-terminal domains of A20 and Cezanne, without TRAFB, is not sufficient to control NF- κ B activation (Evans *et al.* 2001; Song *et al.* 1996).

It has recently been found that the cell survival gene, DJ-1 (also known as Park7), which plays a role in chemotherapy resistance and is associated with poor prognosis, binds to Cezanne and inhibits its de-ubiquitinating activity, leading to increased NF- κ B activation and cell survival. This indicates that Cezanne may be an important regulator of tumour progression and metastasis (McNally *et al.* 2011). It may be that DJ-1 plays a similar role in suppressing the activity of Cezanne in RA, thus leading to enhanced NF- κ B activation and the expression of proinflammatory and anti-apoptotic genes.

A20, ABIN-1, ABIN-2 and Cezanne have all been shown to inhibit the activation of NF- κ B in response to inflammatory stimuli (summarised in Fig. 1.8) and thus are potential targets as therapeutic agents in the resolution of RA. Indeed, adenovirus expression of ABIN-1 in the lungs of mice with allergen-induced asthma led to a substantial decrease in allergen-induced NF- κ B activation (Versteppen *et al.* 2009). Furthermore, lentiviral-mediated overexpression of A20 in endothelial progenitor cells (EPCs) led to the generation of cells that are less sensitive to inflammatory stimuli (Liu *et al.* 2010). Therefore, a means to regulate these proteins at a cellular level may prove beneficial in the control of inflammatory diseases such as RA.

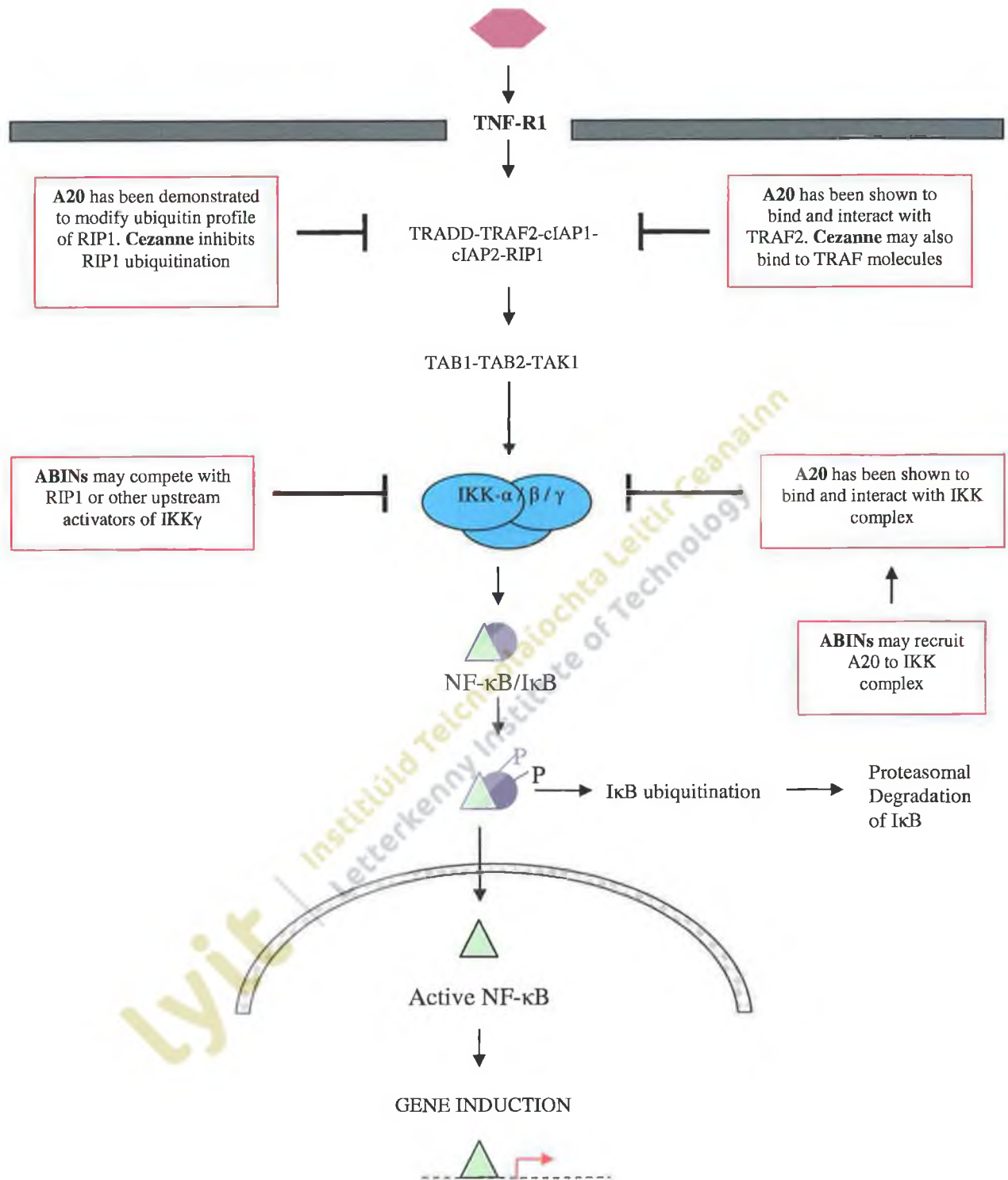


Fig. 1.8 Proposed mechanisms by which A20, ABIN-1, ABIN-2 and Cezanne inhibit TNF- α -induced NF- κ B activation (Beyaert *et al.* 2000; Enesa *et al.* 2008; Evans *et al.* 2001; Harhaj and Dixit 2011; Heyninck and Beyaert 2005; Liu *et al.* 2004; Mauro *et al.* 2006; Song *et al.* 1996; Verstrepren *et al.* 2009; Zetoune *et al.* 2001).

1.7 NR4A subfamily of nuclear orphan receptors

The nuclear receptor-4A (NR4A) or nerve growth factor-induced B factor (NGFI-B) subfamily is part of a large superfamily of nuclear receptors which consists of structurally related, ligand-activated transcription factors, involved in many biological processes. Lipophilic hormones can cross the cell membrane and activate these nuclear receptors to regulate gene expression (Ohkura *et al.* 1998). There are three classes of nuclear receptors: a) the classic group of steroid- and thyroid-hormone receptors which includes glucocorticoid receptors; b) the orphan nuclear receptors, including the NR4A subfamily, for which ligands have not yet been identified; and c) the adopted orphan receptors for which ligands have recently been found (Wang and Wan 2008). The NR4A subfamily includes three members, NR4A1 (NUR77), NR4A2 (nuclear receptor related 1, NURR1) and NR4A3 (neuron derived orphan receptor-1, NOR-1). These receptors exhibit extraordinary evolutionary conservation, having counterparts in *Caenorhabditis elegans* and *Drosophila*, illustrating their biological significance (Ohkura *et al.* 1998).

The structure of NR4A nuclear receptors is shown in Fig. 1.9. It consists of an N-terminal transactivation domain, containing activation function-1 (AF-1) which binds co-activators, a central DNA-binding domain (DBD) and a C-terminal domain containing activation function-2 (AF-2). The DBD is highly conserved among the subfamily members. It consists of two zinc fingers that bind as a monomer to the DNA consensus sequence, AAAGGTCA, known as the NGFI-B responsive element (NBRE) (Bonta *et al.* 2007). The DBDs within NURR1, NUR77 and NOR-1 are over 90 % homologous and are more closely related to each other than to other nuclear receptors (Ohkura *et al.* 1998). The NR4A subfamily may also form homodimers or heterodimers and bind to the palindromic Nur-responsive element (NurRE), TGATATTTX₆AAAGTCCA. In addition, both NURR1 and NUR77 can form heterodimers with the 9-*cis* retinoic acid receptor (RXR) and bind to a motif termed DR5, a retinoic acid response element made up of direct repeats separated by five nucleotides. Heterodimerization of RXR with NURR1 or NUR77 leads to efficient activation in response to RXR ligands (Perlmann and Jansson 1995; Maxwell and Muscat 2005). The ligand-binding domain (LBD) of NR4A members differs from other nuclear receptors in that it contains hydrophobic and aromatic amino acid side chains, meaning these receptors may not have functional ligands. Instead, their primary mode of regulation may be via expression regulation, post-translational modification, transrepression or co-activator and co-repressor recruitment (Bonta *et al.* 2007). The C-terminal

domain of the NR4A receptors shares 20-30 % homology with the LBD of nuclear receptors with known ligands and therefore contain the structural features of ligand-activated transcription factors and are classed as such (Ohkura *et al.* 1998). Activators of NR4A members have been identified which augment their activity: 6-mercaptopurine which is a metabolite of azathioprine, an immunosuppressive drug; prostaglandin A₂ (PGA₂); and benzimidazole derivatives (Bonta *et al.* 2007). It is thought that the agonist 6-mercaptopurine may activate NURR1 through its AF-1 domain, suggesting that it acts as a co-activator of this nuclear receptor (Ordentlich *et al.* 2003).

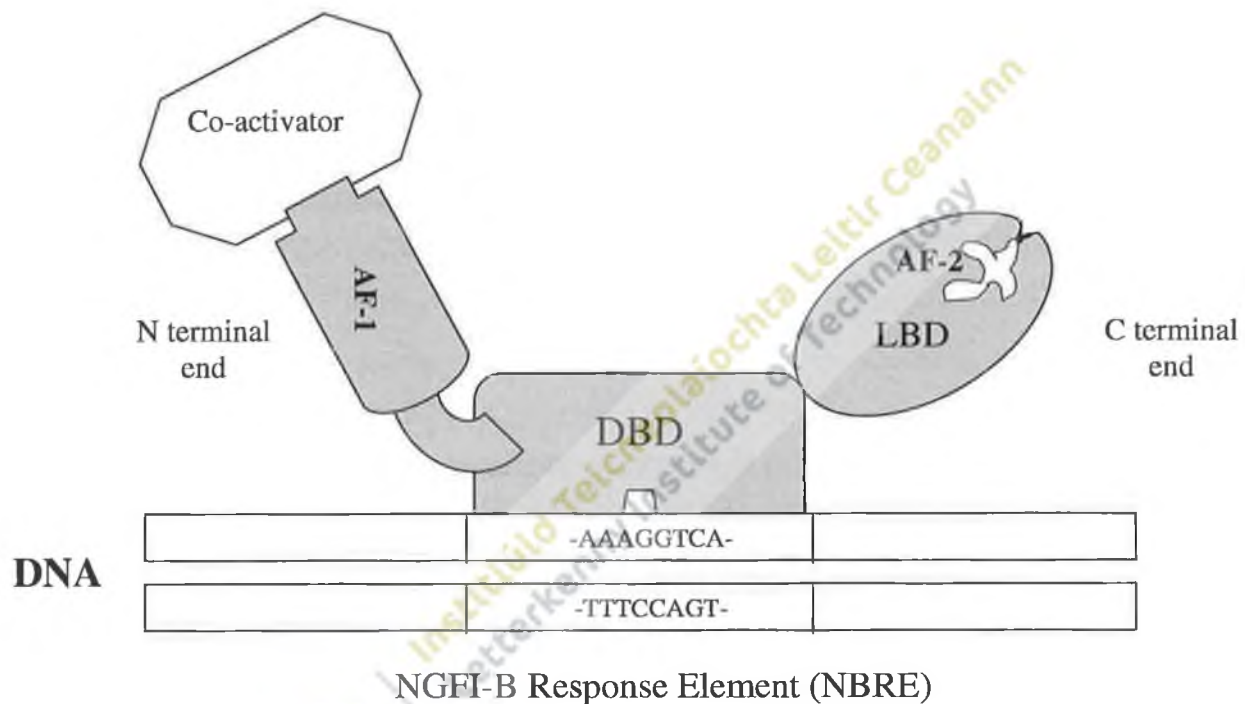


Fig 1.9 The structure of NR4A nuclear receptors binding to the NBRE sequence as a monomer. DBD: DNA binding domain; LBD: ligand binding domain; AF-1: activation function-1; AF-2: activation function-2 (Bonta *et al.* 2007).

NR4A receptors, unlike most nuclear receptors, are products of immediate early genes and are differentially induced by a wide variety of stimuli, including hormones, growth factors, membrane depolarisation, magnetic fields and apoptotic and inflammatory signals (Pei *et al.* 2005; Maxwell and Muscat 2005). NR4A subfamily members have roles in regulating the differentiation, proliferation, apoptosis and survival of many types of cells (Wang and Wan 2008). NUR77 was the first member of this subfamily to be identified and was found to be an

immediate response gene expressed by rat pheochromocytoma PC12 cells when stimulated by nerve growth factors. The other members, NURR1 and NOR-1, were subsequently identified (Wang and Wan 2008).

1.7.1 Functions of NR4A receptors

Several studies have been carried out to elucidate the importance of the NR4A subfamily of orphan nuclear receptors. The NR4A receptors were found to be ubiquitously expressed in adult rat tissue, with the majority of expression in the central nervous system. During rat fetal development, the three subfamily members were found to be expressed in the brain at different stages. NURR1 is more highly expressed at the earlier stages, while NOR-1 expression is strongest at later stages of fetal development. The highest levels of NUR77 are in the adult rat brain. NURR1 is thought to be essential for the differentiation of midbrain dopaminergic neurons which are involved in the control of involuntary movement (Ohkura *et al.* 1998). Furthermore, mutations in the NURR1 gene have been associated with the development of Parkinson's disease (Le *et al.* 2003). NOR-1 is also thought to play a role in the development of neurons in the foetus (Ohkura *et al.* 1998).

Studies indicate that the NR4A subfamily is involved in the apoptosis of self-reactive T cells, a process known as clonal deletion or negative selection. Expression of a dominant negative NUR77 mutant in T cell hybridoma cells suppresses T cell receptor-mediated apoptosis and prevents antigen-induced apoptosis of T cells *in vivo*. In addition, a lesser number of T cells (thymocytes and peripheral T cells) are present in transgenic mice overexpressing NUR77 (Ohkura *et al.* 1998).

Studies have illustrated that NR4A subfamily members may be important regulators of lipid and glucose metabolism. NOR-1, in particular, is induced in high levels in skeletal muscle during recovery from endurance exercise (Maxwell and Muscat 2005). Knock-down of NUR77 in C2C12 cells (a mouse myoblast cell line) led to a reduction in the expression of genes associated with energy expenditure and lipid homeostasis. Induction of adipocyte differentiation results in the upregulation of the NR4A subfamily members (Maxwell and Muscat 2005). Furthermore, a study in 2009 found that common polymorphisms within the NOR-1 locus determine insulin

secretion by β -cells suggesting that NOR-1 may be involved in the development of diabetes (Weyrich *et al.* 2009).

NR4A nuclear receptors are important in the regulation of genes involved in steroidogenesis, including POMC (proopiomelanocortin) and hydroxylase enzymes (Maxwell and Muscat 2005; Murphy and Conneely 1997).

Transcripts made up of NOR-1 fused with EWS (Ewing's sarcoma gene) resulting from a chromosomal translocation have been identified in myxoid chondrosarcomas (Ohkura *et al.* 1998). According to Zhang (2007), the location of NUR77 within the cell controls its effects on cancer cells. NUR77 acts as an oncogenic survival factor, inducing the expression of genes promoting proliferation, when present in the nucleus of the cell. When NUR77 migrates from the nucleus to the mitochondria however, it triggers the release of cytochrome c and apoptosis. It was found that the synthetic retinoid 6-[3-(1-adamantyl)-4-hydroxyphenyl]-2-naphthalene carboxylic acid (AHPN/CD437), which induces apoptosis in human cancer cells, acts via NUR77. AHPN promotes the translocation of NUR77 to the mitochondria, a process thought to be controlled by the RXR. This demonstrates that NUR77 expression is vital for the induction of apoptosis by AHPN (Zhang 2007).

1.7.2 Evidence of a proinflammatory role for NR4A receptors

Studies have found that the NR4A nuclear orphan receptors play a role in inflammation. McEvoy *et al.* (2002) demonstrated that increased levels of NURR1 are found in the synovial lining layer, subsynovial synoviocytes and vascular endothelial cells of RA synovial tissue compared to normal synovial tissue. This study also found that NURR1 expression in RA synovial cells is induced by the inflammatory mediators, TNF- α , IL-1 β and prostaglandin E₂ (PGE₂). This expression is due to TNF- α - and IL-1 β -induced activation of NF- κ B binding to the NURR1 promoter. The NF- κ B heterodimer, p65-p50, and homodimer, p50, are the main NF- κ B subunits responsible for binding of the NURR1 promoter. Furthermore, McEvoy *et al.* (2002) demonstrated that stimulation by PGE₂ resulted in the binding of cyclic adenosine 5'-monophosphate response element-binding protein (CREB) to the NURR1 promoter, leading to its induction. This study indicates that members of the NR4A receptor subfamily may be potential

mediators of cytokine signaling and illustrates the involvement of NURR1 in inflammatory pathways that are pivotal in the pathogenesis of RA.

Davies *et al.* (2005) demonstrated that overexpression of NURR1 in immortalized fibroblast-like synoviocytes (K4 IM cells) led to induction of the proinflammatory genes IL-8, amphiregulin and kit ligand. The proinflammatory cytokine IL-8 plays an important role in neutrophil recruitment during the inflammatory response. Amphiregulin is thought to be involved in early-onset synovial inflammation and severe skin inflammation and may have a role in psoriasis and psoriatic arthritis. Kit ligand (or stem cell factor) is involved in mast cell activation and activation of its receptor leads to the phosphorylation of Akt in the IL-1-dependent NF- κ B activation pathway (Davies *et al.* 2005). A further study by Aherne *et al.* (2009) found that NURR1 co-operates with NF- κ B to upregulate transcription of IL-8 in a mechanism which is independent of NURR1 binding to its DNA binding site or heterodimerization with other nuclear receptors.

Ralph *et al.* (2005) found that treatment with the disease-modifying anti-rheumatic drug, methotrexate, significantly reduces NURR1 expression in patients with inflammatory joint disease and this reduction correlates with improvements in disease activity. Methotrexate selectively and directly down-regulates NURR1 expression in synovial tissue in response to inflammatory stimuli and growth factors, including TNF- α , PGE₂ and VEGF (Ralph *et al.* 2005). Immunostaining of NURR1 revealed that, during methotrexate treatment, the NURR1 present is predominantly confined to the cytoplasm compared with the nuclear localization of NURR1 prior to treatment. It was also found that methotrexate suppresses endogenous and PGE₂-induced NURR1 expression in a dose-dependent manner. This suppression is mediated through the release of adenosine and activation of its A_{2A} receptor (Ralph *et al.* 2005). If NURR1 is retained in the cytoplasm of cells, it therefore cannot induce the expression of pro-inflammatory genes.

Increased NURR1 expression and nuclear localization has been detected in psoriasis skin. Psoriasis is an autoimmune inflammatory skin disease and approximately 15 % of patients develop inflammatory seronegative arthritis, termed psoriatic arthritis. Anti-TNF- α therapies reduce NURR1 levels in psoriasis skin and reinstate its cytoplasmic distribution, indicating that the clinical improvements of this therapy may be mediated through down-regulation of NURR1 and inhibition of its transcriptional activities (O’Kane *et al.* 2008).

A study by Zeng *et al.* (2006) reported that the angiogenic factor, VEGF-A, induces angiogenesis through the up-regulation of NUR77. Overexpression of NUR77 stimulates angiogenesis and leads to the proliferation and survival of human umbilical vein endothelial cells (HUVECs). NUR77 requires its transactivation domain and its DNA binding domain in order to do this, illustrating that this NUR77 mediates angiogenesis and proliferation of HUVECs via its transcriptional activity (Zeng *et al.* 2006). VEGF induces the expression of all three NR4A receptors in HUVECs. Therefore, NR4A receptors are candidate mediators of VEGF-induced functions, including the survival, proliferation and migration of ECs and the synthesis of nitric oxide and prostaglandin I₂ which are involved in the inflammatory response (Liu *et al.* 2003).

In the human monocytic cell line THP-1, stimulation with LPS rapidly induces the expression of all three NR4A subfamily members. LPS-induced expression of NUR77 requires the binding of NF- κ B to its promoter. The NR4A receptors were also found to be strongly induced by 25-hydroxycholesterol and 7 β -cholesterol in THP-1 cells. These oxidized lipids have been implicated in atherosclerosis. Furthermore, NUR77 and NOR-1 expression have been identified in macrophage and smooth muscle cells from human coronary artery atherosclerotic lesions (Pei *et al.* 2005; Nomiya *et al.* 2006). Many patients with RA develop atherosclerosis due to inflammation within the arteries (Buch and Emery 2002).

Smooth muscle cells (SMCs) that have been stimulated by the mitogenic factor PDGF have been shown to rapidly induce NOR-1 expression through an ERK-MAPK dependent signaling pathway. This is mediated via CREB binding to the NOR-1 promoter and initiating transcription (just as PGE₂ stimulation led to CREB binding of the NURR1 promoter in synovial cells). It was also demonstrated that PDGF stimulates NOR-1 transcriptional activity. Furthermore, NOR-1-deficient SMCs exhibit reduced cell proliferation and the cell cycle control genes cyclin D1 and D2 have been identified as target genes for NOR-1 in SMCs. This illustrates that NOR-1 acts as an important transcriptional regulator of SMC proliferation. Activated SMCs are involved in the pathogenesis of atherosclerosis (Nomiya *et al.* 2006).

A study by Pei *et al.* (2006) found that in murine macrophage cells, overexpression of the NR4A subfamily, and NUR77 in particular, leads to the induction of numerous genes involved in inflammation, apoptosis and cell cycle control. These upregulated genes include cyclin D2, which is involved in cell cycle control, and TNF- α and A20, whose roles in inflammation have

been described earlier. Stimulation of cells expressing NUR77 with LPS enhanced the induction of proinflammatory genes compared to cells which did not express NUR77. This illustrates that the NR4A receptors play a role in the regulation of macrophage gene expression during inflammation (Pei *et al.* 2006). The induction of A20 by the NR4A nuclear receptors in murine macrophage cells indicates that, whilst these transcription factors promote the expression of pro-inflammatory genes, they may also trigger the expression of anti-inflammatory genes as a means of protection against an excessive inflammatory response. This warrants further investigation and the interaction between A20 and the NR4A receptors is the focus of this study.

1.7.3 Anti-inflammatory actions of NR4A receptors

Further studies have discovered that the NR4A subfamily members display anti-inflammatory actions. A study by Mix *et al.* (2007) demonstrated that NURR1 selectively inhibits expression of MMP-1, -3 and -9 and suppression of MMP-1 by NURR1 occurs through an NBRE-independent mechanism. This mechanism may involve the interaction of NURR1 with E26 transformation-specific sequence (ETS) transcription factors. This indicates that NURR1 may play a protective role in cartilage homeostasis by controlling the synthesis of MMPs which break down cartilage.

During the development of atherosclerosis, macrophages ingest modified lipids, forming lipid-laden foam cells. In human monocytic leukemia THP-1 cells overexpressing NR4A receptors, the uptake of oxidized low-density lipoprotein was reduced. Furthermore, overexpression of each of the three NR4A subfamily members in human THP-1 and U937 macrophages led to a 2- to 10-fold reduction of the proinflammatory factors IL-1 β , IL-8 and MIP-1 α after stimulation with TNF- α and LPS. However, it should be noted that overexpression of NOR-1 in these cells, when stimulated with TNF- α , led to a 2.5-fold increase in MCP-1 (monocyte chemotactic protein-1) expression and no significant difference was observed in MCP-1 expression when NURR1 was overexpressed (Bonta *et al.* 2006).

Harant and Lindley (2004) discovered that overexpression of NUR77 in the human T cell leukemia Jurkat cell line results in repression of IL-2 promoter activation. Suppression of IL-2 requires the N-terminal domain of NUR77. Alterations of the NF- κ B binding sites on the IL-2 promoter abolish this repression, indicating that it is mediated via the inhibition of NF- κ B. IL-2

induces the proliferation of T and B cells in the inflammatory response (Harant and Lindley 2004).

You *et al.* (2009) revealed that overexpression of NUR77 in HUVECs controls TNF- α - and IL-1 β -induced NF- κ B activation through the induction of I κ B α expression, which binds NF- κ B, preventing it from translocating into the nucleus. Suppression of NF- κ B activation impairs EC activation, blocking expression of the adhesion molecules ICAM-1 and VCAM-1 and suppressing the adherence of monocytes to ECs. This inhibits the infiltration of monocytes to the inflamed area. I κ B α is induced via binding of NUR77 to an NBRE site on its promoter (You *et al.* 2009).

A study by de Waard *et al.* (2006) established that overexpression of NUR77 leads to a decrease in the proliferation of venous SMCs and may help to prevent vein-graft disease.

Overall, evidence suggests that the positive and negative transcriptional regulation carried out by the NR4A subfamily of nuclear receptors is most likely to be dependent on a complex interplay between the receptor, promoter and cellular context (Aherne *et al.* 2009).

1.7.4 Nuclear receptors as targets for therapeutics

The importance of nuclear receptor signaling is demonstrated when it becomes dysregulated, resulting in the development of proliferative, reproductive and metabolic diseases, including cancer, infertility and diabetes. Therefore, nuclear receptors have become key targets for drug discovery and nuclear receptor agonists/antagonists have been developed to treat these diseases (Gronemeyer *et al.* 2004).

One such example is tamoxifen, which is a hormone used for the treatment of breast cancer and also for its prevention in women with a high risk of developing breast cancer. Tamoxifen binds to the oestrogen receptor, preventing the binding of oestrogen (Gronemeyer *et al.* 2004) and therefore, is known as an antioestrogen. It acts as a partial agonist, exhibiting mixed agonist and antagonist activities. Oestrogen-regulated gene transcription is mediated by the two activation functions, AF-1 and AF-2, of the oestrogen receptor. The AFs recruit co-activators or co-repressors to the general transcription complex. However, the binding of tamoxifen to the

oestrogen receptor leads to a conformational change in the receptor, resulting in a non-functional AF-2, while AF-1 retains its function (Wakeling 2000). Therefore, tamoxifen may act as an agonist or as an antagonist, depending on the cell and promoter context, on the structure of the hormone response element to which the receptor binds and on the additional transcription factors recruited (Gronemeyer *et al.* 2004).

Another example of drugs which target nuclear receptors for the treatment of disease is corticosteroids. These act as ligands for glucocorticoid receptors and are used to treat inflammatory diseases, including RA (Gronemeyer *et al.* 2004). Corticosteroids are described in more detail in section 1.8.1 below.

While treatment of diseases by targeting nuclear receptors usually involves the use of alternative ligands, it may be possible to modulate the activity of orphan receptors through harnessing the crosstalk between nuclear receptor-mediated signal transduction pathways and other signal transduction pathways. These other pathways can result in post-transcriptional modification of nuclear receptors via phosphorylation, ubiquitylation or acetylation, altering their function. For example, in response to stimuli such as growth factors or cytokines, mitogen-activated protein kinases (MAPKs) have the ability to phosphorylate certain nuclear receptors which can affect their function (Gronemeyer *et al.* 2004). In addition, a ligand for the glucocorticoid receptor has been identified that has the ability to repress and activate only a subset of genes usually controlled by corticosteroids. This ligand, termed AL-438, still maintains the anti-inflammatory properties of steroids but exhibits a reduction in the adverse effects on bone metabolism and glucose control associated with conventional corticosteroids. This mechanism is thought to involve differential co-factor recruitment in response to ligand (Coghlan *et al.* 2003). Therefore, it may be possible to harness the anti-inflammatory actions of the NR4A receptors whilst preventing the proinflammatory effects of these receptors. The identification of agonists of NR4A receptors (such as 6-mercaptopurine) aids the potential for development of drugs for the selective therapeutic regulation of these receptors in the treatment of diseases (Ordentlich *et al.* 2003).

1.8 Current Treatment for Rheumatoid Arthritis

Traditionally, RA treatment was focused on managing the pain and inflammation associated with the disease. Now however, the aim of treatment is to suppress inflammation, reduce the progression of RA, and even to establish remission, with the use of new drugs along with more conventional therapies (Combe 2009). Until the mid-1980s, treatment for RA began with a non-steroidal anti-inflammatory drug (NSAID), sometimes along with a corticosteroid. This was then followed by a disease-modifying anti-rheumatic drug (DMARD). If this DMARD failed, another one was prescribed in its place. This is known as sequential monotherapy (Nurmohamed and Dijkmans 2008). A low dose of the DMARD methotrexate was increasingly used from the 1980s onwards and, during this time, DMARDs started to be prescribed much earlier (Nurmohamed and Dijkmans 2008). An important development in the treatment of RA came with the introduction of biological therapies in the late 1990s. These are agents which target molecules involved in inflammatory pathways and came about from an increased understanding of the pathogenesis of RA (Klareskog *et al.* 2009). Biological therapies are much more expensive than DMARDs, but can be an effective treatment for RA and offer an alternative for patients who fail to respond to existing DMARDs. It has become apparent that intensive and early intervention with treatment such as combination DMARDs and/or biological therapies can be highly beneficial in the control of joint damage and may induce high rates of remission (Combe 2009; Smolen *et al.* 2010).

1.8.1 Corticosteroids

Corticosteroids (or glucocorticoids/adrenal steroids) are extremely effective in suppressing the inflammatory response and the immune system. They are synthesized and secreted by the adrenal cortex in the brain and are important for normal metabolism and resistance to stress (Mycek *et al.* 2000). Corticosteroids act as ligands, binding to glucocorticoid receptors which belong to the same superfamily of nuclear receptor transcription factors that include the NR4A subfamily. When the steroid binds, the receptor becomes activated and the steroid-receptor complex translocates into the nucleus, where it can repress or induce target gene transcription (Rang *et al.* 2007). Apart from the enzymes involved in metabolism, the corticosteroids induce the synthesis of I κ B, which retains NF- κ B in the cytoplasm, inhibiting its action. They also induce the synthesis of anti-inflammatory proteins such as annexin-1. Treatment with corticosteroids results in a decline in the production of inflammatory cytokines and cell adhesion

molecules, a reduction in the concentration and actions of leucocytes and a decrease in angiogenesis (Rang *et al.* 2007).

The adverse effects of long-term usage of corticosteroids include the redistribution of body fat, poor wound healing and osteoporosis. Another important adverse effect is suppression of the protective immune response to infection (Rang *et al.* 2007).

1.8.2 Non-steroidal anti-inflammatory drugs (NSAIDs)

Non-steroidal anti-inflammatory drugs (NSAIDs) such as aspirin, ibuprofen and indometacin, have anti-inflammatory effects and also reduce pain and fever. They comprise a group of chemically diverse agents, many of which act by reducing the production of prostaglandins in inflammatory cells through the inhibition of cyclooxygenase enzymes. Prostaglandins are among the chemical mediators which are released in inflammatory processes (Mycek *et al.* 2000). Some prostaglandins act as vasodilators, allowing increased blood flow to the inflamed area and leading to the influx of proinflammatory cells and mediators (Rang *et al.* 2007). Prostaglandins sensitize nerve endings to the action of chemical mediators such as bradykinin and histamine, causing pain (Mycek *et al.* 2000). In addition, E-type prostaglandins (PGEs) in the hypothalamus cause a rise in the hypothalamic set-point for temperature control in the body and this results in fever. COX-1 and COX-2 are two cyclooxygenase enzymes which have been identified and NSAIDs inhibit both of these by hydrogen bonding to an arginine residue on the enzymes (Rang *et al.* 2007).

A side effect of NSAIDs is gastrointestinal disturbances and this is attributed to their inhibition of COX-1. This enzyme leads to the synthesis of prostaglandins that protect the mucosa and inhibit acid secretion. COX-2 is induced by the inflammatory response, producing mediators of inflammation (Rang *et al.* 2007). The COX-2 selective inhibitor celecoxib is available which has less of an effect on the gastrointestinal tract (Mycek *et al.* 2000). However, other COX-2 inhibitors have been taken off the market due to safety concerns (European Medicines Agency 2005). Along with diarrhoea, indigestion, vomiting and possible gastric damage, other side effects of NSAIDs are skin reactions, renal problems and, less commonly, liver disorders (Rang *et al.* 2007). NSAIDs reduce the symptoms of RA but they do not halt disease progression or induce remission (Mycek *et al.* 2000).

1.8.3 Disease-modifying anti-rheumatic drugs (DMARDs)

Disease-modifying anti-rheumatic drugs (DMARDs) improve symptoms, reduce disease activity and can induce remission of RA. These include sulphasalazine, cyclosporin, gold, antimalarial drugs, methotrexate and biological therapies, as discussed below (Smolen *et al.* 2010). DMARDs are slow-acting, in contrast to NSAIDs, and may take several months to take effect (Rang *et al.* 2007).

1.8.3.1 Sulphasalazine

Sulphasalazine is widely used for RA and chronic inflammatory bowel disease. It is composed of sulfapyridine and 5-aminosalicylate (5-ASA). Bacteria in the colon split the bond between these molecules, releasing them. The active metabolite in sulfasalazine is 5-ASA, which is thought to scavenge the toxic oxygen metabolites produced by neutrophils. The adverse effects of this drug include gastrointestinal problems, headache and skin reactions. Folic acid absorption may be inhibited and, therefore, folic acid supplements are sometimes required (Rang *et al.* 2007).

1.8.3.2 Methotrexate

Methotrexate is a commonly used, effective treatment for RA (Smolen *et al.* 2010). It is an immunosuppressant and acts faster than other DMARDs (Mycek *et al.* 2000). It inhibits T-cell activation (Klareskog *et al.* 2009) and enhances the release of adenosine at inflamed sites. Activation of the adenosine receptor A2A reduces inflammation and tissue damage (Gomez and Sitkovsky 2003). Methotrexate also acts as a folate antagonist and, at higher doses, is widely used as a chemotherapeutic agent (Rang *et al.* 2007). Folates are required for purine and thymidylate production which are necessary for the synthesis of DNA, RNA and proteins. Methotrexate inhibits the enzyme dihydrofolate reductase. This enzyme catalyses the reduction of folate to tetrahydrofolate (FH₄). FH₄ acts as a co-factor in the formation of thymidylate and purines (Rang *et al.* 2007). Thus, methotrexate suppresses the synthesis of DNA, RNA and proteins, eventually causing the death of proliferating cells. The side effects of using methotrexate include nausea, vomiting, diarrhoea and myelosuppression (decrease in the production of blood cells by bone marrow). Many of these effects can be avoided with use of the drug leucovorin (Mycek *et al.* 2000).

Methotrexate is most commonly administered orally as it is readily absorbed from the gastrointestinal tract. It may also be given by intramuscular, intravenous or intrathecal (under the arachnoid membrane of the brain or spinal cord) routes (Mycek *et al.* 2000). It is often used as an initial treatment for RA. If this does not result in sufficient amelioration, additional or alternative DMARDs may be introduced, followed by biological therapies (Klareskog *et al.* 2009; Smolen *et al.* 2010).

1.8.4 Biological Therapies

Several biological therapies for RA are now available. The first of these were anti-TNF- α agents which were approved for clinical use in 1998 (Wong *et al.* 2008). There are now several TNF- α inhibitors available for inflammatory arthritis, including etanercept, infliximab and adalimumab (Rubbert-Roth and Finckh 2009; Tak and Kalden 2011).

1.8.4.1 Etanercept

Etanercept (brand name Enbrel) is a soluble TNF- α receptor joined to the Fc fragment of a human immunoglobulin (IgG1) which binds to TNF- α and sequesters it. The TNF- α , therefore, cannot bind to its membrane-bound receptors on target cells and initiate its proinflammatory pathways. There are two isomers of the TNF receptor, a p55 (TNFR1) and a p75 receptor (TNFR11), which may be membrane-bound or soluble, circulating in the serum. Etanercept consists of two extracellular regions of the human soluble p75 TNF receptor (sTNFR11) which captures and binds TNF- α at two of its three receptor-binding sites, thereby preventing TNF- α -induced signaling. Subcutaneous injections of etanercept are given either twice weekly at a concentration of 25 mg or once a week at a concentration of 50 mg. It is indicated for treatment of RA, juvenile chronic arthritis, psoriatic arthritis, ankylosing spondylitis and psoriasis (Wong *et al.* 2008).

1.8.4.2 Infliximab

Infliximab (brand name Remicade) is a monoclonal antibody consisting of human constant regions of the IgG1 κ antibody with murine variable regions. It can bind to soluble and transmembrane TNF- α , and has a high affinity and specificity for the cytokine. It has been reported that the murine variable fragment induces synthesis of human anti-mouse antibodies which would limit the efficacy of this treatment. The mode of administration is by intravenous infusion every 8 weeks at a concentration of 3 – 10 mg/kg. Along with RA, infliximab is also

indicated for use in ulcerative arthritis, psoriatic arthritis, chronic severe plaque psoriasis and Crohn's disease (Wong *et al.* 2008).

1.8.4.3 Adalimumab

Adalimumab (brand name Humira) is a complete human IgG1 monoclonal antibody. Like infliximab, it binds to both soluble and transmembrane TNF- α and prevents it from binding to its receptors. Adalimumab is given subcutaneously every two weeks at a concentration of 40 mg or once a week at a higher concentration. Adalimumab is indicated for RA and also moderate to severe Crohn's disease, psoriatic arthritis and ankylosing spondylitis (Wong *et al.* 2008).

1.8.4.4 Modes of Action of Anti-TNF- α Agents

Despite the frequent use of anti-TNF- α agents, much remains to be discovered about their modes of action. Studies suggest that the binding of anti-TNF- α agents to TNF- α receptors may result in several effects (Wong *et al.* 2008). It may elicit complement-dependant lysis of the cell and antibody-dependant cytotoxicity. This binding could also induce apoptosis mediated by reverse intracellular signaling (outside to inside signaling), a reduction in cytokine production or a halt in cell growth (Wong *et al.* 2008). Studies show that reverse intracellular signaling, initiated by infliximab, can also lead to the inhibition of NF- κ B activation in RA patients (Meusch *et al.* 2009).

Treatment with TNF- α antagonists can result in a reduction of other proinflammatory cytokines, such as IL-1 and IL-6, both in serum and in the synovium of RA patients, in addition to a decrease in TNF- α levels. Infiltration of inflammatory cells including T and B cells, macrophages and synoviocytes into the inflamed joint is suppressed by anti-TNF- α agents. This is due to the control of cell migration and the induction of apoptosis of these cells. It has been demonstrated that in the synovial membrane, the level of VEGF, which induces angiogenesis, is diminished following anti-TNF- α treatment. The expression of endothelial adhesion molecules is also reduced. An increase in the number of regulatory T (Treg) cells in circulation was found after treatment with anti-TNF- α agents in one study. Treg cells inhibit the synthesis of proinflammatory mediators by activated T cells. TNF- α inhibition also results in a reduction in levels of RANKL. Overall, treatment with TNF- α antagonists can result in reduced inflammation and joint destruction and has a clear, beneficial effect in some patients (Wong *et al.* 2008). It has been demonstrated that the use of methotrexate along with TNF- α antagonists enhances their

effectiveness and, as a result, these drugs are commonly used in combination (Klareskog *et al.* 2009).

1.8.4.5 Other Biological Therapies

The success of anti-TNF- α agents in some patients has led to the development of drugs which target other mediators of inflammation, such as IL-1, and those which target T and B lymphocytes (Tak and Kalden 2011).

Abatacept (brand name Orencia) has been approved for the treatment of RA in adults who did not have an adequate response to DMARDs or TNF- α inhibitors. Abatacept inhibits the activation of T-cells through the suppression of essential co-stimulatory signals. It is made up of an extracellular CTLA4 domain along with the Fc domain of an IgG molecule. Rituximab (brand name Rituxan) is approved for use by adult RA patients who failed to respond to at least one TNF- α inhibitor. Rituximab consists of a monoclonal antibody for the CD20 molecule on the surface of mature and immature B cells. The binding of this antibody reduces the concentration of B cells in circulation, leading to reduced T cell activation and less antibody and immune complex formation (Klareskog *et al.* 2009; Tak and Kalden 2011). Anakinra (brand name Kineret) is an IL-1 receptor antagonist which inhibits IL-1 signaling by binding to the IL-1 receptor. Studies have illustrated that it improves disease activity in some patients (den Broeder *et al.* 2006). Tocilizumab (brand name RoActemra or Actemra) is an antibody developed as an IL-6 receptor antagonist and is used for patients who have not responded to, or are unsuitable for, anti-TNF- α treatment. It may be used in conjunction with methotrexate and has shown effectiveness in controlling disease activity (Oldfield *et al.* 2009). Denosumab is a newly developed monoclonal antibody against RANKL and it has been shown to inhibit bone damage and joint destruction in RA patients when combined with methotrexate (Cohen *et al.* 2008).

Pathological Inflammatory Response

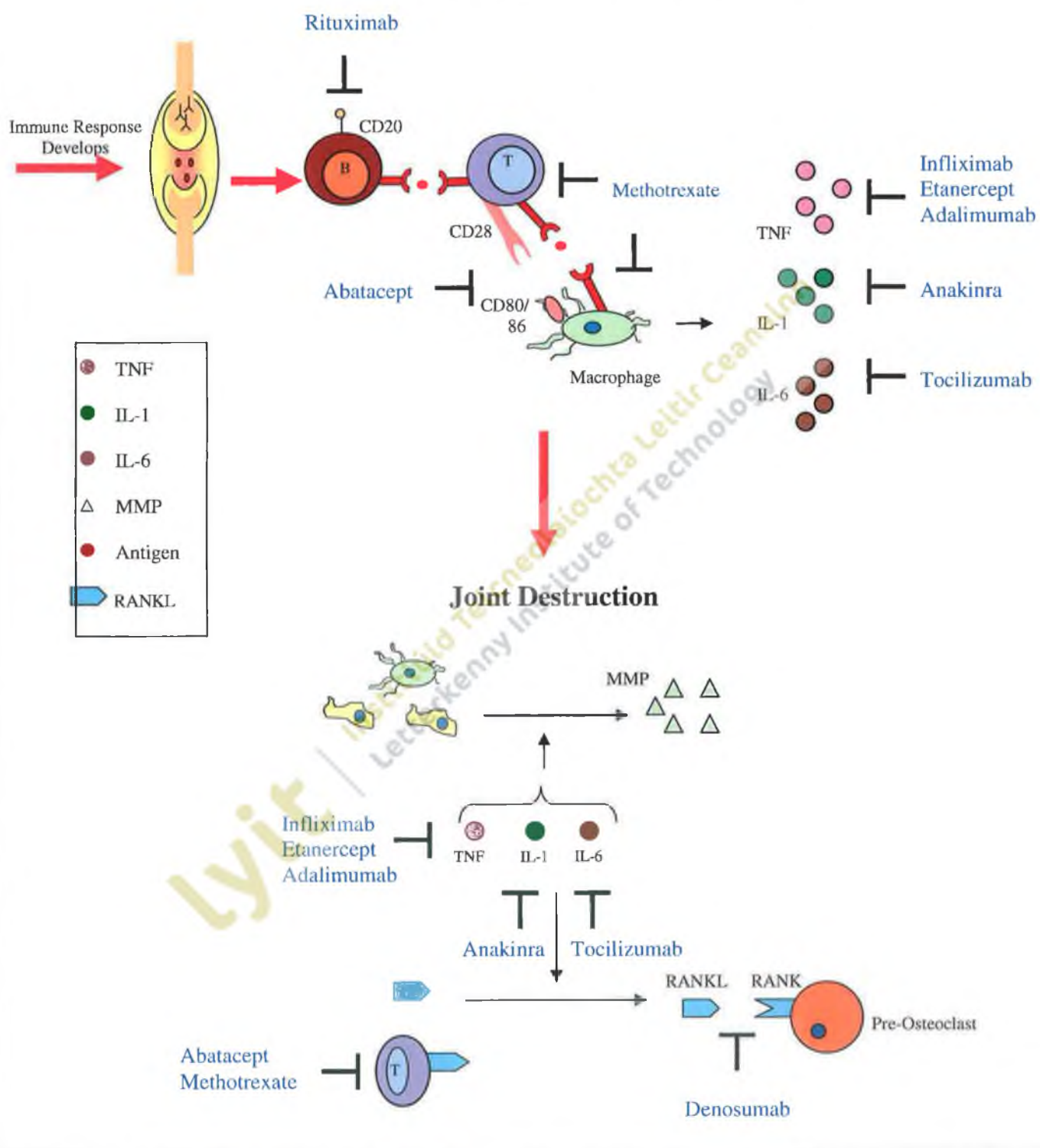


Fig. 1.10 Sites of action of biological therapies and other agents for the treatment of RA (Adapted from Klareskog *et al.* 2009; Rang *et al.* 2007).

1.8.4.6 Adverse Effects of Biological Therapies

There are serious adverse effects associated with the use of biological therapies, but these are infrequent. It is strongly recommended that patients are screened for latent tuberculosis (TB) prior to receiving anti-TNF- α treatment. This is due to a concern that this therapy may induce reactivation of TB. If detected, patients should be treated for this before commencing anti-TNF- α therapy. The most frequent side effect of TNF- α inhibition is injection or infusion reactions, although these are not usually serious. There is an increased risk of developing infections when receiving anti-TNF- α treatment because of the role TNF- α naturally plays in the immune system. It is uncertain whether TNF- α inhibition increases the risk of lymphoma or solid malignancies in RA patients and this is because RA patients are at a higher risk of developing these conditions initially. Further studies are required to establish definitively if there is an increased risk of lymphoma and solid malignancies associated with anti-TNF- α therapy. Patients who have advanced congestive heart failure are not suitable for treatment with TNF- α inhibitors (Lin *et al* 2008). Other adverse reactions associated with TNF- α inhibition include neutropenia and hepatotoxicity (Gartehner *et al.* 2005).

Common adverse effects associated with the use of other biological therapies, such as abatacept, rituximab and tocilizumab, include injection/infusion site reactions, nausea, abnormal results of liver function tests, neutropenia, gastrointestinal complaints and musculoskeletal disorders. In addition, patients receiving these treatments have a higher risk of developing serious infections. Furthermore, the long-term safety profiles of these drugs have yet to be established (Nogid and Pham 2006; Kimby 2005; Plushner 2008).

Whilst the use of TNF- α antagonists can be a very effective treatment for RA, between 20 % and 40 % of patients administered with one of these agents do not gain a 20 % improvement in American College of Rheumatology criteria (ACR20 response). Over 50 % of RA patients treated with a TNF- α inhibitor fail to obtain a 50 % improvement in ACR criteria (ACR50 response). Furthermore, during treatment, additional patients lose efficacy or develop side effects. In these situations, often an alternative TNF- α inhibitor is then used, which may be beneficial, due to differences in the bioavailability and stability of anti-TNF- α agents. However, most patients still fail to improve adequately (that is, attain an ACR50 response) after changing to a different TNF- α antagonist. Biological agents which target other cytokines or immune cells, such as those describe above, offer an alternative to TNF- α inhibition, having different modes of

action. However, studies have yet to be carried out comparing the efficacy of these therapies in patients who have not responded to treatment with TNF- α antagonists (Rubbert-Roth and Finckh 2009). Information thus far relating to combination biological therapy indicates that there is an increased risk of serious infections (Wong *et al.* 2008). Therefore, further research into finding other targets for the treatment of RA is necessary, in order to develop additional/alternative forms of therapy.

1.9 Project Objectives

A20, ABIN-1, ABIN-2 and Cezanne have all been shown to inhibit the activation of NF- κ B in response to inflammatory stimuli. The NR4A subfamily of nuclear receptors may be potential targets for the control of inflammation, through controlling their proinflammatory activities and/or enhancing their anti-inflammatory properties. The study by Pei *et al.* (2006) demonstrating that overexpression of the NR4A members in macrophages leads to the induction of A20 gene expression indicates that this subfamily of nuclear receptors may have a role in regulating A20 and A20-interacting genes. This also suggests that NR4A receptors may, in turn, be regulated by A20.

The objectives of this project were to:

- Examine the promoter regions of A20 and the A20-interacting genes ABIN-1, ABIN-2 and Cezanne for the presence of the NR4A transcription factor binding site (NBRE site) using bioinformatic analysis, potentially linking the NR4A receptors to expression of these genes.
- Determine the effects of the inflammatory cytokine TNF- α on the expression of A20, ABIN-1, ABIN-2 and Cezanne in the multicellular environment of RA, elucidating the expression of these genes in human synoviocyte and chondrocyte cells in an inflammatory environment. This was achieved by performing reverse transcription (RT)-PCR and quantitative (q)PCR analyses of RNA extracted from cells stimulated with TNF- α .
- Examine the potential of A20 as a means of modulating the transcriptional activity of the NR4A subfamily of nuclear receptors in cell culture models of inflammatory arthritis. This was achieved by performing transient transfection experiments in which an NBRE-

luciferase reporter construct and a constitutively active NURR1 expression vector were co-transfected into synoviocyte and chondrocyte cells. An A20 expression plasmid was also co-transfected into these cells. The luciferase activity was measured and compared to controls transfected in a similar manner without A20. In addition, further transfection experiments were carried out to investigate the effect of A20 on the transcriptional activation of the NR4A target gene IL-8 by NURR1. It has previously been established that NURR1 induces expression of the proinflammatory chemokine IL-8 and that NURR1 also enhances NF- κ B p65 induction of IL-8 independently of the NBRE binding site (Aherne *et al.* 2009). Therefore, cells were co-transfected with an IL-8 human promoter luciferase reporter construct, a NURR1 expression vector and an A20 expression construct with and without a p65 expression vector. The luciferase assay results were compared to those obtained without the presence of A20 overexpression. In this manner, the effects of A20 on the transcriptional activity of NURR1 were elucidated.

Chapter 2

Materials and Methods

lyit | Institiúid Teicneolaíochta Litrí Ceanainn
Letterkenny Institute of Technology

2. Materials and Methods

2.1 Biological Materials

2.1.1 Cell Lines

The human synoviocyte cell line K4 IM was established by C. Haas at the Clinical Research Unit for Rheumatology, University Hospital, Freiburg, Germany from a healthy donor and immortalized using a SV40 T antigen (TAg) (Haas *et al.* 1997).

The human chondrocyte cell line SW 1353 (HTB-94) was initiated by A. Leibovitz at the Scott and White Clinic, Temple, Texas in 1977 from a primary grade II chondrosarcoma of the right humerus obtained from a 72 year old Caucasian female (Gebauer *et al.* 2005)

2.1.2 Plasmids

The pCAGGS-GFP/A20 plasmid was constructed by inserting the blunted *Bsp* HI-*Bam* HI fragment, containing the mutated *Aequorea Victoria* green-fluorescent protein (GFP) coding sequence fused to the mouse zinc finger protein A20 coding sequence, into the blunted *Xho* I site of pCAGGS. This plasmid was a gift to Dr. Joanne Gallagher by Prof. R. Beyaert, Unit of Molecular Signal Transduction in Inflammation, Ghent University, Belgium.

The pCMX-NURR1 expression plasmid contains the full-length mouse NURR1 coding cDNA cloned into a pCMX plasmid. This plasmid was kindly provided to Dr. Evelyn Murphy by Professor T. Perlmann, Karolinska Institute, Stockholm.

The pNBRE₃-tk-luciferase reporter construct contains three copies of the NGFI-B binding response element (NBRE) cloned upstream of the herpes simplex virus thymidine kinase promoter linked to the coding region of the luciferase gene. This plasmid was kindly donated to Dr. Evelyn Murphy by Professor T. Perlmann, Karolinska Institute, Stockholm.

The pcDNA6/*myc*-His C empty expression vector from Invitrogen contains a human cytomegalovirus immediate-early (CMV) promoter, a reading frame to facilitate in-frame cloning with a C-terminal peptide encoding the *myc* (*c-myc*) epitope and a polyhistidine (6xHis) metal binding tag for detection and purification of a recombinant protein. The plasmid was used in this study to ensure that the concentration of transfected DNA was equal in all samples.

Renilla luciferase pRL-SV40 vector from Promega was used as an internal control reporter and contains cDNA encoding *Renilla* luciferase cloned from the marine organism *Renilla reniformis* (sea pansy).

The IL-8 human promoter luciferase reporter construct contains the human IL-8 gene cloned into the pGL3 basic vector and was a gift to Dr. Evelyn Murphy from Dr. Xiaolan Zhang, The Dorothy M. Davis Heart and Lung Research Institute, Columbus.

The p65-RFP expression vector encodes the p65 subunit of NF- κ B cloned upstream of the DsRed-Express gene (*Discosoma sp.* red fluorescent protein) in the pIREs2-DSRed Express expression vector. This plasmid was kindly provided to Dr. Evelyn Murphy by Prof. Paul Moynagh, National University of Ireland, Maynooth.

The pmaxGFP is a positive control vector from Amara Biosystems encoding the green fluorescent protein from the marine organism *Pontellina sp.*

2.1.3 Standard End-Point PCR Primers

Sigma-Aldrich

B-actin	5'	3'
Forward Primer	GGACTTCGAGCAAGAGATGG	
Reverse Primer	AGCACTGTGTTGGCGTACAG	

ICAM-1

Forward Primer	TAAGCCAAGAGGAAGGAGCA
Reverse Primer	CATATCATCAAGGGTTGGGG

VCAM-1	5'	3'
Forward Primer	CTGTTCCAGCGAGGGTCTAC	
Reverse Primer	CGCTCAGAGGGCTGTCTATC	

A20		
Forward Primer	ATGCACCGATACACACTGGA	
Reverse Primer	CACAAGCTTCCGGACTTCTC	

ABIN-1		
Forward Primer	TGAGCAATGGCAACAAAGAG	
Reverse Primer	GCTCCAGCATCTTCACCTTC	

ABIN-2		
Forward Primer	GAACACACAGATGGGCACAC	
Reverse Primer	CCACTTGGCATTGAGGTCTT	

Cezanne		
Forward Primer	CACGTCTTTGTCCTTGCTCA	
Reverse Primer	GCAAGGGCAGCAGCTTATAC	

2.1.4 Quantitative PCR Oligonucleotides

Thermo Scientific

Solaris Human qPCR Gene Expression Assays

GAPDH	5'	3'
Forward Primer	GCCTCAAGATCATCAGCAATG	
Reverse Primer	CTTCCACGATACCAAAGTTGTC	
Probe	GCCAAGGTCATCCATGA	

A20		
Forward Primer	ATTTTCGGGAGATCATCCAC	
Reverse Primer	AATTGCCGTCACCGTTC	
Probe	CTTGTGGCGCTGAAAACG	

ABIN-1	5'	3'
Forward Primer	CCTGTCAAATGCCCAGCTAA	
Reverse Primer	ATGGTAACGCTCTCCTGAG	
Probe	AAGAGGAAAGCAAAGGCC	

2.1.5 Other Biological Materials

Competent *E. coli* cells JM109, genotype: *endA1*, *recA1*, *gyrA96*, *thi*, *hsdR17* (r_K^- , m_K^+), *relA1*, *supE44*, $\Delta(lac-proAB)$, [F' , *traD36*, *proAB*, *lacI*^q Δ M15] Promega

<i>Eco</i> R1, <i>Bam</i> H1 and <i>Hind</i> III restriction enzymes and 10X restriction enzyme buffers	Sigma Aldrich
GeneJuice	EMD Chemical
Go Taq DNA Polymerase	Promega
M-MLV Reverse Transcriptase	Promega
Recombinant human TNF- α	R & D Systems
RQ1 RNase-free DNase	Promega
Turbofect	Fermentas

2.2 Chemical Materials

Acetic acid	Fluka
Ampicillin	Molekula
Chloroform	Fluka
Ethanol	Merck
Isopropanol	Merck
LB agar	Oxoid
LB broth	Oxoid
Formaldehyde	Fisher Scientific
Phosphate buffered saline tablets	Oxoid

Promega

1 kb DNA ladder, 100 bp DNA ladder, RNA marker, loading dye, 5X Green Go Taq buffer, dNTPs, RNasin inhibitor, Agarose analytical grade, Ethidium Bromide (molecular biology grade), Random Primers, Formamide (molecular biology grade).

Riedel-de Haën

Sodium hydroxide pellets, Glycerol, Sodium Dodecyl Sulphate (SDS), Potassium Acetate, Trizma base, Ethylenediaminetetraacetic acid (EDTA).

Sigma Aldrich

10X MOPS running buffer, Chloroform (molecular biology grade), TRI Reagent, RPMI-1640 medium (HEPES modification, with 25 mM HEPES, without L-glutamine, sterile-filtered, cell culture tested), 0.25 % Trypsin-EDTA solution (sterile-filtered, cell culture tested), 200 mM L-glutamine (sterile-filtered, cell culture tested), Fetal Bovine Serum (sterile-filtered, cell culture tested), Penicillin-Streptomycin (10,000 units penicillin and 10 mg streptomycin per ml in 0.9 % NaCl, sterile-filtered, cell culture tested), Diethylpyrocarbonate (DEPC), Dimethyl Sulfoxide (DMSO), Trypan blue solution (0.4 %).

2.2.1 Commercial Kits

QIAGEN Plasmid Midi Kit	QIAGEN
Dual Luciferase Reporter Assay System	Promega
Go Script Reverse Transcription System	Promega
Solaris qPCR Gene Expression Master Mix	Thermo Scientific
Venor GeM Mycoplasma Detection Kit	Minerva Biolabs

2.3 DNA Manipulation

The preparation of solutions used in Chapter 2 is described in Appendix A.

2.3.1 Bacterial Transformation

Transformation is based on the natural ability of some bacteria to take up 'naked' DNA. DNA of interest is introduced into bacterial cells by ligating it to a vector such as a plasmid which can replicate autonomously inside the cells. The transformed bacterial cells are then allowed to grow and divide, during which time the recombinant plasmid DNA replicates many times within the cells. Plasmids contain one or more antibiotic resistance genes and, after transformation, the bacteria which were formerly sensitive to the antibiotic become resistant, allowing for the selection of transformants (Hames and Hooper 2000). Bacterial cells were transformed with the desired plasmid for storage and amplification purposes.

Two hundred and fifty nanograms of QIAGEN-purified plasmid DNA were added to 50 μ l of commercially obtained competent *E. Coli* cells in a 1.5 ml eppendorf. The contents were mixed and the eppendorf was centrifuged briefly to collect the contents at the bottom of the tube. The eppendorf was stored on ice for 10 min. It was then placed in a waterbath at 42°C for 50 s to heat shock the cells. The eppendorf was returned to ice for 2 min. Four hundred and fifty microlitres of sterile LB broth at 4°C were added and the eppendorf was placed in a shaking incubator at 37°C for 1 hr to allow amplification of the cells. One hundred microlitres of the amplified cells were spread onto an LB with selective antibiotic agar plate. A 10⁻¹ dilution was also plated. The plates were incubated at 37°C overnight. Controls were carried out by plating competent cells which were not transformed on both LB agar and LB plus selective antibiotic agar to determine the viability of the competent cells and to verify that the untransformed cells were sensitive to the selective antibiotic.

2.3.2 Plasmid DNA Miniprep

A plasmid DNA miniprep is a rapid method of isolating small quantities of plasmid DNA from bacterial cells. The method involves separating the plasmid DNA from the chromosomal DNA, which may be achieved using alkaline lysis. This method takes advantage of the fact that, at an

alkaline pH, plasmid DNA (being supercoiled) remains relatively intact, while chromosomal DNA separates completely into two strands. The plasmids revert back into their original form upon lowering the pH, while the chromosomal DNA cannot reanneal and forms an insoluble complex which can then be removed by centrifugation, along with other cell debris (Dale and von Schantz 2002).

Plasmid DNA minipreps were carried out to ascertain whether the bacterial transformations were successful and restriction enzyme digestions were subsequently conducted on the isolated DNA to establish that the correct plasmids were present. One transformed colony was selected and inoculated into 5 ml of sterile LB broth containing the selective antibiotic in a 50 ml sterile container. The container lid was loosely capped and the container was incubated overnight at 37°C in a shaking incubator. One millilitre of the overnight culture of transformed cells was transferred to a 1.5 ml eppendorf and centrifuged at maximum speed for 30 min at 4°C. The supernatant was removed and the pellet was resuspended in 100 µl of ice cold alkaline lysis solution I by vigorous vortexing. Two hundred microlitres of freshly prepared solution II were then added. The tube contents were mixed by inverting the tube rapidly five times, not vortexing. One hundred and fifty microlitres of solution III were added and the contents mixed by inverting several times. The lysate became viscous at this point and the eppendorf was stored on ice for 3-5 min. The eppendorf was centrifuged at maximum speed for 5 min at 4°C. The supernatant was transferred to a fresh 1.5 ml eppendorf. The nucleic acids were precipitated by adding 1 ml of 100 % ethanol at room temperature. The eppendorf was vortexed and allowed to stand for 2 min followed by centrifugation at maximum speed for 5 min at 4°C. The supernatant was removed and the DNA pellet was dried by inverting the tube and allowing it to stand on a clean paper towel. Fluid adhering to the tube wall was removed using a pipette. The DNA pellet was washed with the addition of 1 ml of 70 % ethanol and inverted several times. The eppendorf was centrifuged at maximum speed for 2 min at 4°C. The supernatant was removed and the remaining ethanol was allowed to evaporate at room temperature for 5-10 min. The nucleic acids were dissolved in 50 µl of sterile ultrapure H₂O. The eppendorf was vortexed gently and the DNA plasmid solution was stored at -20°C.

2.3.3 Plasmid Glycerol Stocks

Plasmid glycerol stocks of transformed bacterial cells were prepared to obtain a stock of the desired plasmids. An isolated colony of transformed cells was selected and inoculated into 5 ml of LB broth containing the selective antibiotic. The inoculated broth was incubated overnight at 37°C in a shaking incubator. Plasmid minipreps were performed on all overnight cultures to ensure the plasmid was present. Zero point five millilitres of the overnight culture were added to 0.5 ml of 50 % sterile glycerol solution and mixed. The plasmid glycerol stock solution was placed in a -20°C freezer overnight and then stored at -80°C.

2.3.4 QIAGEN Plasmid Purification

A QIAGEN Plasmid Midi Kit was used to obtain ultrapure, transfection grade plasmid DNA. A single colony was selected from a freshly streaked glycerol plasmid stock LB agar plate containing the selective antibiotic. In a 50 ml tube, a starter culture of 5 ml sterile LB broth with selective antibiotic was inoculated. The tube was loosely capped and incubated for approximately 8 hr at 37 °C in a shaking incubator (approximately 250 rpm). The starter culture was then diluted 1/500. This was carried out by inoculating 25 ml LB broth with selective antibiotic in a 50 ml tube with 50 µl of starter culture. The diluted culture tube was loosely capped and incubated overnight at 37 °C in a shaking incubator. The bacterial cells were harvested by centrifugation at 4500 rpm for 15 min at 4 °C. The cell pellet was resuspended in 4 ml of Buffer P1 and pipetted up and down until no cell clumps remained. Four millilitres of Buffer P2 were added to the tube and the contents were mixed thoroughly by inverting the sealed tube 4-6 times (not vortexing). The tube was then incubated at room temperature (15–25 °C) for 5 min. Four millilitres of chilled Buffer P3 were added and mixed thoroughly by inverting 4-6 times. The tube was incubated on ice for 15 min. It was then centrifuged at 4500 rpm for 30 min at 4 °C. The supernatant containing the plasmid was removed promptly and placed in a fresh 10 ml centrifuge tube. This was centrifuged again at 4500 rpm for 15 min at 4 °C. Meanwhile, a QIAGEN-tip 100 was equilibrated by applying 4 ml of Buffer QBT and the column was allowed to empty completely by gravity flow. The supernatant containing the plasmid was removed promptly and loaded onto the QIAGEN-tip where it was allowed to enter the resin by gravity flow. The QIAGEN-tip was washed with 2 x 10 ml of Buffer QC. The plasmid DNA was eluted from the resin by applying 5 ml Buffer QF. The eluate was collected in a 15 ml tube. The

plasmid DNA was precipitated by adding 3.5 ml room-temperature isopropanol to the eluted DNA. The tube contents were mixed and centrifuged at 4500 rpm for 60 min. The supernatant was carefully decanted and the plasmid DNA pellet was washed with 2 ml of room-temperature 70 % ethanol. The tube was centrifuged at 4500 rpm for 60 min at 4 °C. The supernatant was carefully decanted without disturbing the pellet. The pellet was air-dried for 5 min and the plasmid DNA was dissolved in 100 µl of sterile ultrapure H₂O. The purified plasmid DNA was stored at -20 °C.

2.3.5 Spectrophotometric Analysis of Nucleic Acids

DNA and RNA were quantified by measuring its absorbance at 260 nm (A_{260}). This is the wavelength at which nucleic acids absorb maximally. One microlitre of DNA/RNA was dissolved in 19 µl of sterile ultrapure H₂O in a 20 µl quartz cuvette. The absorbance was measured using a Perkin Elmer Lambda Bio UV spectrometer and the concentration of DNA was calculated using the formula:

$$A_{260} \times \text{Dilution Factor (i.e. 20)} \times 50 \text{ (50}\mu\text{g of pure DNA has } A_{260} \text{ of 1)} \\ = \text{Concentration of DNA (}\mu\text{g/ml)}$$

The concentration of RNA was calculated using the formula:

$$A_{260} \times \text{Dilution factor (i.e. 20)} \times 40 \text{ (40}\mu\text{g of pure DNA has } A_{260} \text{ of 1)} \\ = \text{Concentration of RNA (}\mu\text{g/ml)}$$

The purity of the extracted RNA was determined by calculating the ratio of its absorbance at 260 nm versus its absorbance at 280 nm (A_{260}/A_{280}). Pure RNA has an A_{260}/A_{280} ratio of 2.

2.3.6 Restriction Enzyme Digestion of DNA

Restriction enzymes are isolated from certain bacteria and allow DNA to be cut at specific sites. They are used to determine the length of DNA sequences by using gel electrophoresis, containing DNA markers, following restriction digests. In this way, DNA vectors or fragments may be

identified (Hames and Hooper 2000). A DNA digest was carried out by adding the following components into a 0.5 ml sterile eppendorf:

1 μ g DNA	X μ l
Restriction Enzyme (10U)	1 μ l
RE Buffer (10X)	2 μ l
Sterile Ultrapure H ₂ O	<u>X μl</u>
Final Volume	20 μ l

The tube was placed in a Techne TC-3000 thermocycler and incubated at 37°C for 2 hr. The digested DNA was electrophoresed on a 0.8 % agarose gel, along with a 1 kb DNA ladder and a 100 bp DNA ladder.

2.3.7 DNA Gel Electrophoresis

Agarose gel electrophoreses is used for separating DNA fragments greater than 500 bp in length. The DNA is separated into a series of bands, with the smaller bands migrating through the gel further. The size of each fragment may be determined by comparison to standard DNA fragments of known size in commercial DNA ladders. The DNA may be located on the gel by staining with ethidium bromide which intercalates with the DNA and can be visualised using a UV transilluminator (Hames and Hooper 2000).

Undigested plasmid DNA was electrophoresed on a 1.2 % agarose gel. Restriction enzyme digested DNA plasmids were electrophoresed on 0.8 % agarose gel, while PCR products were electrophoresed on a 1.5 % agarose gel. The appropriate amount of agarose was measured out and added to 50 ml of 1X TAE buffer in a conical flask. The agarose was melted using a microwave. The gel was gently poured into the pre-assembled gel tray and the comb was added. The gel was allowed to set for 30 min. The two temporary sides for the gel tray were removed and the tray with the agarose gel was placed in the gel electrophoresis chamber. The gel was immersed in 1X TAE buffer and the comb was removed from the gel. The samples were prepared by adding loading dye to a 1X final concentration to the DNA samples in a 0.5 ml eppendorf which was then centrifuged briefly to gather the contents at the bottom of the tube. A 1 kb DNA ladder (0.5 μ g) and a 100 bp DNA ladder (1 μ g) were also prepared to determine the

size of the DNA samples run on the gel. The samples were loaded and the power source was switched on and set at 75 V. The gel was allowed to run for 45 min. The power was switched off. The gel was removed from the gel tray and immersed in 400 ml of ultrapure H₂O containing 0.03 mg ethidium bromide. The gel was stained for 15 min. It was then destained for 10 min in ultrapure H₂O. The DNA in the gel was viewed using an Alpha Innotech AlphaImager HP gel imaging system.

2.4 RNA Analysis

2.4.1 RNase-free Environment

RNA, unlike DNA, is easily degraded by hydrolysis, due to the extra -OH group. RNase enzymes degrade RNA and are ubiquitous and resistant to degradation. It is extremely difficult to prevent them from contaminating the RNA in a sample. Precautions must be carried out to prevent or minimize this, such as wearing clean gloves at all times, using aseptic technique and working in a laminar flow cabinet. RNases are resistant to autoclaving and sterile RNase-free plastic pipettes, tips and containers must be used. To ensure solutions are free of RNase contamination, they can be treated with diethylpyrocarbonate (DEPC) and then autoclaved. This is a hazardous chemical and, along with other chemicals used, must be treated with caution (Sambrook and Russell 2001).

2.4.2 RNA Extraction from Cultured Cells

The medium was firstly removed from the culture vessel and 1 ml of TriReagent was added per 10 cm³ of culture vessel surface area. The TriReagent was pipetted up and down several times to mix and the lysate was transferred to a 1.5 ml sterile eppendorf. The eppendorf was left to stand at room temperature for 5 min to allow complete dissociation of nucleoprotein complexes. Two hundred microlitres of chloroform were then added per 1 ml of TriReagent to the eppendorf, the lid closed tightly and vigorously shaken by hand for 15 s. The eppendorf was allowed to stand at room temperature for 5 min. The eppendorf was centrifuged at 12,000 rpm for 15 min at 4°C. The mixture separated into a lower pink phenol-chloroform phase containing protein, a white interphase containing DNA and an upper aqueous phase containing RNA. The upper aqueous phase was transferred to a fresh 1.5 ml sterile eppendorf and the RNA was precipitated by adding

0.5 ml isopropyl alcohol per 1 ml TriReagent used in sample preparation. The contents were mixed by pipetting up and down and the eppendorf was then allowed to stand at room temperature for 10 min. The eppendorf was then centrifuged at 12,000 rpm for 10 min at 4°C. The supernatant was carefully removed after centrifugation and the RNA pellet was washed with the addition of 1 ml 70 % ice-cold ethanol per 1 ml of TriReagent used. The tube was inverted several times (not vortexed) and centrifuged at 7,500 rpm at 4°C for 5 min. The supernatant was removed and the RNA pellet was allowed to air-dry for 5 min. The RNA pellet was then dissolved in 40 µl of DEPC-treated H₂O and pipetted up and down gently to ease dissolution. The eppendorf was incubated at 60°C for 10 min and then stored at -20°C.

2.4.3 RNA Gel Electrophoresis

The extracted RNA was quantified as described above. The quality of the RNA extracted from the cells was then determined using denaturing gel electrophoresis. In order to remove any RNases from the RNA gel electrophoresis apparatus, the RNA gel electrophoresis tank, gel tray, comb and lid were washed in detergent and rinsed with DEPC-treated H₂O. The apparatus was then rinsed with 100 % ethanol and allowed to air dry. It was then rinsed thoroughly with DEPC-treated H₂O and again allowed to air dry.

A 1 % formaldehyde denaturing gel was made up by mixing the following:

Agarose	0.5 g
DEPC-treated H ₂ O	43.5 ml

The agarose was dissolved using a microwave. The agarose gel solution was cooled to 60 °C and the following were added in the fume hood, forming a 50 ml gel:

10X MOPS running buffer	5.0 ml
Formaldehyde 37 %	1.5 ml

The gel was poured in the fume hood, the comb was added and the gel was allowed to set for 30 min. The gel was immersed in 1X MOPS running buffer and pre-run for 5 min at 75 V. Each RNA sample was prepared by mixing the following in an eppendorf:

RNA	6.0 μ l
10X MOPS Running Buffer	1.0 μ l
Formaldehyde	1.0 μ l
Formamide	3.0 μ l
Loading dye	1.0 μ l

The eppendorf was briefly centrifuged to collect the contents at the bottom of the tube. The samples were loaded into the wells and the gel was electrophoresed for 45 min at 75 V. The gel was stained in 400 ml of ultrapure H₂O containing 0.03 mg ethidium bromide for 1 hr. The gel was destained in DEPC-treated H₂O for 10 min. The RNA samples were then visualized on the gel using an Alpha Innotech AlphaImager HP gel imaging system.

2.4.4 Reverse-Transcription (RT)

Reverse-transcription is the conversion of messenger RNA (mRNA) to its complementary DNA (cDNA) using a reverse transcriptase enzyme. This enzyme uses the mRNA strand as a template while directing deoxyribonucleotides into the growing chain. Thus, when an A,G,C or U nucleotide of the template RNA strand is encountered, the complementary deoxyribonucleotide (i.e., T, C, G or A) is incorporated into the growing DNA strand. This strand is called the first strand cDNA (Glick and Pasternak 2003). Reverse transcriptase produced by the Moloney Murine Leukemia Virus (M-MLV) was used in this study.

2.4.4.1 Reverse Transcription for Standard End-Point PCR

In a sterile 0.5 ml eppendorf, 2 μ g of RNA were added to 1 μ g of random primers. To this, nuclease-free H₂O was added to a final volume of 15 μ l. The eppendorf was placed in a Techne TC-3000 thermocycler and heated to 70°C for 5 min to melt secondary structures within the template RNA. The eppendorf was then immediately placed on ice to prevent secondary structures from reforming. The following components were then added to the tube:

M-MLV 5X Reaction Buffer	5.00 μ l
dNTP mixture (Final concentration 10 mM each dNTP)	5.00 μ l
RNasin® Ribonuclease Inhibitor (25 units)	0.63 μ l
M-MLV RT (200 units)	1.00 μ l
Sterile Ultrapure H ₂ O	<u>13.37 μl</u>
Final Volume	25.00 μ l

The eppendorf was centrifuged briefly to collect the contents at the bottom. It was then placed in the thermocycler at 37°C for 60 min. Afterwards, the eppendorf containing the first strand cDNA produced was stored at -20°C.

2.4.4.2 Reverse Transcription for qPCR using the GoScript Reverse Transcription System

The RNA samples were treated with DNase prior to reverse transcription for qPCR analysis to remove any contaminating genomic DNA. This was carried out by placing the following in a sterile eppendorf:

RNA (3 μ g)	X μ l
RQ1 RNase-free DNase 10X Reaction Buffer	1 μ l
RQ1 RNase-free DNase (1 u/ μ g RNA)	3 μ l
Nuclease-free H ₂ O	<u>X μl</u>
Final Volume	10 μ l

The eppendorf was incubated at 37°C for 30 min. One microlitre of RQ1 DNase Stop Solution was then added to terminate the reaction. The eppendorf was incubated at 65°C for 10 min to inactivate the DNase.

In a 0.5 ml sterile eppendorf, 1 μ g of DNase-treated RNA was added to 0.5 μ g of random primers and nuclease-free H₂O to give a total final volume of 5 μ l. The eppendorf was placed in a thermocycler and heated to 70°C for 5 min to melt secondary structures within the template RNA. The tube was then immediately placed on ice to prevent secondary structures from reforming. The following components were then added to the eppendorf in the order listed:

GoScript 5X Reaction Buffer	4.0 μ l
MgCl ₂ (Final concentration 1.5 mM)	1.2 μ l
PCR Nucleotide Mix (Final concentration 0.5 mM each dNTP)	1.0 μ l
Recombinant RNasin Ribonuclease Inhibitor (20 units)	0.5 μ l
Go Script Reverse Transcriptase	1.0 μ l
Nuclease-Free H ₂ O	<u>7.3 μl</u>
Final Volume	15 μ l

The tube was centrifuged briefly to collect the contents at the bottom. It was then placed in the thermocycler at 25°C for 5 min to anneal. The eppendorf was then incubated in the thermocycler at 42°C for 1 hr. The resulting cDNA was stored at -20°C. Prior to qPCR, the reverse transcriptase was inactivated by heating to 70°C for 5 min.

2.4.5 Polymerase Chain Reaction (PCR) Primer Design

Primers for end-point PCR analysis were designed using the Primer3 online program (<http://primer3.sourceforge.net/>) with the default settings.

Real-time PCR primers and probes were designed by the manufacturers (Thermo Scientific Dharmacon) on submission of the accession numbers of the genes of interest.

2.4.6 End-Point PCR Analysis

Polymerase chain reaction (PCR) is an extremely simple yet powerful technique. It allows enormous amplification of any specific sequence of DNA provided that short sequences either side of it are known. A PCR reaction contains the target DNA, two primers that hybridise to flanking sequences on opposing strands of the target, all four deoxyribonucleotide triphosphates and a DNA polymerase. PCR consists of three steps: denaturation, primer annealing and elongation, which take place at different temperatures. Automated thermocyclers are used to cycle the reaction many times, taking only a few hours (Hames and Hooper 2000).

Per 50µl reaction:	µl
5X Green Go Taq Buffer	10.00
dNTP mix (Final concentration 10 mM each dNTP)	1.00
Go Taq DNA polymerase (5 U/µl)	0.25
Forward primer 10µM	1.00
Reverse primer 10µM	1.00
Template cDNA	2.00
Sterile Ultrapure H ₂ O	<u>34.75</u>
Total volume	50.00

The reaction tubes were briefly centrifuged and placed in a Techne TC-3000 thermocycler. The corresponding PCR program was run (with a heated lid at 105°C).

B-actin, ICAM-1 and VCAM-1 PCR Program:

Initial Denaturation	95°C for 3 min	1 cycle
Denaturation	95°C for 45 s	β-actin: 18 cycles ICAM-1, VCAM-1: 30 cycles
Annealing	61°C for 45 s	
Extension	72°C for 45 s	
Final Extension	72°C for 7 min	1 cycle

A20, ABIN-1, ABIN-2 and Cezanne PCR Program:

Initial Denaturation	95°C for 3 min	1 cycle
Denaturation	95°C for 45 s	A20, ABIN-1: 23 cycles ABIN-2, Cezanne: 25 cycles
Annealing	60°C for 45 s	
Extension	72°C for 45 s	
Final Extension	72°C for 7 min	1 cycle

The PCR products were visualised on agarose gels (without the addition of loading dye, due to the use of Green Go Taq buffer in the PCR reaction mixture) as described in section 2.3.7 above.

2.4.7 Quantitative PCR (qPCR)

Quantitative or real-time PCR is a technique which amplifies specific DNA sequences and measures their concentration simultaneously using fluorescence-detecting thermocyclers. The rate of accumulation of amplified DNA is plotted over the course of an entire PCR. Therefore, qPCR has the ability to quantify the DNA product during the exponential phase of the PCR, yielding improved precision in quantifying the DNA. It is also less sensitive to differences in the efficiency of amplification (Sambrook and Russell 2001).

The fluorescent reporter probe method was used to detect amplified DNA. This method uses an oligonucleotide probe that binds to an internal sequence with the target DNA sequence. The probe has a fluorescent group attached at the 5' end and a fluorescent quencher at the 3' end (Sambrook and Russell 2001). Eclipse probes were used which, in the unhybridised form, are quenched due to their coil formation, where the reporter and quencher are close together. When hybridised to a sequence within the target with the aid of minor groove binders, however, the probe is linearised and the reporter is separated from the quencher, resulting in fluorescence. The amount of target DNA produced is directly proportional to the intensity of the fluorescence (Bio-Rad Laboratories Inc. 2011).

The reagents were thawed on ice, mixed and briefly centrifuged before use. The Solaris Master Mix was not vortexed. The reaction mix was prepared for a Thermo-Fast non-skirted 96-well PCR plate (Abgene) as follows:

	Per well
Solaris qPCR Master Mix (2X)	12.50 μ l
Solaris Primer/Probe Set (20X)	1.25 μ l
cDNA Template	2.00 μ l
PCR grade H ₂ O	<u>4.25 μl</u>
Final Volume	25.00 μ l

The plate was sealed with SealPlate (Excel Scientific) optically clear film and the wells were checked for bubbles. Any bubbles, if present, were removed. Each sample was analysed in triplicate and a no template control (containing PCR grade H₂O) was included to assess any potential reagent contamination. The plate was placed into a Bio-Rad iCycler iQ Optical Module qPCR instrument and the following thermal cycle was run:

Enzyme Activation	95°C for 10 min	1 cycle
Denaturation	95°C for 15 s	} 40 cycles
Annealing/Extension	60°C for 60 s	

The fluorescent data was collected at the annealing/extension step at each cycle. This program was run for each of the genes of interest (A20, ABIN-1, ABIN-2, Cezanne) and for the control gene, GAPDH). The $2^{-\Delta\Delta CT}$ (Livak) method (Livak and Schmittgen 2001) was used to calculate the change in gene expression levels using the cycle threshold (C_T) values obtained (the cycle number at which the fluorescence produced crosses the threshold) as described below.

1. The C_T of the target gene was normalized to that of the reference gene, for both the test sample and the calibrator sample as follows:

$$\Delta C_{T(\text{test})} = C_{T(\text{A20 TNF 4 h})} - C_{T(\text{GAPDH TNF 4 h})}$$

$$\Delta C_{T(\text{calibrator})} = C_{T(\text{A20 TNF 0 h})} - C_{T(\text{GAPDH TNF 0 h})}$$

2. The ΔC_T of the test sample was normalized to the ΔC_T of the calibrator:

$$\Delta\Delta C_T = \Delta C_{T(\text{test})} - \Delta C_{T(\text{calibrator})}$$

3. The expression ratio was then calculated:

$$2^{-\Delta\Delta CT} = \text{Normalised expression ratio}$$

The data obtained was statistically analysed using Student's *t* tests in Microsoft Excel.

2.5 Cell Culture Techniques

Cell culture involves the growth of cells in the laboratory where the appropriate conditions for survival and proliferation of the cells are provided. Cell culture techniques are widely used for research and diagnostic purposes and in the pharmaceutical industry. Strict adherence to aseptic technique and the use of sterile solutions and equipment are necessary to avoid bacterial, viral and/or fungal contamination of cells in culture (Phelan 1998).

Cell culture techniques were carried out aseptically, in a sterile environment using a Faster Ultrasafe Grade II Biohazard laminar flow cabinet. The cells were visualised using an Olympus CKX41 inverted microscope.

2.5.1 Cell Culture

Human immortalised synovial fibroblasts (K4 IM cell line) and human immortalised chondrocytes (SW 1353 cell line) were grown in RPMI-1640 medium supplemented with 10 % (v/v) heat-inactivated fetal bovine serum (FBS), 100 U/ml penicillin, 100 µg/ml streptomycin and 10 mM/ml L-glutamine in Sarstedt 75 cm³ culture flasks which were incubated in a humid environment at 37°C with 5 % CO² in a Binder cell culture incubator. Cells were fed when required by removing the used medium which was discarded into disinfectant and replacing it with an appropriate volume of fresh supplemented media (pre-heated to 37°C). If feeding for the first time since thawing and seeding cells, only half of the used medium was removed and replaced with fresh medium. Prior to feeding, the cells were viewed under the microscope to determine % confluency and checked for the presence of contamination. The cells were subcultured when approximately 80 % confluent. The medium was removed from the flask and the cells were washed with approximately 2 ml sterile phosphate-buffered saline (PBS) which was then removed. The cells were trypsinized by adding the appropriate volume of trypsin-EDTA (enough to cover the bottom surface of the flask) and placed back in the incubator (at 37°C) for 5 min or until the cells were observed to detach from the surface of the flask. An equal volume of supplemented medium was then added to the flask to neutralise the trypsin-EDTA solution. The cell suspension was transferred into a sterile centrifuge tube and centrifuged at 400 rpm for 5 min. The supernatant was removed and discarded into disinfectant. The cell pellet was resuspended in the appropriate volume of supplemented medium and transferred into a new cell

culture flask. Approximately 15 ml of supplemented medium were added to the flask. The passage number of the cells was recorded. The flask was then placed in the CO² incubator.

2.5.2 Cryopreservation of Cells

Early passage number cells were grown up and then cryopreserved in a mixture of dimethyl sulfoxide (DMSO), FBS and supplemented medium and stored at -80°C in order to build up cell stocks. The cells were grown to approximately 70 % confluency. The cells were trypsinized as described above. The cell suspension was centrifuged at 800 rpm for 5 min. The supernatant was removed and discarded. One millilitre of FBS and 3.5 ml of supplemented media were placed in a fresh sterile 15 ml tube. The cell pellet was transferred into the FBS/supplemented medium mixture and mixed by pipetting up and down once or twice. The mixture was aliquotted into five 1 ml sterile cryotubes which were pre-labelled with the cell type, date and passage number. One hundred microlitres of DMSO were then added to each cryotube. The cryotubes were stored in a New Brunswick Scientific Ultra-Low Temperature Freezer at -80°C.

2.5.3 Heat Inactivation of Serum

Fetal bovine serum (FBS) at room temperature was placed in a clean waterbath at 56°C for 30 min. The serum was aseptically aliquotted into 50 ml sterile containers, labelled and stored at -20°C.

2.5.4 Supplementation of Media

Supplemented RPMI (500 ml) was prepared as follows:

RPMI culture medium	440 ml
Inactivated FBS	50 ml
Penicillin 10,000 U/ml Streptomycin 10 mg/ml	5 ml
L-glutamine 2 mM/ml	5 ml

The bottle of media was labelled “supplemented” and dated and placed in the cell incubator at 37°C for 24 hr to check for the presence of contamination. The supplemented medium was then stored at 4°C.

2.5.5 Counting Cells

Cell counts were obtained using an Improved Neubauer haemocytometer. The cell monolayer was trypsinized and the trypsin was neutralised with the addition of supplemented medium. The cell suspension was mixed thoroughly to disperse any clumps and 90 µl were transferred into a sterile eppendorf. Ten microlitres of Trypan blue solution were added to the eppendorf and mixed. Trypan blue is a viability stain which dyes dead cells blue. Viable cells are not stained and remain clear. The haemocytometer and a coverslip were cleaned with lens tissue dipped in 70 % ethanol. The coverslip was then placed over the grooves and semi-silvered counting area of the haemocytometer. Twenty microlitres of the cell suspension/Trypan blue mixture were transferred to the haemocytometer counting chamber. The viable cells were visualised and counted using a light microscope and 10X objective lens. The number of viable cells/ml was determined using the following formula:

$$\text{Average cell count} \times \text{Dilution factor} \times \text{Volume of Haemocytometer}$$

2.5.6 TNF- α Stimulation of Cells

Cells were grown in Sarstedt 25 cm² culture flasks to approximately 80 % confluence and then serum-starved by replacing the supplemented medium with serum-free RPMI-1640 medium containing 100U/ml penicillin, 100µg/ml streptomycin and 2mM/ml L-glutamine for 24 hr. The cells were then stimulated with 10ng/ml recombinant human TNF- α which had been resuspended in PBS with 0.1 % BSA (+TNF). The medium in control wells/flasks was replaced with either fresh serum-free medium (-TNF) or serum-free medium containing 1µl/ml vehicle (containing only PBS with 0.1 % BSA) (Veh). The flasks were then incubated until the appropriate time period had elapsed.

2.5.7 Transfection of Cells using Turbofect Transfection Reagent

Cells were grown in Sarstedt 75 cm³ cell culture flasks to 70-80 % confluency. The cells were then trypsinized and counted using a haemocytometer. Cells were seeded into Thermo Scientific Nunc Nunclon Delta Surface 24-well culture plates at a concentration of 1.4×10^4 cells per well. Twenty-four hours later, the cells were serum-starved by replacing the supplemented medium with serum-free medium, as described above. Transfections using Turbofect were carried out 24 hr later in triplicate, according to the manufacturer's instructions (Turbofect, Fermentas). A total of 900 ng of Qiagen-purified plasmid DNA were added to 50 μ l of serum-free medium (SFM) in a sterile eppendorf, followed by the addition of 1 μ l of the transfection reagent, Turbofect, for each well. The contents were mixed and briefly centrifuged, before incubating at room temperature for 15 min. The medium in each well was removed. The DNA/SFM/Turbofect mixture was added to 0.5 ml of SFM, mixed and then added to the well. The plate was incubated at 37°C in a CO₂ incubator for 24 hours.

2.5.8 Transfection of Cells using GeneJuice Transfection Reagent

Cells were grown in 75 cm³ Greiner Bio-one cellstar cell culture flasks to 70-80 % confluency. The cells were then trypsinized and counted using a haemocytometer. Cells were seeded into a 24-well culture plate at a concentration of 0.5×10^5 cells per well. Twenty-four hours later the cells were transfected using GeneJuice as follows: Working solutions of Qiagen-purified plasmid DNA were prepared at a concentration of 100 μ g/ μ l using TE buffer. Using the plasmid working solutions, a total of 325 ng of DNA were diluted to a volume of 25 μ l with SFM for each well to be transfected. In a separate eppendorf, 0.75 μ l of Genejuice were diluted to a volume of 25 μ l with SFM for each well to be transfected. This was incubated at room temperature for 5 min and then added to the diluted plasmid DNA and mixed. The DNA/GeneJuice/SFM mixture was incubated at room temperature for 10 min. The medium in each well was removed. The DNA/GeneJuice/SFM mixture was added to 450 μ l of supplemented medium, mixed and then added to the well. The plate was incubated at 37°C in a CO₂ incubator for 24 hours.

2.5.9 Luciferase Assays

The luciferase assays were carried out 24 hours post transfection, as per the manufacturer's instructions (Promega). The medium was removed from the wells of the 24-well plate and each well was rinsed with 0.5 ml sterile PBS. The cells in each well were lysed with the addition of 100 μ l of 1X Passive Lysis Buffer and the plate was placed in a shaking incubator for 15 min at room temperature. The lysates were assayed for firefly (*Photinus pyralis*) luciferase and *Renilla* (*Renilla reniformis*) luciferase activities using the Dual Luciferase® Reporter (DLR™) Assay System and a manual single-sample Modulus luminometer. For each sample to be assayed, 100 μ l of Luciferase Assay Reagent II (LARII) were predispensed into a 1.5 ml eppendorf. Twenty microlitres of cell lysate were transferred into the eppendorf and pipetted up and down five times to mix (not vortexed). The eppendorf was placed into a Turner Biosystems Modulus single sample luminometer and the firefly luciferase activity was measured. To the same eppendorf, 100 μ l of Stop & Glo® Reagent were added and the contents were vortexed briefly to mix. The eppendorf was placed back in the luminometer and the *Renilla* luciferase activity was measured. Firefly luciferase values were normalised to *Renilla* luciferase activity and the results were presented in terms of the mean fold change plus the standard error of the mean (SEM) compared to the NBRE reporter construct alone. The data obtained was statistically analysed using Student's *t* tests in Microsoft Excel.

2.5.10 Green Fluorescent Protein (GFP) Assay

In order to ascertain the transfection efficiency of the transfection reagent Turbofect for each of the two cell lines, K4 IM synoviocytes and SW 1353 chondrocytes, GFP assays were carried out on both cell lines and the results compared. Both cell types were seeded into 24-well culture plates at densities of 1.4×10^4 cells/well and 2.5×10^4 cells/well. The pmaxGFP expression vector was transfected into each cell line at concentrations of 100, 250 and 500 ng/well using Turbofect, as described in section 2.5.7 above, and 24 hr later both cell types were viewed and photographed using the Olympus IX51 inverted fluorescent microscope with a mercury lamp and Olympus DP70 digital camera system. The percentage transfection efficiency was determined by calculating the ratio of the number of cells expressing GFP to the total number of cells present.

2.5.11 Test for Mycoplasma

Mycoplasmas are one of the smallest free-living forms of bacteria and lack a bacterial cell wall. They are found widely in nature, the majority being host-specific commensals colonizing many species including plants, insects, mammals and humans. Mycoplasmas are a major cause of cell culture contamination resulting in a substantial change in the biological characteristics of cells (Volokhov *et al.* 2011). The Venor® GeM Mycoplasma Detection Kit for conventional PCR was used to test cell cultures for the presence of Mycoplasma contamination. The kit allows for the detection of *Mycoplasma (M.) orale*, *M. hyorhinitis*, *M. arginini*, *M. fermentans*, *M. salivarium*, *M. hominis*, *M. pneumoniae*, *M. synoviae*, *Acholeplasma laidlawii* and *Ureaplasma* species. Mycoplasmas are identified by amplifying the 16S rRNA coding region of the mycoplasma genome. The test was carried out according to the manufacturer's instructions (Minerva Biolabs). All reagents used in the test (including 10 X Reaction buffer) were provided in the kit except for the DNA polymerase.

One hundred microlitres of cell culture supernatant from cultures at 90 – 100 % confluence were transferred into a sterile 0.5 ml eppendorf. The sample was incubated at 95°C for 5 min and briefly centrifuged to pellet cellular debris. Two microlitres of this sample were used in the PCR reaction. Samples were tested in duplicate. An internal control was included in all samples. PCR grade water was used for the negative control.

Per 25 µl reaction:	µl
PCR grade water	15.3
10X Reaction buffer	2.5
Primer/Nucleotide mix	2.5
Internal Control DNA	2.5
Go Taq DNA Polymerase (5 U/ µl)	0.2
Sample/Positive/Negative Control	<u>2.0</u>
Total volume	25.0

The reaction tubes were briefly centrifuged and placed in a Techne TC-3000 thermocycler. The following PCR program was run (with a heated lid at 105°C).

Initial Denaturation	94°C for 2 min	1 cycle
Denaturation	94°C for 30 s	} 39 cycles
Annealing	55°C for 30 s	
Extension	72°C for 30 s	
Cooled to 4° C		

The PCR products, along with DNA markers, were electrophoresed on a 1.5 % agarose gel at 100 V for 40 min. The gel was stained in approximately 400 ml of ultrapure H₂O containing 0.03 mg ethidium bromide. The gel was stained for 15 min. It was then destained for 10 min in ultrapure H₂O. The DNA in the gel was viewed using an Alpha Innotech AlphaImager® HP gel imaging system.

An internal control DNA band at 191 bp in all samples indicated that the PCR was successful. A band at approximately 267 bp (other than in positive control) would have indicated the presence of mycoplasma contamination.

lyit | Institiúid Teicneolaíochta Leictreonaigh
 Letterkenny Institute of Technology

Chapter 3

Bioinformatic Analysis of A20, ABIN-1, ABIN-2 and Cezanne

lyit | Institiúid Teicneolaíochtaí Leictreonaíochtaí
Letterkenny Institute of Technology

3. Bioinformatic Analysis of A20, ABIN-1, ABIN-2 and Cezanne

3.1 Introduction

The objectives of the study were to investigate the potential role of the NR4A subfamily of nuclear receptors in the regulation of A20 and A20-interacting proteins and to examine the potential of A20 as a means of modulating the NR4A subfamily in the pathogenesis of rheumatoid arthritis. The three members of the NR4A subfamily bind to the same *cis*-acting consensus sequence (AAAGGTCA), known as NBRE or NGFI-beta (nerve growth factor-induced clone B) response element, in order to regulate target gene expression (Wilson *et al.* 1991). Bioinformatic analysis of A20 and the A20-interacting genes was carried out to determine whether the transcription factor binding site for the NR4A subfamily (the NBRE site) is present in these genes. If the NBRE binding site is identified in these genes, this would give an indication that the NR4A subfamily of nuclear receptors may directly lead to the induction of A20, ABIN-1, ABIN-2 and Cezanne gene expression, potentially adding to the few known target genes of this subfamily of orphan nuclear receptors.

3.2 Bioinformatic Analysis

The Genomatix software package (<http://www.genomatix.de>) was used for all bioinformatic analyses. The promoter regions of the genes of interest were identified using Gene2Promoter, a Genomatix software tool. Gene2Promoter permits the extraction and analysis of the promoter sequences of genes. The Gene IDs of the genes of interest were obtained from the National Center for Biotechnology Information (NCBI) and entered into the Gene2Promoter input page. The resulting promoter regions were analysed from 1000 bp upstream of the transcription start site to 100 bp downstream. MatInspector, another Genomatix software tool, was used for the identification of transcription factor binding sites (TFBSs) within these promoter regions.

Potential consensus NBRE sequences were identified in the promoter regions of A20, ABIN-1, ABIN-2 and in two Cezanne promoters identified by Gene2Promoter (see Table 3.1 and Fig. 3.1). However, this transcription factor binding site was located in the promoter of what Genomatix termed a “less relevant transcript” of ABIN-2. Genomatix defines a less relevant transcript as

being one that is most likely not relevant in creating the main product of a gene, based on evaluation of the exon/intron structure of all alternative transcripts within a locus.

Genomatix provides the DNA sequences identified within DNA sequences with core similarity and matrix similarity scores (given in Table 3.1). Core similarity is the score given for the similarity between the highest conserved bases or “core sequence” (usually four bases written in capital letters) within the defined TFBS and the putative binding site identified in the promoter of interest. The maximum core similarity score is 1.0 and is given when the core sequence of the identified binding site matches the predefined TFBS exactly. The matrix similarity is the value given for the complete sequence of the binding site. Genomatix describes a “good” match as having a matrix similarity of > 0.80.

The NR4A binding site (NBRE) sequence is AAAGGTCA (Wilson *et al.* 1991).

Table 3.1 Potential NBRE sequences identified within A20 and A20-interacting Genes using Genomatix Software

Gene	Potential NBRE sequence	Position from – to	Strand	Core Similarity	Matrix Similarity
A20	cca aGAGGtca tgtg	379-393	(+)	0.763	0.862
ABIN-1	caa aAAGGtta gatg	214-228	(-)	1.000	0.869
ABIN-2	gga aAAGGtcg cctc	536-550	(+)	1.000	0.871
Cezanne	tag aAAGGtga gaga	184-198	(-)	1.000	0.860
Cezanne	gtc cAAGGtca catg	102-116	(-)	1.000	0.929

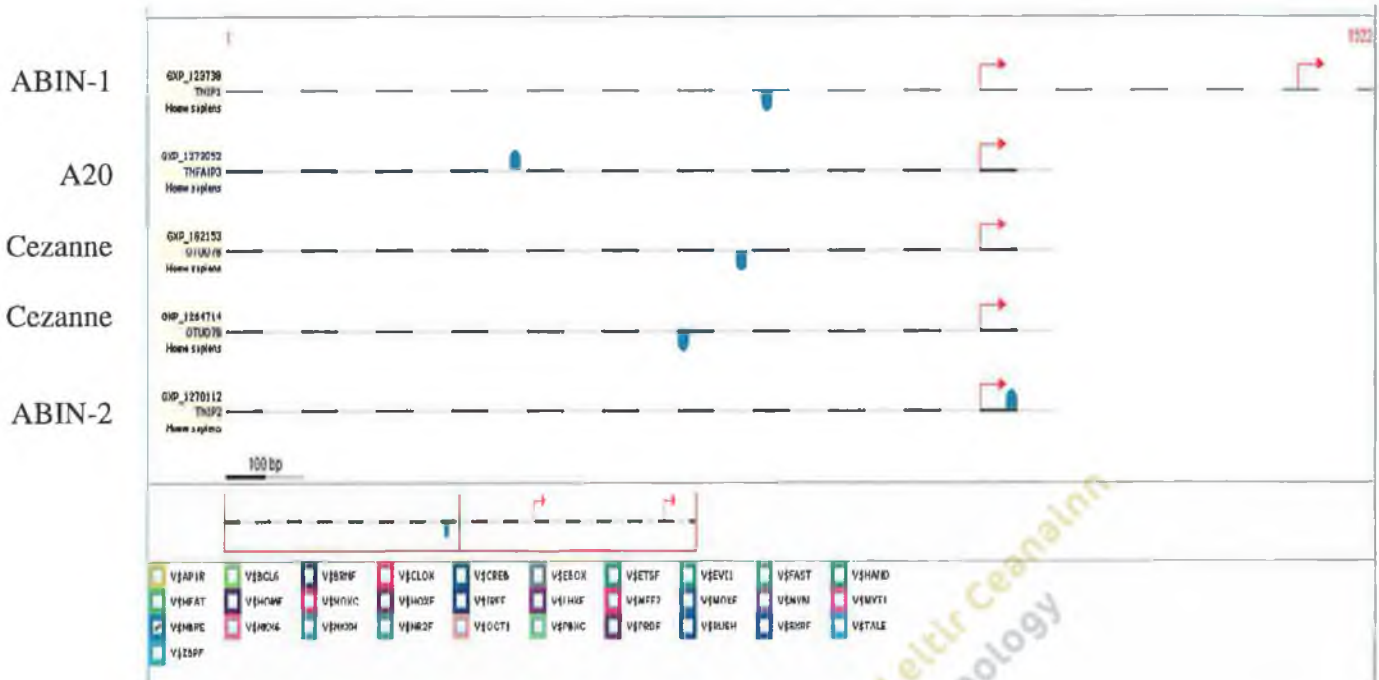


Fig. 3.1 Schematic representation of potential consensus NBRE sites (in blue) in the promoter regions of A20 (TNFAIP3), ABIN-1 (TNIP1), ABIN-2 (TNIP2) and in two Cezanne (OTUD7B) promoters generated using Genomatix. The black and grey patterned lines represent the sequence of the promoters. — 100 bp □ Transcription Start Site

The promoters identified were analyzed for the NF-κB transcriptional binding site using MatInspector. The results are shown in Fig. 3.2 below.

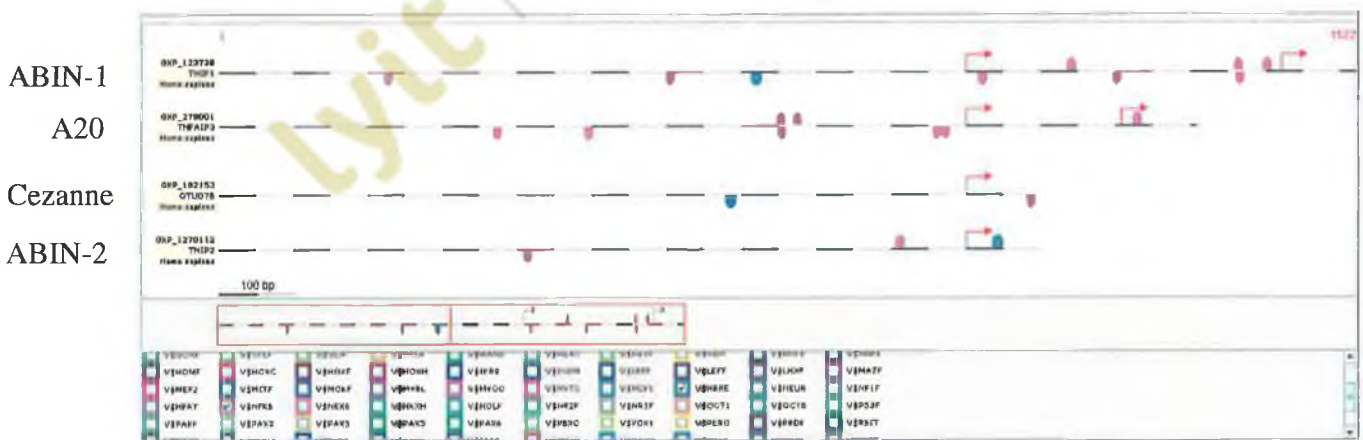


Fig. 3.2 Potential consensus NBRE sites (blue) and NF-κB binding sites (pink) identified in the promoter regions of A20, ABIN-1, ABIN-2 and Cezanne using Genomatix software. The black and grey patterned lines represent the promoter sequences. □ Transcription Start Site.

Genomatix extracts several promoters for each gene of interest from the information available in the databases. The promoter of A20 in which the NBRE site was detected does not contain any NF- κ B binding sites. NF- κ B is known to bind to the promoter of A20 and induce its transcription. A study by Krikos *et al.* (1992) found that TNF- α induction of A20 required two NF- κ B elements located 54 and 66 bp upstream of the transcription start site. These two NF- κ B binding sites appear to be present in the A20 promoter above, however. The NBRE TFBS was identified in the promoters of Cezanne and ABIN-1 which also contain NF- κ B binding site(s). ABIN-1 has been identified as an NF- κ B target gene in the Hodgkin's disease derived cell lines L428 and HDLM2 and in keratinocytes (Hinz *et al.* 2002; Hinata *et al.* 2003). Therefore, the NF- κ B transcriptional binding sites identified within the ABIN-1 promoter may mediate induction of this gene. Furthermore, the NBRE site found within this promoter may be involved in the induction of ABIN-1.

In order to elucidate whether the potential NBRE TFBSs identified may be functional, the A20 and the A20-related gene promoters were analysed to determine if a common promoter model containing the NBRE site is present. According to Genomatix, functionality may be determined by the context of the promoter sequence. If a TFBS is located within a framework of two or more binding sites, this provides evidence that the individual sites in the framework may be functional. Therefore, identification of a promoter model representing a framework of two or more TFBSs within a defined distance and strand orientation can provide an indication that the matching sites are functional because it is more specific (Genomatix 2009).

In order to search for a promoter model containing the NBRE site, Frameworker was used which is a Genomatix software tool designed for the comparative analysis of promoter sequences and allows the extraction of a common framework of TFBSs from a set of DNA sequences (Genomatix 2009).

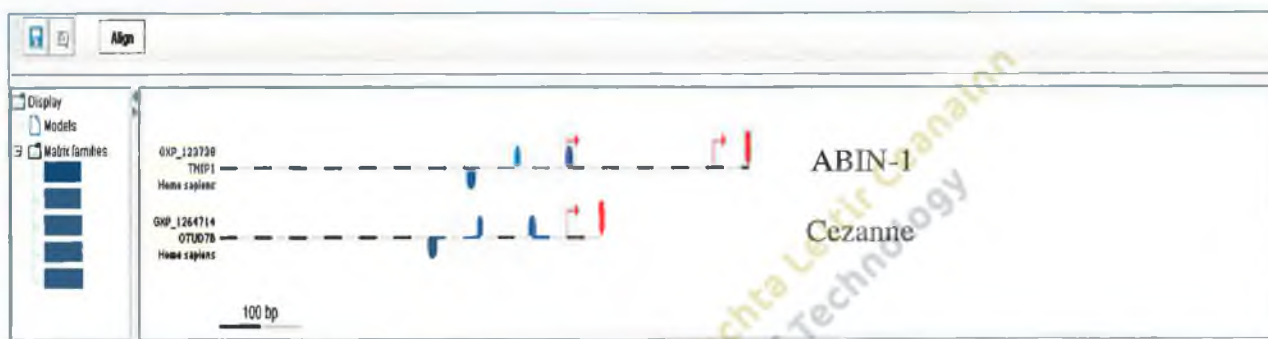
The promoters containing the NBRE site were selected for Frameworker analysis and the default parameters were used. It should be noted that Frameworker uses strand-specific TFBSs for constructing promoter models, meaning that Frameworker only compares TF sites with the same strand orientation. Several promoter models containing the NBRE site were found that were common to both ABIN-1 and Cezanne genes (see Fig.3.2), indicating that this binding site may be functional in these A20-interacting genes. These models included the TF matrix families

E2FF, MOKF, MYT1, NR2F, RXRF and SORY. The definition of these TF matrix families are given in Table 3.2.

A

Element	Strand	Matrix sim.	Distance to next element	Common to	p-value
1 V\$NBRE	-	Optimized (min. 0.87)	3 - 3 bp		
2 V\$NR2F	-	Optimized (min. 0.76)	2 - 2 bp		
3 V\$RXRF	-	Optimized (min. 0.81)	134 - 137 bp	2 matches in 2 seq. (40 %), 2 non-overlapping	7.98562e-07
4 V\$SORY	+	Optimized (min. 0.87)	149 - 151 bp		
5 V\$MOKF	+	Optimized (min. 0.98)	---		

Graphical output:



B

Element	Strand	Matrix sim.	Distance to next element	Common to	p-value
1 V\$MYT1	+	Optimized (min. 0.80)	141 - 150 bp		
2 V\$NBRE	-	Optimized (min. 0.86)	5 - 6 bp	2 matches in 2 seq. (50 %), 2 non-overlapping	4.79329e-07
3 V\$RXRF	-	Optimized (min. 0.81)	141 - 144 bp		
4 V\$E2FF	+	Optimized (min. 0.76)	---		

Graphical output:

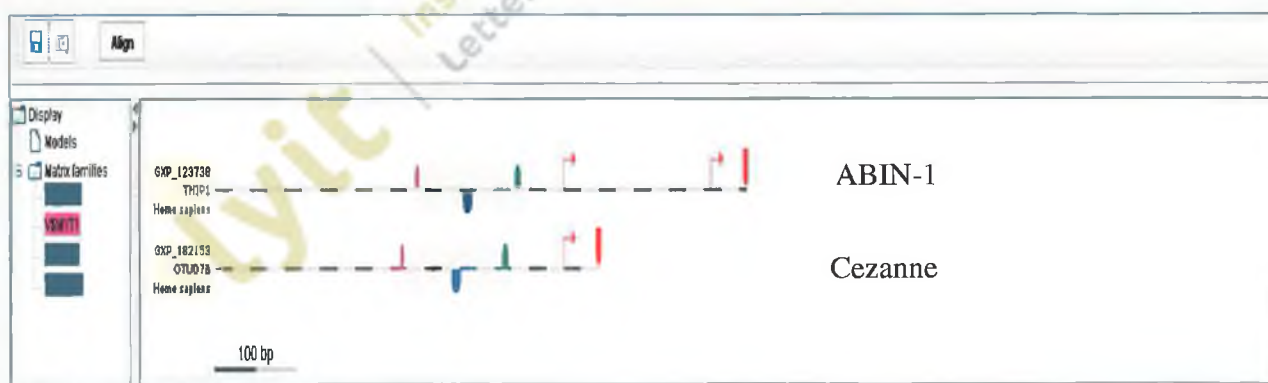



Fig. 3.3 Examples of promoter TF models containing the NBRE site which were identified by Frameworker as being common to the promoters of ABIN-1 and Cezanne. The coloured semi-circles represent the matrix families of TFBSs. The black and grey patterned lines represent the sequence of the promoters. Symbols above or below the sequence line represent the TFBSs present on the positive or negative strand, respectively.  Transcription Start Site — 100 bp

Table 3.2 Definitions of TF matrix families that have been identified in promoter models which are common to the promoters of ABIN-1 and Cezanne and which also contain the NBRE site.

TF matrix family	Definition (Genomatix 2009)
E2FF	E2F-myc activator/cell cycle regulator
MOKF	Mouse Krueppel-like factor
MYT1	Myelin transcription factor 1 neuronal C2HC zinc finger protein
NR2F	Nuclear receptor subfamily 2 factors
RXRF	Retinoid X receptor heterodimer binding sites
SORY	SOX/SRY-sex/testis determining and related HMG box factors

Another Genomatix software tool, ModelInspector, was also used to analyse the promoter sequences. ModelInspector uses a library of predefined promoter modules to examine DNA sequences for matches to these models. This library contains models for functional subunits of promoters. All promoter modules in the library are experimentally verified. The promoters were searched for promoter modules containing the NBRE binding site. The NBRE AP1F 01 module (from the Module Library Version 5.4) was identified within the ABIN-1 promoter. Genomatix states that NUR77 and c-Jun have additive effects on the StAR (mouse steroidogenic acute regulatory protein) promoter. The fact that the NBRE site detected is part of a promoter module provides further evidence that this site may be functional in ABIN-1.

In addition, ModelInspector also found several NF- κ B-containing promoter modules within the NBRE-containing ABIN-1 promoter. These were ETSF NF- κ B 02, NF- κ B NF- κ B NF- κ B 01, NF- κ B RBPF 01 and NF- κ B SP1F 04. As the NF- κ B sites identified within ABIN-1 form part of several promoter modules, this supports the theory that they may mediate transcriptional activation of this gene.

The NBRE site, being present in the promoter of a less relevant transcript of ABIN-2, indicates that this TF site is not likely to be functionally significant in this gene. The NBRE site is present in a promoter of A20 in which no NF- κ B TFBSs were detected and NF- κ B is known to induce A20 expression (Krikos *et al.* 1992). This also indicates that the NBRE site identified in this

gene may not be functionally significant. However, the Frameworker and ModelInspector results point to the NBRE binding site being functional in ABIN-1 and Cezanne.

The promoter regions of the A20-related genes were examined further in order to ascertain if they have a similar promoter organizational structure. If a common promoter model is found in all four genes, it could then be used to search the human genome for potential co-regulated genes not previously identified as being functionally related.

ModelInspector was again used for this analysis. The promoters identified by Gene2Promoter can be assigned to several alternative transcripts within a locus. Genomatix assigns the alternative transcripts with three possible quality levels. Gold transcripts are experimentally verified 5' complete transcripts. Silver transcripts are those with a 5' end confirmed by PromoterInspector prediction and bronze transcripts are annotated with no confirmation for 5' completeness. Using ModelInspector, the Genomatix-defined gold transcript promoters of A20, ABIN-1, ABIN-2 and Cezanne genes were searched for common promoter modules from Promoter Module Library Version 5.0 and default parameters were used. Two common promoter modules were identified as being present in the gold transcript promoters of the four genes of interest and these are given in Table 3.3. The first was SP1F SP1F 04. According to Genomatix (2009) two SP1 binding sites are essential for podoplanin promoter activity. Podoplanin promotes the formation of elongated cell extensions and increases endothelial cell adhesion, migration and tube formation (Hartz 2009). The second was EGRF SP1F 01. Egr-1 and Sp family proteins play a reciprocal role in the control of expression from the PTPIB (protein tyrosine phosphatase) and the ABCA2 (adenosine 5'triphosphate-binding cassette, subfamily A, member 2) promoters (Genomatix 2009).

Table 3.3 Promoter modules identified using ModelInspector as being common to A20, ABIN-1, ABIN-2 and Cezanne promoters

Module	Function
SP1F SP1F 04	Two SP1 binding sites are essential for podoplanin promoter activity
EGRF SP1F 01	Egr-1 and Sp family proteins play a reciprocal role in the control of expression from the PTPIB (protein tyrosine phosphatase) and the ABCA2 (adenosine 5'triphosphate-binding cassette, subfamily A, member 2) promoters

Several other promoter modules were identified using ModelInspector in three out of the four genes analyzed and these are given in Table 3.4, along with their functions.

Table 3.4 Promoter modules and their functions identified within A20 and A20-interacting genes using ModelInspector (Genomatix 2009)

Module	Function	Genes Identified
ETSF SP1F 02	Mannose receptor C type 1 (MRC1) gene expression is regulated in part by co-operative interaction between the ubiquitously expressed transcription factor SP1 and the lymphoid/myeloid factor PU 1.	A20, ABIN-1, ABIN-2
IKRS AP2F 01	Ap-2 is the main activator and Ikaros functions cooperatively with it for maximal expression of the human P-LAP (placental leucine aminopeptidase) gene. Ikaros family members function as activators of the CD8A gene and that their associated activities are critical for appropriate chromatin remodeling transitions during thymocyte differentiation and lineage commitment.	A20, ABIN-1, ABIN-2
SP1F ETSF 02	Essential for transcriptional activation of the leukocyte surface antigen CD53 gene in different cell lines.	ABIN-1, ABIN-2, Cezanne
SP1F SP1F 05	Specificity protein (Sp) 1 and Sp3 can cooperatively regulate survivin (apoptosis inhibitor 4) promoter activity.	A20, ABIN-2, Cezanne

Frameworker was used to identify other common promoter models not present in the ModelInspector library (and therefore not verified experimentally) within the Genomatix-defined gold transcript promoters of A20, ABIN-1, ABIN-2 and Cezanne. The parameter settings were as default except for the minimum distance between elements parameter, which was set as 1bp. The promoter models identified in all four genes in this manner are given in Table 3.5, along with the model p values assigned by Genomatix. The p value is the probability of obtaining an equal or greater number of sequences containing the model in a set of randomly drawn human promoters. The lower the p value, the higher the specificity of the model.

Table 3.5 Promoter models identified by Frameworker as being common to A20, ABIN-1, ABIN-2 and Cezanne promoters and their p values indicating their specificity

Promoter Model	p value
HESF SP1F	1.4×10^{-7}
SP1F ZBPF	6.6×10^{-4}
EGRF EGRF	0.0021
ZBPF EKLF	0.0034
ZBPF SP1F	0.0073
ZBPF ZBPF	0.0115
NRF1 NRF1	0.0238

A definition of the transcription factor matrix families within these promoter models are given in Table 3.6.

Table 3.6 Definition of TF matrix families within promoter models identified by Frameworker as being common to A20, ABIN-1, ABIN-2 and Cezanne (Genomatix 2009)

TF matrix family	Function
EGRF	Early growth response/nerve growth factor induced protein C & related factors
EKLF	Erythroid Kruppel-like factor
HESF	Vertebrate homologues of enhancer of split complex
NRF1	Nuclear respiratory factor 1 bZIP transcription factor that acts on nuclear genes encoding mitochondrial proteins
SP1F	GC-Box factors SP1/GC

The Genomatix Promoter Database “Promoters of annotated genes” was searched for both the modules identified using ModelInspector and the models found using Frameworker. This database contains a subset of all human promoters. Promoters of hypothetical proteins or genes that are annotated as “similar to” are excluded from this database. Numerous genes were identified which contain each of the promoter module/model (~ 1500 genes). The search was

then restricted to search only the sense (+) strand. The number of genes containing the model HESF SP1F for example, was found to be approximately 650. Among these 650 genes were regulatory factor X, 2 (involved in HLA class II expression), serpin peptidase inhibitor clade B (ovalbumin) member 9 (a serine protease inhibitor involved in many cellular processes), ephrin-A3 (receptor protein-tyrosine kinase), and proteasome subunit, alpha type, 2. Some of these genes may be co-regulated with the A20-related genes. However, the models would need to be further refined in order to identify them. Future work may elucidate these genes.

3.3 Discussion

The NR4A subfamily of nuclear orphan receptors bind to the NBRE (nerve growth factor-induced clone B response element) transcription factor binding site in the promoter of target genes to control their expression. The NBRE site consists of the sequence AAAGGTCA (Wilson *et al.* 1991). A20, ABIN-1, ABIN-2 and Cezanne were analysed using bioinformatic software (Genomatix) to determine whether the NBRE site is present in these genes, potentially linking the expression of these genes to the NR4A subfamily of nuclear receptors.

The Genomatix tool Gene2Promoter was utilised to identify and extract the promoter regions of A20, ABIN-1, ABIN-2 and Cezanne from the EIDorado human genome database for analysis. Gene2Promoter extracts more than one promoter sequence for a given gene. These include promoter sequences for alternative transcripts of a gene. The promoter regions analysed for each gene consisted of 1000 bp upstream of the transcription start site and 100 bp downstream. The Genomatix tool MatInspector was used to analyse these regions for the presence of the NBRE site. The NBRE binding site was indeed located within the promoters of each of the genes of interest (Fig. 3.1), including two Cezanne promoters identified by Gene2Promoter. The NR4A binding site was found to be present on the sense strand of A20 and ABIN-2 promoters and on the antisense strand of ABIN-1 and both Cezanne promoters. The NBRE site was detected within ABIN-1 and Cezanne promoters and Genomatix describes these promoters as corresponding to gold ABIN-1 and Cezanne transcripts. When promoters are identified by Gene2Promoter, it also provides a quality assessment for their corresponding transcripts – gold, silver or bronze. Gold transcripts are experimentally verified and derived from mapping of full length cDNAs. Silver transcripts are supported by PromoterInspector prediction at the 5' end. Bronze transcripts are without additional evidence of their completeness.

However, the ABIN-2 promoter on which the NBRE site was found was, according to Genomatix, the promoter of a “less relevant transcript” of ABIN-2 – one which is not thought to be relevant in creating the main gene product. In addition, the A20 promoter in which the NBRE site was identified does not contain NF- κ B binding sites. NF- κ B is a known inducer of A20 and this indicates that the NBRE site found within A20 may not be functional and that the NR4A binding site found within ABIN-2 may not be relevant. NF- κ B binding elements were identified in the promoters of experimentally verified 5' complete transcripts of each of the genes of interest (Fig. 3.3), including two NF- κ B sites at approximately 50 bp upstream of the A20 promoter transcription start site. TNF- α induction of A20 requires two NF- κ B elements located 54 and 66 bp upstream of the transcription start site (Krikos *et al.* 1992) and the sites identified, among others, appear to correspond with these. This means that the NBRE site found in an alternative promoter may not be functional in controlling A20 expression. However, it may be that this A20 transcript is regulated by an alternative TF to NF- κ B.

The sequences of the NBRE sites found within the promoters of the genes of interest are given in Table 3.1, along with their locations. Genomatix provides the DNA sequences identified within DNA sequences with core similarity and matrix similarity scores (also given in Table 3.1). Core similarity is the score given for the similarity between the highest conserved bases or “core sequence” (usually four bases written in capital letters) within the defined TFBS and the putative binding site identified in the promoter of interest. The maximum core similarity score is 1.0 and is given when the core sequence of the identified binding site matches the predefined TFBS exactly, as is the case for the NBRE sites found within ABIN-1, ABIN-2 and Cezanne. The matrix similarity is the value given for the complete sequence of the binding site. Genomatix describes a “good” match as having a matrix similarity of >0.80. All NBRE sites identified within A20, ABIN-1, ABIN-2 and Cezanne have a score of between 0.860 and 0.929.

While none of the TFBSs identified in the genes of interest match the NBRE sequence exactly, a perfect match is not necessarily required for the site to be functional. Murphy *et al.* (1996) discovered three *cis*-acting sequences which bind specifically to NURR1 and NUR77 and are similar, but not identical, to the original NBRE site. The sequences of these binding sites are: GAAGGTCA, GAAGGTCG and AAAGGTCG. The latter sequence is identical to the sequence of the NBRE site identified within ABIN-2. Furthermore, a study by You *et al.* (2009) found that an NBRE site with one-point mutation (consisting of the sequence AAAGATCA) is present in

the human I κ B α promoter and that NUR77 binds specifically to this site. Mutation of this sequence halted induction of the I κ B α promoter by NUR77. Therefore, while the sequences of the NBRE sites identified by Genomatix within A20, ABIN-1, ABIN-2 and Cezanne are not identical to the original NBRE site, they may still be functional.

It should be noted that the palindromic Nur-responsive element (NurRE), TGATATTTX₆AAAGTCCA, to which the NR4A subfamily bind as homodimers or heterodimers, was not available as an option to search for within the promoters of interest in Genomatix, thus limiting the results obtained.

Further analysis of the promoter sequence of genes can provide evidence whether or not the TFBS(s) identified may be functional. The context within which the TFBS is found can offer clues to the site's functionality. If the TFBS forms part of a framework (or model) consisting of two or more binding sites, this indicates that the individual sites within the framework may be functional (Genomatix). The Genomatix tool Frameworker was used to construct promoter models which contained the NBRE site and which were common to the genes of interest. Frameworker is used for the comparative analysis of promoter sequences and allows the extraction of a common framework of TFBSs from a set of DNA sequences. The promoters identified as containing the NBRE site were selected and analysed. Several common models containing this site were found within the promoters of ABIN-1 and Cezanne. The two most complex models are given in Fig. 3.2. (The other models identified were subsets of these two models and therefore are not shown.) The most complex common promoter model consisted of the binding sites: RXRF, NR2F, MOKF, SORY and NBRE. The second model consisted of the sites: RXRF, MYT1, E2FF and NBRE. The definitions of these TFBSs are given in Table 3.2. Both models contain the retinoid X receptor heterodimer binding site (RXRF). NURR1 and NUR77 can both bind to the 9-*cis* retinoic acid receptor to form heterodimers. These NR4A subfamily members then enhance transcriptional activation of the RXR in response to RXR ligands (Perlmann and Jansson 1995). The identification of promoter models containing NBRE binding sites within the promoters of ABIN-1 and Cezanne provides stronger evidence that these sites may be functionally significant in these genes.

The Genomatix software tool ModelInspector was used to search the A20-related gene promoters for experimentally-verified promoter modules containing the NBRE binding site. One such

module was detected within the ABIN-1 promoter – NBRE AP1F 01. Since the NBRE binding site is part of an experimentally-verified promoter module, this supports the idea that the NBRE site identified within ABIN-1 may be functional and that the NR4A subfamily members may be involved in the regulation of this gene.

Genes containing TFBSs that are conserved in distance and orientation within their promoter regions can be involved in the same biological processes due to the necessity of the interaction of their gene products (Cohen *et al.* 2006). Therefore, the promoter regions of A20, ABIN-1, ABIN-2 and Cezanne were analyzed further to ascertain if they have a similar promoter organizational structure. ModelInspector was used to examine these promoters for common, pre-defined, experimentally-verified promoter modules from the Promoter Module Library Version 5.0. Promoters of Genomatix-defined gold transcripts of A20, ABIN-1, ABIN-2 and Cezanne were used for this analysis. The promoter modules SP1F SP1F 04 and EGRF SP1F 01 were found to be common to all four genes of interest (Table 3.3). Two SP1 binding sites are essential for podoplanin promoter activity (Genomatix 2009). Podoplanin promotes the formation of elongated cell extensions and increases endothelial cell adhesion, migration and tube formation (Hartz 2009). Perhaps the A20-related genes are induced by some of the same activators as the podoplanin gene which has a role in cell adhesion, aiding in the recruitment of inflammatory cells. Further work may elucidate this. The second module common to all A20-related genes analysed was EGRF SP1F 01. Egr-1 and Sp family proteins play a reciprocal role in the control of expression from the PTP1B (protein tyrosine phosphatase 1B) and the ABCA2 (adenosine 5'triphosphate-binding cassette, subfamily A, member 2) promoters (Genomatix 2009). PTP1B has been implicated in the negative regulation of insulin (Olefsky 2004). ABCA2 is a transporter protein involved in lipid homeostasis (Torres 2007). Several other promoter modules were found to be common to three of the four genes of interest and these are given in Table 3.4.

In order to find other promoter frameworks which may be common to the four genes of interest and important in their regulation, Frameworker was used to analyse gold transcript-promoters for common promoter models not necessarily containing the NBRE site. In contrast to the promoter modules found by ModelInspector, these models are not experimentally verified. Seven such models were identified by Frameworker using default parameters apart from the minimum distance between elements parameter, which was set at 1 bp. The p values of these models

increased from 1.4×10^{-7} for the first model (HESF SP1F) to 0.02 for the last model identified (NRF1 NRF1).

ModelInspector was used to search the human genome for other genes containing these promoter modules or models in order to find other potential co-regulated genes. The Genomatix Promoter Database Promoter of annotated genes was searched. However, approximately 1500 genes were identified that contain each of the promoter modules/models. When the search was restricted to only the sense (+) strand, approximately 650 genes were identified for model HESF SP1F for example. Further work on refining the promoter models found in the A20-related genes may lead to the identification of co-regulated genes, followed by verification through experimental work on the promoters of these genes.

A study by Sacchetti *et al.* (2001) found that NURR1 activates transcription of one of its target genes, the human dopamine transporter gene (hDAT), through an NBRE-independent mechanism, although a canonical NBRE sequence was identified in the promoter of this gene, along with several NBRE-like sequences. A NURR1 mutant without the canonical DNA-binding domain retained the ability to induce transcription of the hDAT gene in a dose-dependant manner. They suggested that NURR1 may act as a transcriptional co-activator of an unidentified protein, or that NURR1 may act indirectly by sequestering co-repressor complexes. This means that even if an NBRE binding site is identified using bioinformatic analysis, experimentation in the laboratory is required to establish whether the site is functionally significant.

An electrophoretic mobility shift assay (EMSA) is a procedure which is used to characterise protein-DNA interactions and could be used in future studies to ascertain if the NR4A subfamily of nuclear receptors actually bind to the promoters of A20, ABIN-1, ABIN-2 and Cezanne, providing evidence that the NBRE sites identified are functional. However, such analysis is beyond the scope of this study.

3.4 Conclusions

Using bioinformatic analysis, the NR4A transcription factor binding site, the NBRE site, was identified within the promoters of A20, ABIN-1, ABIN-2 and Cezanne. The NBRE site was detected in the promoter of a less relevant transcript of ABIN-2, indicating that this TF site may not be functionally significant in this gene. The NBRE site is present in a promoter of A20 in which NF- κ B TFBSs were not detected and NF- κ B is known to induce A20 expression. This also indicates that the NBRE site identified in the A20 gene may not be functionally significant. However, the ModelInspector and Frameworker results, along with the fact that NF- κ B sites were found in the NBRE-containing ABIN-1 promoter, strongly support the hypothesis that the NBRE binding site is functional in ABIN-1 and Cezanne and that the NR4A subfamily is involved in the regulation of these genes. Further studies would elucidate these findings. However, they were beyond the scope of the current investigation.

Chapter 4

Analysis of Changes in Expression of Genes which are Functionally Related to A20 in Response to TNF- α

lyit | Institiúid Teicneolaíochta Ictiúil Éireann
Letterkenny Institute of Technology

4. Analysis of Changes in Expression of Genes which are Functionally Related to A20 in Response to TNF- α

4.1 Cell Lines

In these studies, in vitro cell culture models of inflammatory arthritis were employed to investigate the roles of TNF- α on the expression of A20 and related gene transcripts. The K4 IM human immortalized synoviocyte cell line was utilized. This cell line was established to investigate the factors leading to synovial fibroblast activation in inflammatory arthritis. They have fibroblast-like morphology and analyses have demonstrated that they retain the fibroblast-like phenotype. These cells express the cell surface markers ICAM-1 and CD44 at comparable levels to primary synovial fibroblasts, although expression of VCAM-1 and the receptors for IL-1 and PDGF are lower. K4 IM cells, like their primary counterparts, are activated by growth factors, synovial fluid and serum, resulting in the induction of immediate early genes such as Egr-1 (Haas *et al.* 1997). Therefore, K4 IM cells are useful as a model to study gene expression in activated synoviocytes which are key cells in the pathogenesis of RA.

The human chondrocyte SW 1353 cell line was also used in this study. These cells have been found to be an appropriate model for primary chondrocytes when treated with inflammatory cytokines. These cells express aggrecan, type II collagen, Cart-1 and TGF- β , which are among the genes expressed in the chondrogenic phenotype (Vincenti and Brinckerhoff 2001; Ah-Kim *et al.* 2000). This cell line also conserves several Sox9 signaling pathways identified in murine chondrocytes (Schaefer *et al.* 2003). Activated chondrocytes play an important role in maintaining the inflammatory environment within the RA joint, producing many proinflammatory cytokines, chemokines and MMPs, contributing to joint damage (Otero and Goldring 2007; Rannou *et al.* 2006).

4.1.1 Mycoplasma Testing of Cells

Mycoplasmas are one of the smallest free-living forms of bacteria and lack a bacterial cell wall. They are a major cause of cell culture contamination resulting in a substantial change in the biological characteristics of cells (Volokhov *et al.* 2011). The Venor® GeM Mycoplasma Detection Kit for conventional PCR was used to test the cultured cells for the presence of Mycoplasma contamination and the test was carried out as described in section 2.5.11.

4.1.1.1 Mycoplasma Test Results for K4 IM and SW 1353 Cells

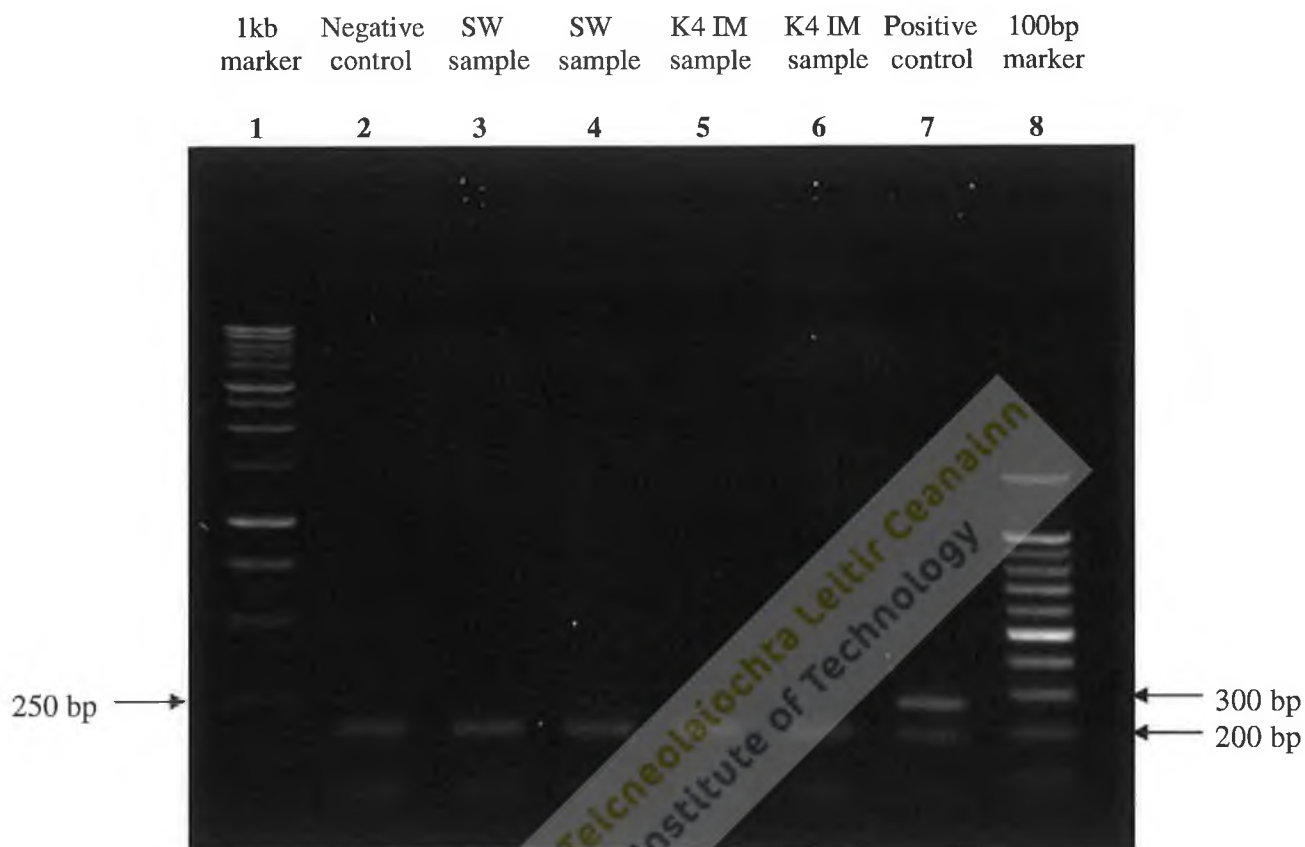


Fig. 4.1 RT-PCR analysis for the detection of mycoplasma in K4 IM and SW 1353 cells. Products were electrophoresed on a 1.5 % agarose gel and visualised by staining with ethidium bromide solution. All samples contained an internal control (191 bp). Test samples are negative (lanes 3-6). A PCR product of the expected size of 267 bp was detected in the positive control sample.

Lane	Sample
1	1 kb DNA ladder
2	Negative control
3	SW 1353 sample
4	SW 1353 sample
5	K4 IM sample
6	K4 IM sample
7	Positive control
8	100 bp DNA ladder

The test for the presence of mycoplasma contamination utilised end-point PCR. All samples contained an internal control which is clearly visible, demonstrating that the RT-PCR reaction was carried out successfully in each of the samples. The positive control band at 267 bp in lane 7 is also evident, demonstrating that a valid test was carried out. Mycoplasma contamination was not detected in the K4 IM or SW 1353 cells. Primer dimers are visible at the bottom of the image.

4.2 Analysis of Differential Gene Expression in Response to TNF- α

In order to ascertain the effect of the inflammatory cytokine TNF- α on the expression of A20 and the A20-interacting genes, ABIN-1, ABIN-2 and Cezanne in the multicellular environment of RA, two cell models of inflammatory arthritis were stimulated with the cytokine, followed by reverse transcription-PCR (RT-PCR) of the resulting RNA.

Human immortalized K4 synovial fibroblasts and human immortalized SW chondrocytes were grown in 25cm² culture flasks to approximately 80 % confluence and then serum-starved for 24 hr. The cells were then stimulated with 10 ng/ml recombinant human TNF- α (+TNF). The medium in control flasks was replaced with either fresh serum-free medium (-TNF) or serum-free medium containing 1 μ l/ml vehicle (containing PBS with 0.1 % BSA) (Veh). Following stimulation, the cells were incubated for the appropriate time period (4 hr or 24 hr). Total RNA was then extracted from the cells using TRI Reagent. The integrity of the isolated RNA was determined by gel electrophoresis and total RNA concentrations were determined by UV spectrophotometric analysis, as described in section 2.3.5. Two micrograms of total RNA was reverse transcribed into cDNA using random primers and Moloney murine leukemia virus reverse transcriptase. Following first strand cDNA synthesis, end-point PCR of the genes of interest was carried out using Go Taq DNA polymerase. PCR products were run out on a 1.5 % TAE agarose gel and then visualised by staining with ethidium bromide and viewed using an Alpha Innotech AlphaImager® HP gel imaging system.

The induction of differential gene expression by TNF- α in K4 IM synovial fibroblasts and SW 1353 chondrocytes was confirmed by RT-PCR analysis of intercellular adhesion molecule-1 (ICAM-1) and vascular cell adhesion molecule-1 (VCAM-1), as these genes have previously been shown to be upregulated in response to TNF- α stimulation (Tessier *et al.* 1993; Marlor *et al.*

1992). The housekeeping gene β -actin was used as a positive control which displayed equal levels of gene expression across all samples.

A time-course stimulation of SW 1353 cells with TNF- α was also carried out to determine the time at which maximal A20 and ABIN-1 expression is induced by this cytokine in these cells. Cells were stimulated over a 24 hr period and total RNA was extracted. The RNA was treated with DNase to remove any contaminating genomic DNA. Reverse-transcription was carried out using the Go Script Reverse Transcription System. Quantitative PCR (qPCR) analysis was carried out on the resulting cDNA.

4.3 K4 IM Synoviocyte Results

4.3.1 Determination of the Integrity of Extracted RNA

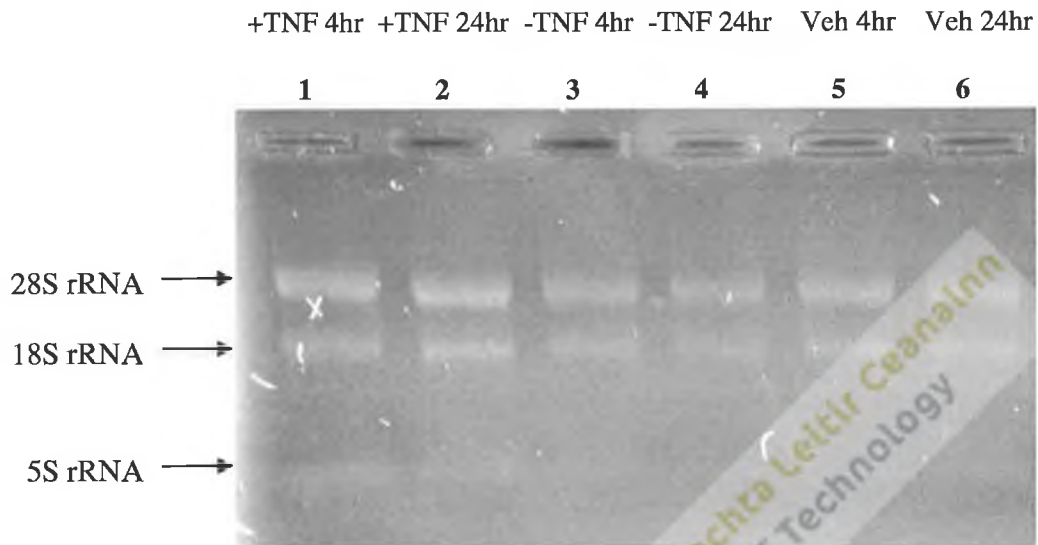


Fig. 4.2 Total intact RNA isolated from K4 IM cells which were untreated, treated with vehicle or treated with TNF- α for the times indicated. The RNA was electrophoresed on a denaturing gel and visualized by staining with ethidium bromide.

Lane	RNA Sample
1	+ TNF- α 4 hr
2	+ TNF- α 24 hr
3	- TNF- α 4 hr
4	- TNF- α 24 hr
5	Vehicle 4 hr
6	Vehicle 24 hr

4.3.2 Reverse Transcription-Polymerase Chain Reaction (RT-PCR) Results

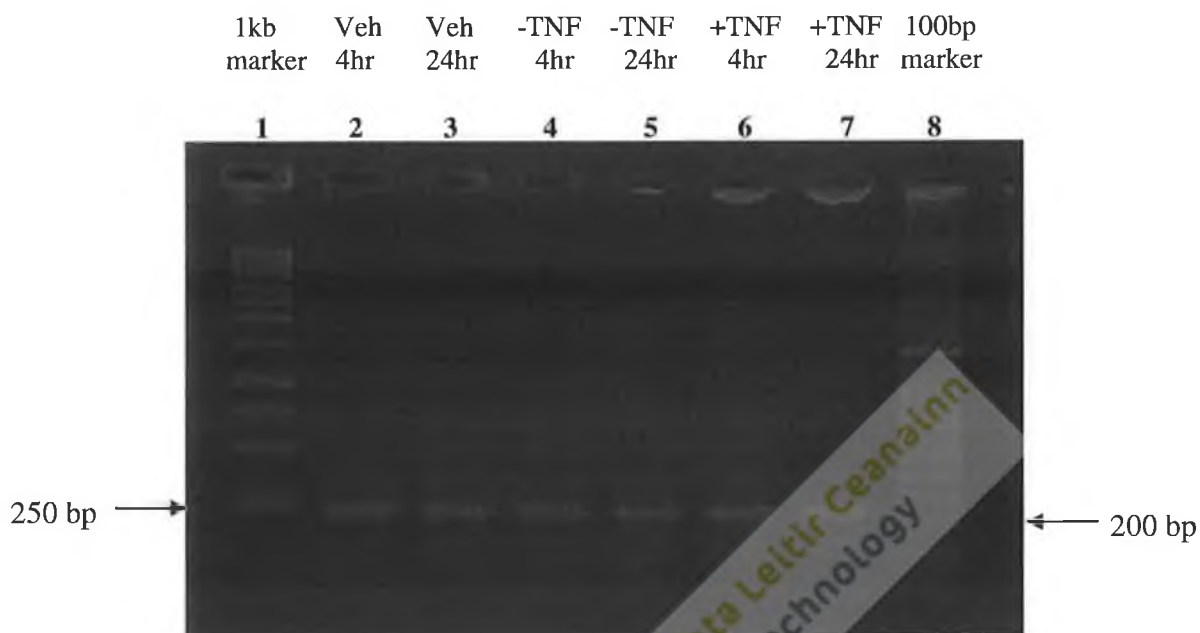


Fig. 4.3 RT-PCR analysis of the housekeeping gene β -actin (234 bp) performed on RNA isolated from K4 IM cells which were untreated, treated with vehicle or treated with TNF- α for the times indicated. The PCR products were electrophoresed on a 1.5 % agarose gel and visualised by staining with ethidium bromide.

Lane	Sample
1	1 kb DNA ladder
2	Vehicle 4 hr β -actin
3	Vehicle 24 hr β -actin
4	- TNF- α 4 hr β -actin
5	- TNF- α 24 hr β -actin
6	+ TNF- α 4 hr β -actin
7	+ TNF- α 24 hr β -actin
8	100 bp DNA ladder

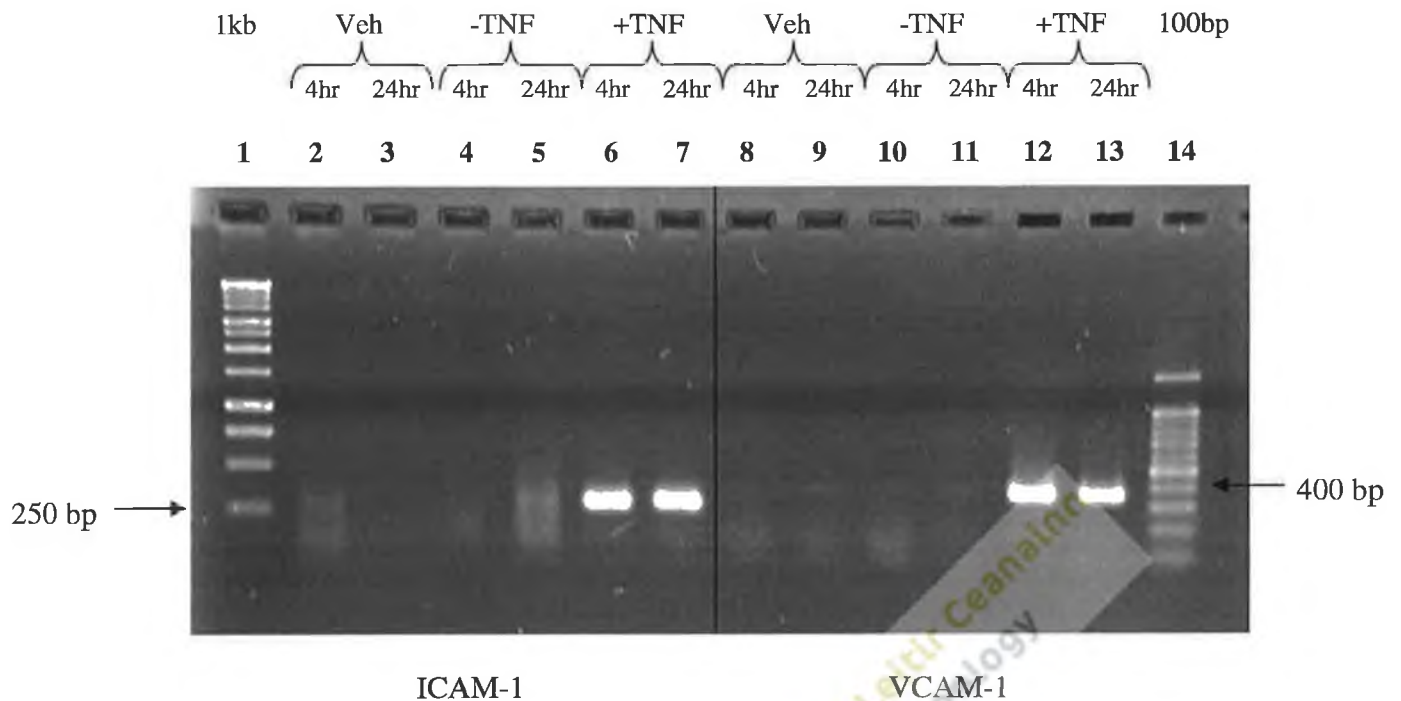


Fig. 4.4 RT-PCR analysis of ICAM-1 (295 bp) and VCAM-1 (350 bp) performed on RNA isolated from K4 IM cells which were untreated, treated with vehicle or treated with TNF- α for the times indicated. The PCR products were electrophoresed on a 1.5 % agarose gel and visualised by staining with ethidium bromide solution.

Lane	Sample
1	1 kb DNA ladder
2	Vehicle 4 hr ICAM-1
3	Vehicle 24 hr ICAM-1
4	- TNF- α 4 hr ICAM-1
5	- TNF- α 24 hr ICAM-1
6	+ TNF- α 4 hr ICAM-1
7	+ TNF- α 24 hr ICAM-1
8	Vehicle 4 hr VCAM-1
9	Vehicle 24 hr VCAM-1
10	- TNF- α 4 hr VCAM-1
11	- TNF- α 24 hr VCAM-1
12	+ TNF- α 4 hr VCAM-1
13	+ TNF- α 24 hr VCAM-1
14	100 bp DNA ladder

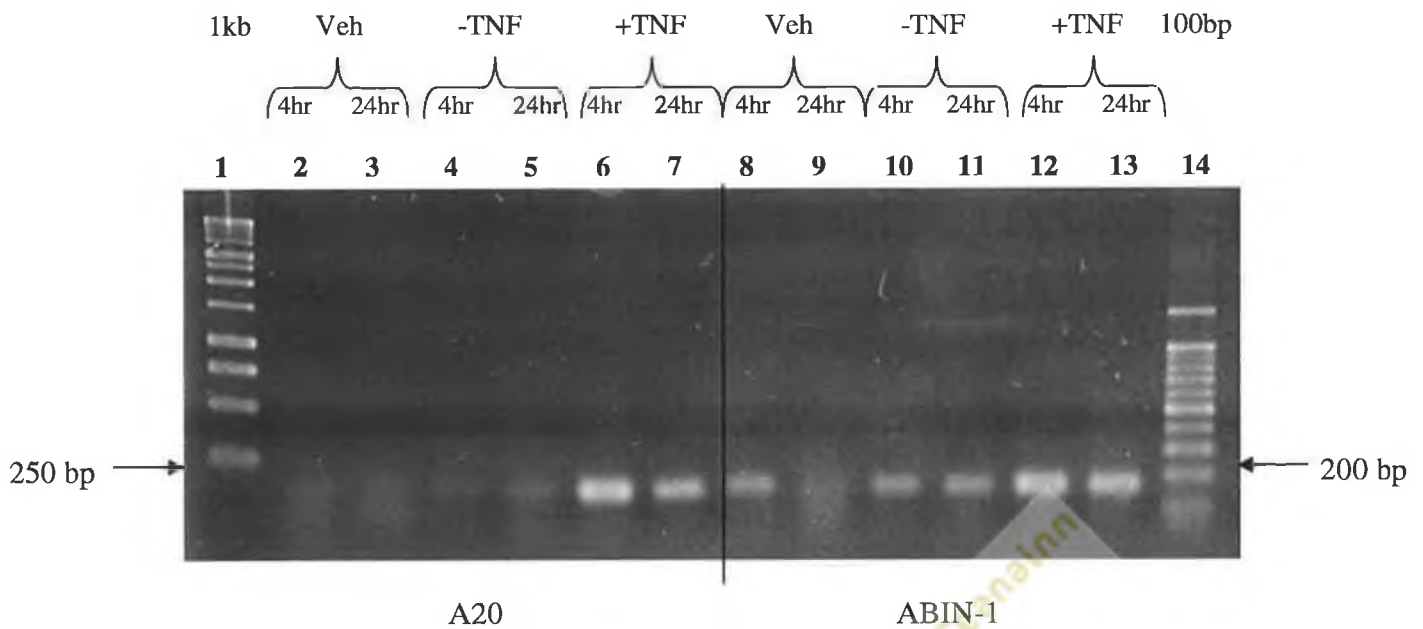


Fig. 4.5 RT-PCR analysis of A20 (153 bp) and ABIN-1 (168 bp) performed on RNA isolated from K4 IM cells which were untreated, treated with vehicle or treated with TNF- α for the times indicated. The PCR products were electrophoresed on a 1.5 % agarose gel and visualised by staining with ethidium bromide.

Lane	Sample
1	1 kb DNA ladder
2	Vehicle 4 hr A20
3	Vehicle 24 hr A20
4	- TNF- α 4 hr A20
5	- TNF- α 24 hr A20
6	+ TNF- α 4 hr A20
7	+ TNF- α 24 hr A20
8	Vehicle 4 hr ABIN-1
9	Vehicle 24 hr ABIN-1
10	- TNF- α 4 hr ABIN-1
11	- TNF- α 24 hr ABIN-1
12	+ TNF- α 4 hr ABIN-1
13	+ TNF- α 24 hr ABIN-1
14	100 bp DNA ladder

4.4 SW 1353 Chondrocyte Results

4.4.1 Determination of the Integrity of RNA Extracted

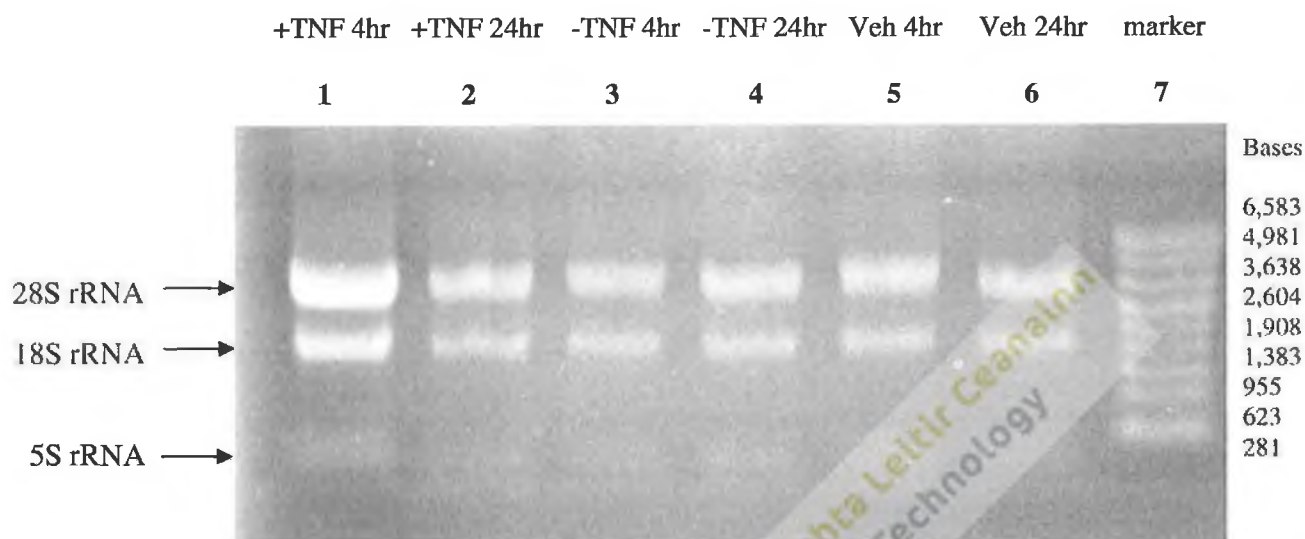


Fig. 4.7 Total intact RNA isolated from SW 1353 cells which were untreated, treated with vehicle or treated with TNF- α for the times indicated. The RNA was electrophoresed on a denaturing gel and visualized by staining with ethidium bromide solution.

Lane	RNA Sample
1	+ TNF- α 4 hr
2	+ TNF- α 24 hr
3	- TNF- α 4 hr
4	- TNF- α 24 hr
5	Vehicle 4 hr
6	Vehicle 24 hr
7	RNA marker

4.4.2 RT-PCR Results

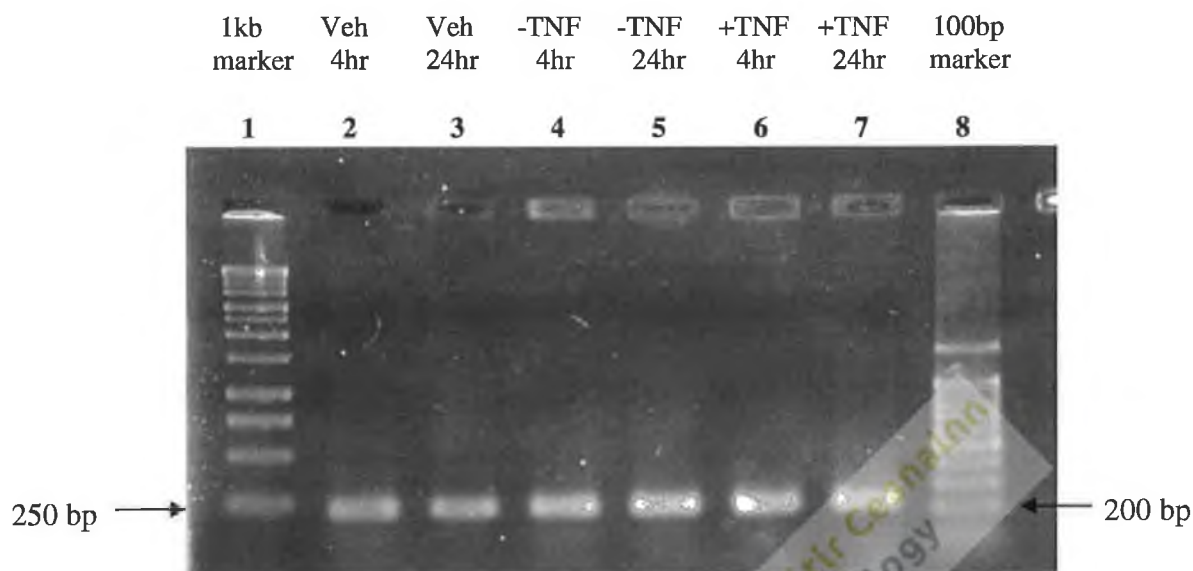


Fig. 4.8 RT-PCR analysis of the housekeeping gene β -actin (234 bp) performed on RNA isolated from SW 1353 cells which were untreated, treated with vehicle or treated with TNF- α for the times indicated. The PCR products were electrophoresed on a 1.5 % agarose gel and visualised by staining with ethidium bromide.

Lane	Sample
1	1 kb DNA ladder
2	Vehicle 4 hr β -actin
3	Vehicle 24 hr β -actin
4	- TNF- α 4 hr β -actin
5	- TNF- α 24 hr β -actin
6	+ TNF- α 4 hr β -actin
7	+ TNF- α 24 hr β -actin
8	100 bp DNA ladder

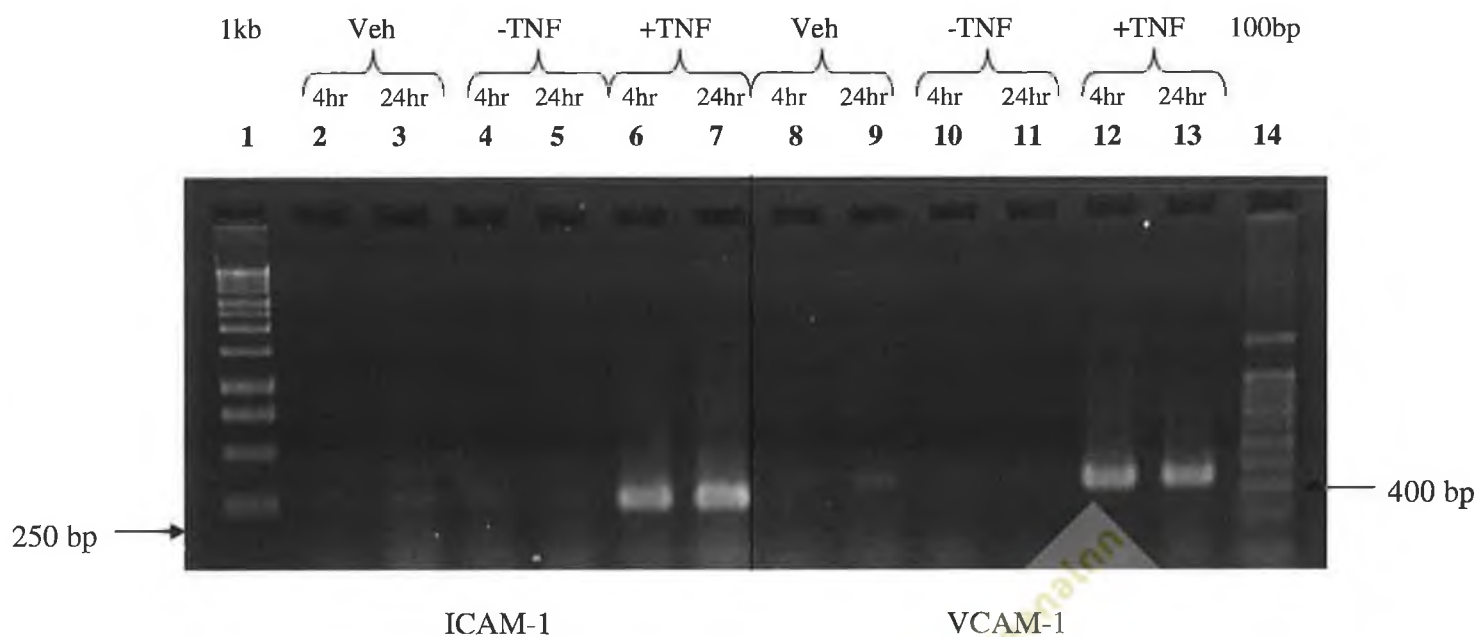


Fig. 4.9 RT-PCR analysis of ICAM-1 (295 bp) and VCAM-1 (350 bp) performed on RNA isolated from SW 1353 cells which were untreated, treated with vehicle or treated with TNF- α for the times indicated. The PCR products were electrophoresed on a 1.5 % agarose gel and visualised by staining with ethidium bromide.

Lane	Sample
1	1 kb DNA ladder
2	Vehicle 4 hr ICAM-1
3	Vehicle 24 hr ICAM-1
4	- TNF- α 4 hr ICAM-1
5	- TNF- α 24 hr ICAM-1
6	+ TNF- α 4 hr ICAM-1
7	+ TNF- α 24 hr ICAM-1
8	Vehicle 4 hr VCAM-1
9	Vehicle 24 hr VCAM-1
10	- TNF- α 4 hr VCAM-1
11	- TNF- α 24 hr VCAM-1
12	+ TNF- α 4 hr VCAM-1
13	+ TNF- α 24 hr VCAM-1
14	100 bp DNA ladder

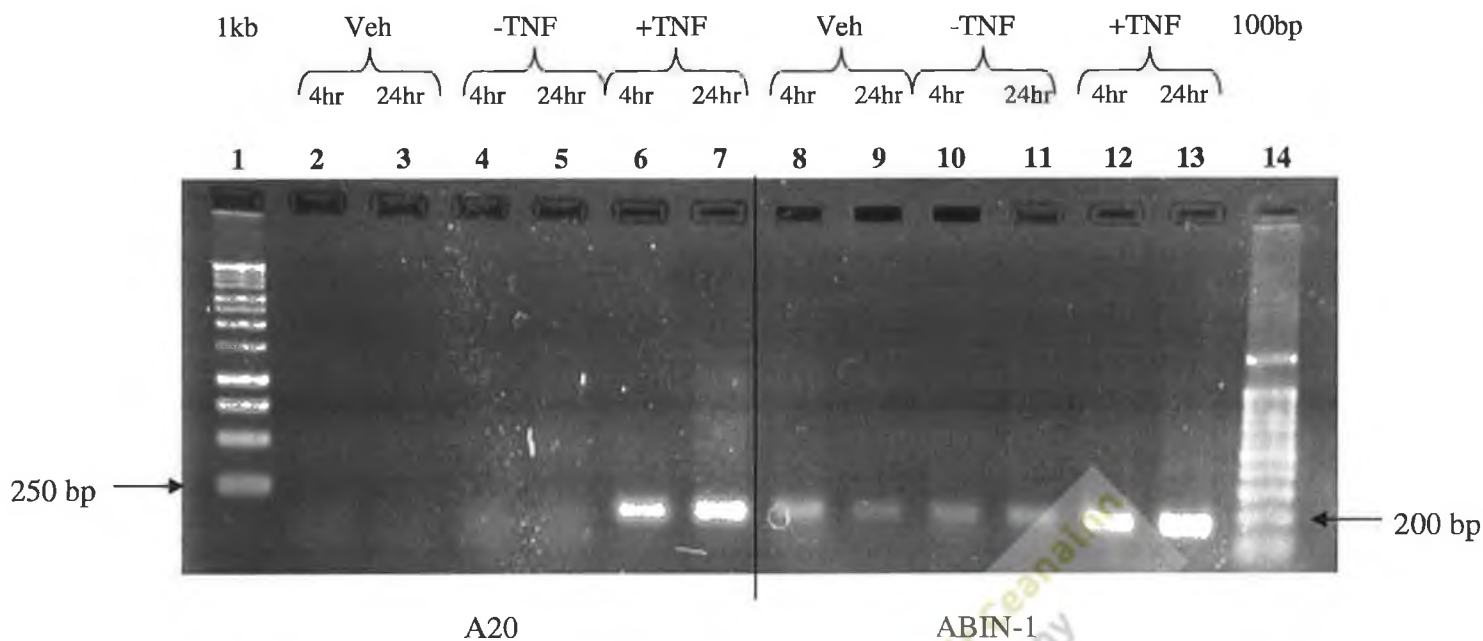


Fig. 4.10 RT-PCR analysis of A20 (153 bp) and ABIN-1 (168 bp) performed on RNA isolated from SW 1353 cells which were untreated, treated with vehicle or treated with TNF- α for the times indicated. The PCR products were electrophoresed on a 1.5 % agarose gel and visualised by staining with ethidium bromide.

Lane	Sample
1	1 kb DNA ladder
2	Vehicle 4 hr A20
3	Vehicle 24 hr A20
4	- TNF- α 4 hr A20
5	- TNF- α 24 hr A20
6	+ TNF- α 4 hr A20
7	+ TNF- α 24 hr A20
8	Vehicle 4 hr ABIN-1
9	Vehicle 24 hr ABIN-1
10	- TNF- α 4 hr ABIN-1
11	- TNF- α 24 hr ABIN-1
12	+ TNF- α 4 hr ABIN-1
13	+ TNF- α 24 hr ABIN-1
14	100 bp DNA ladder

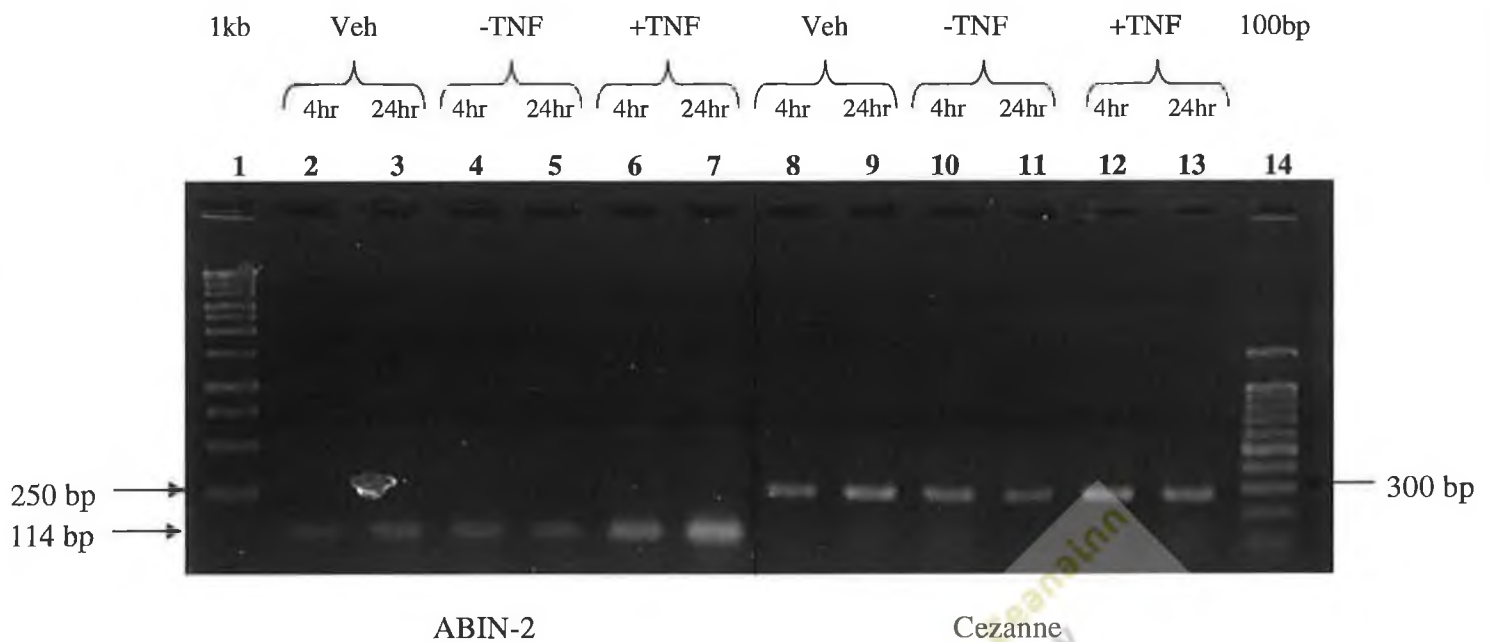


Fig. 4.11 RT-PCR analysis of ABIN-2 (114 bp) and Cezanne (293 bp) performed on RNA isolated from SW 1353 cells which were untreated, treated with vehicle or treated with TNF- α for the times indicated. The PCR products were electrophoresed on a 1.5 % agarose gel and visualised by staining with ethidium bromide.

Lane	Sample
1	1 kb DNA ladder
2	Vehicle 4 hr ABIN-2
3	Vehicle 24 hr ABIN-2
4	- TNF- α 4 hr ABIN-2
5	- TNF- α 24 hr ABIN-2
6	+ TNF- α 4 hr ABIN-2
7	+ TNF- α 24 hr ABIN-2
8	Vehicle 4 hr Cezanne
9	Vehicle 24 hr Cezanne
10	- TNF- α 4 hr Cezanne
11	- TNF- α 24 hr Cezanne
12	+ TNF- α 4 hr Cezanne
13	+ TNF- α 24 h Cezanne
14	100 bp DNA ladder

4.4.3 Determination of the Integrity of Extracted RNA for qPCR

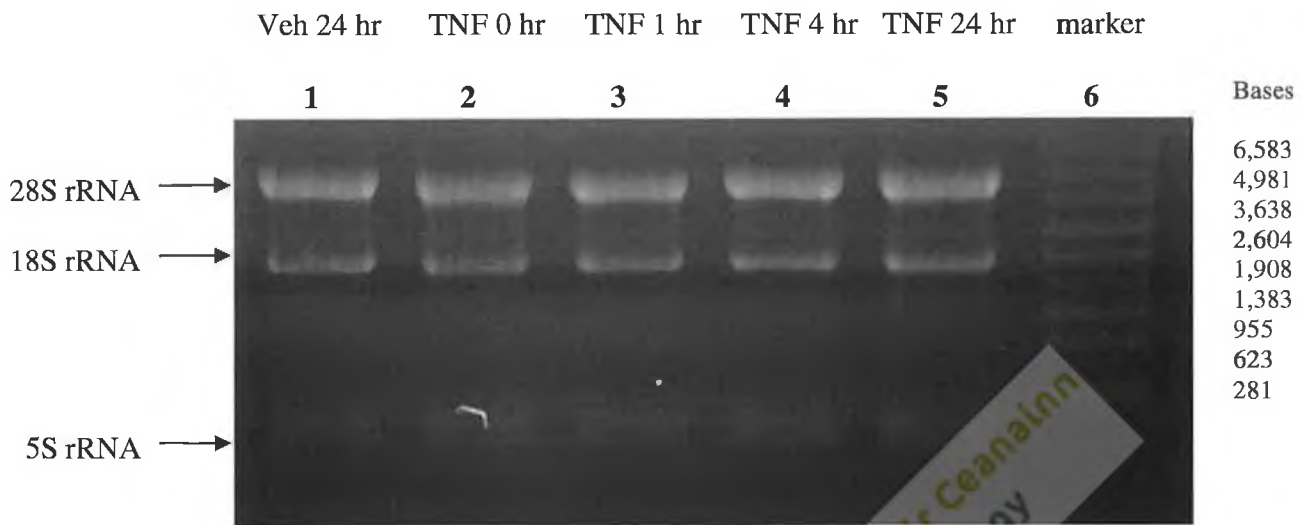


Fig. 4.12 Total intact RNA isolated from SW 1353 cells which were untreated or treated with TNF- α for the times indicated. The RNA was electrophoresed on a denaturing gel and visualised by staining with ethidium bromide.

Lane	RNA Sample
1	Vehicle 24 hr
2	TNF 0 hr
3	TNF 1 hr
4	TNF 4 hr
5	TNF 24 hr
6	RNA marker

4.4.4 Quantitative (q)PCR Results

Quantitative (q)PCR analysis of changes in gene expression in response to the inflammatory stimulus TNF- α was carried out in chondrocytes. The expression of A20 and ABIN-1 were analysed. RNA isolated from SW 1353 cells grown in the presence or absence of TNF- α for defined periods of time was reverse transcribed into cDNA and amplified by qPCR. Results were normalised to expression of the housekeeping gene GAPDH. Experiments were performed in triplicate.

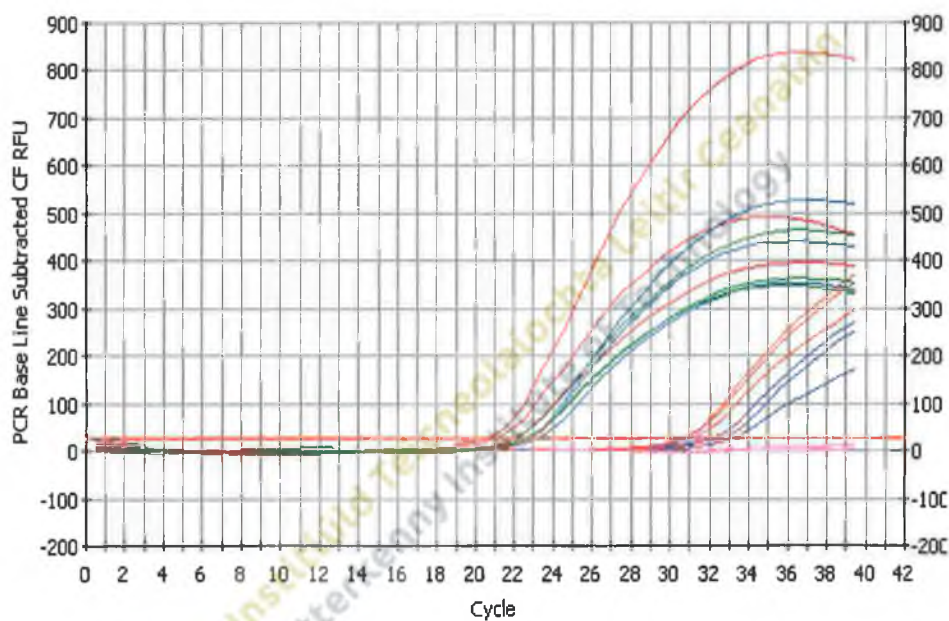


Fig. 4.13 qPCR amplification curves for A20 gene expression. RNA isolated from SW 1353 cells grown in the presence or absence of TNF- α was reverse-transcribed into cDNA and amplified by qPCR in triplicate, along with the reference gene GAPDH. Purple = vehicle, orange = TNF 0 hr, red = TNF 1 hr, blue = TNF 4 hr, green = TNF 24 hr, pink = no template control.

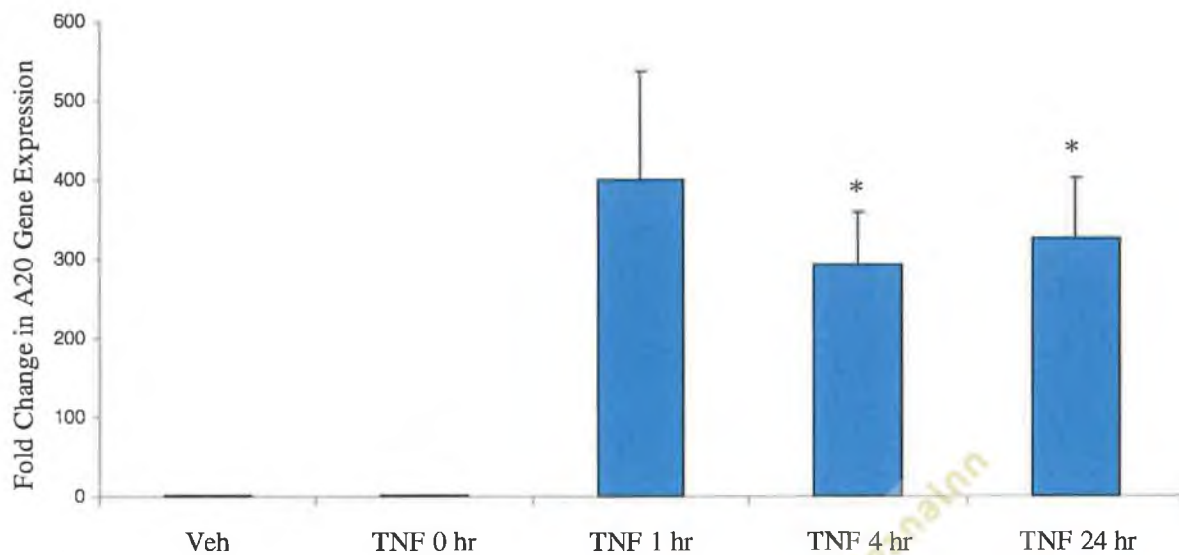


Fig. 4.14 qPCR analysis of A20 mRNA levels in response to TNF- α stimulation in SW 1353 chondrocyte cells. Cells were serum-starved for 24 hr prior to treatment with vehicle for 24 hr or TNF- α (10 ng/ml) for the times indicated and the RNA extracted. The RNA was reverse transcribed into cDNA. A20 mRNA expression levels were assessed by qPCR analysis and levels were normalized to GAPDH. The results are expressed as fold change compared to untreated cells and represent mean plus SEM of three qPCR experiments performed in triplicate. * $p < 0.05$ compared to TNF 0 hr for cumulative data from three qPCR experiments.

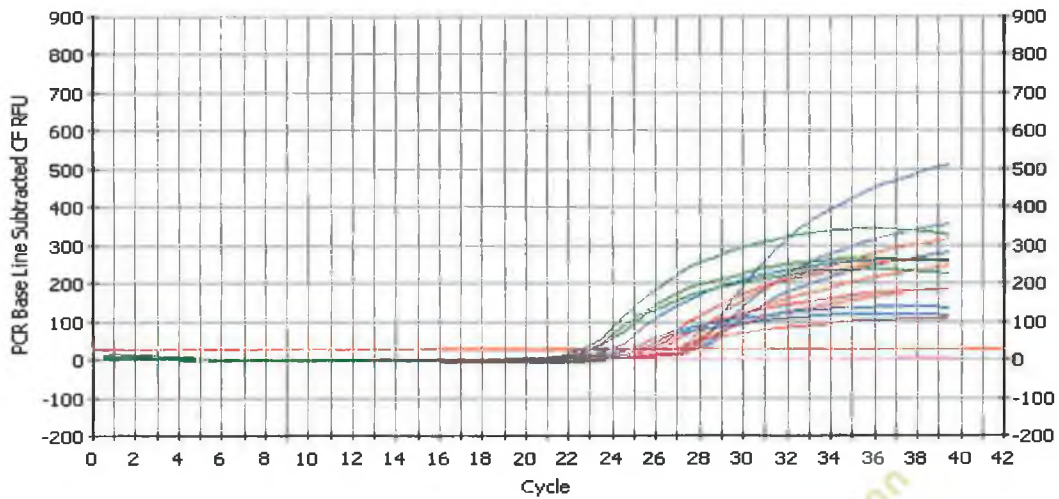


Fig. 4.15 qPCR amplification curves for ABIN-1 gene expression. RNA isolated from SW 1353 cells grown in the presence or absence of TNF- α was reverse-transcribed into cDNA and amplified by qPCR in triplicate, along with the reference gene GAPDH. Purple = vehicle, orange = TNF 0 hr, red = TNF 1 hr, blue = TNF 4 hr, green = TNF 24 hr, pink = no template control.

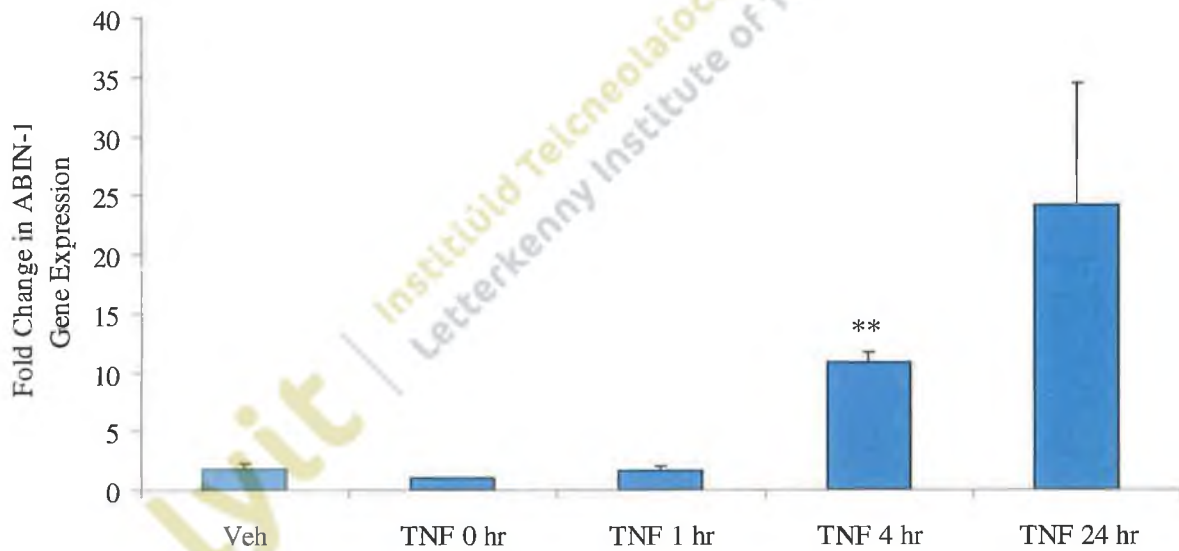


Fig. 4.16 qPCR analysis of ABIN-1 mRNA levels in response to TNF- α stimulation in SW 1353 chondrocyte cells. Cells were serum-starved for 24 hr prior to treatment with either vehicle for 24 hr or TNF- α (10 ng/ml) for the times indicated and the total RNA extracted. The RNA was reverse transcribed into cDNA. ABIN-1 mRNA expression levels were assessed by qPCR analysis and levels were normalized to GAPDH. The results are expressed as fold change compared to untreated cells and represent mean plus SEM of three qPCR experiments performed in triplicate. ** $p < 0.01$ compared to TNF 0 hr for cumulative data from three qPCR experiments.

4.5 Discussion

TNF- α , as stated previously, is a key cytokine in the pathogenesis of RA. It is found in elevated levels in the RA joint. TNF- α stimulates the activation of NF- κ B, which in turn, induces a cascade of proinflammatory cytokines, chemokines and adhesion molecules, including TNF- α itself. This cytokine also stimulates the differentiation of osteoblasts into osteoclasts which resorb bone (Deng and Lenardo 2006; Kast 2005; Yamamoto and Gaynor 2001). The effects of TNF- α stimulation on A20 and the A20-related genes ABIN-1, ABIN-2 and Cezanne in human immortalised synoviocyte and chondrocyte cells was investigated using conventional end-point RT-PCR analysis. End-point RT-PCR is a semi-quantitative method of determining variations in the expression of RNA transcripts (Marone *et al.* 2001). K4 IM synoviocytes and SW 1353 chondrocytes were grown in the presence or absence of TNF- α . The RNA was isolated and reverse transcribed into cDNA. Gene expression was then examined using end-point PCR analysis.

Optimization of the end-point PCR reaction components and cycling parameters was carried out initially to obtain optimum results. Primer and template cDNA concentrations were varied, followed by varying the PCR cycle number to determine the optimum combination.

For end-point PCR analysis, β -actin was used as the housekeeping gene. It encodes a cytoskeletal protein which is important in cell migration, motility, structure and integrity and is one of the main components of contractile apparatus in the cell (NCBI 2011). β -actin was amplified for a lower number of PCR cycles (18) compared to the genes of interest (23-30) to ensure that it was not overcycled and that the actual expression levels of this housekeeping gene were even between the samples in each experiment. RT-PCR analysis of β -actin expression resulted in bands of equal intensity for each of the samples (+TNF- α , -TNF- α , vehicle) as expected (Fig. 4.3 and 4.8).

In order to confirm the induction of differential gene expression by TNF- α in K4 IM synoviocytes and SW 1353 chondrocytes, RT-PCR of ICAM-1 (CD54) and VCAM-1 (CD106) was carried out on the cDNA prior to the genes of interest. Treatment of both cell types by TNF- α resulted in a strong induction of ICAM-1 and VCAM-1 after 4 and 24 hr (Fig. 4.4 and 4.9). TNF- α -induced upregulation of ICAM-1 and VCAM-1 in fibroblast-like synoviocytes has

previously been demonstrated (Tessier *et al.* 1993; Marlor *et al.* 1992). It has also been shown that ICAM-1 and VCAM-1 are expressed at basal levels in SW 1353 cells and upregulated in response to TNF- α (d'Abusco *et al.* 2010; Ju *et al.* 2002) corresponding to the results obtained in this study.

It was ascertained during establishment and characterization of the immortalised K4 IM cell line that expression of ICAM-1 was maintained from the parental primary synovial fibroblasts, whilst VCAM-1 expression was downregulated (Haas *et al.* 1997). In this study however, basal mRNA levels of ICAM-1 and VCAM-1 were detected in unstimulated K4 IM cells (Fig 4.4).

Results obtained illustrate that treatment of K4 IM synoviocytes with TNF- α resulted in upregulation of A20 mRNA expression after 4 hr, with a diminishing effect after 24 hr (Fig. 4.5). Basal expression of A20 was detected in untreated synoviocytes. TNF- α stimulation of SW 1353 cells led to induction of A20 mRNA after 4 and 24 hr (Fig. 4.10). A20 was first discovered as a TNF- α -induced early response gene in primary human umbilical vein endothelial cells (HUVEC) in which A20 induction was strongest after 1 hr and barely detectable after 2 hr (Dixit *et al.* 1990). It has also been demonstrated that A20 is upregulated by TNF- α in HeLa cells, with maximum induction after 30 min, and in Jurkat T cells (Zhou *et al.* 2003; Krikos *et al.* 1992). The A20 promoter contains two NF- κ B transcription factor binding sites and induction of A20 transcription by TNF- α is mediated via these binding elements (Krikos *et al.* 1992). It has been established that NF- κ B activation of primary human epidermal keratinocytes and dermal fibroblasts using p50 and p65 retrovectors led to induction of A20 expression (Hinata *et al.* 2003). Furthermore, it is known that A20 functions as a negative feedback inhibitor of NF- κ B (Jaattela *et al.* 1996). Therefore, it is likely that TNF- α induces A20 expression in synoviocytes and chondrocytes via the transcription factor NF- κ B.

TNF- α stimulation of synoviocytes and chondrocytes resulted in an induction of ABIN-1 mRNA expression after 4 and 24 hr (Fig. 4.4 and 4.10). From these end-point PCR results, the induction appears to be highest after 4 hr in K4 IM cells, with the effect lessening after 24 hr. In the SW 1353 cells however, ABIN-1 transcripts appear to be more abundant after 24 hr. The ABIN-1 gene has two alternatively spliced isoforms, Naf-1 α and Naf-1 β . Naf-1 α is approximately 2800 nucleotides in length with an open reading frame consisting of 1941 nucleotides, whereas Naf-1 β is approximately 2600 bp long and has an open reading frame of 1781 bp (Beyaert *et al.* 2000).

The ABIN-1 primer set was designed so that both α and β isoforms of the gene would be amplified. The primers anneal upstream of the coding sequence for the shorter Naf-1 β isoform, and therefore, were able to amplify both alternatively spliced isoforms of ABIN-1. The results in the K4 IM synoviocytes correlate with a study carried out by Gallagher *et al.* (2003) which used oligonucleotide microarrays and real-time PCR to establish that ABIN-1 is upregulated by TNF- α in primary human synoviocytes. ABIN-1 was maximally expressed after 8 hr, with higher expression levels after 4 hr than 24 hr. It has been established that ABIN-1 is upregulated in HeLa cells 4 hr after stimulation with TNF- α (Zhou *et al.* 2003). Furthermore, ABIN-1 has been identified as an NF- κ B target gene in the Hodgkin's disease derived cell lines L428 and HDLM2 and in keratinocytes (Hinz *et al.* 2002; Hinata *et al.* 2003) indicating that TNF- α induces ABIN-1 expression via the transcription factor NF- κ B and possibly via the NF- κ B binding sites identified within the ABIN-1 promoter in Chapter 3.

RT-PCR analysis indicate that ABIN-2 mRNA expression levels appear to be upregulated with TNF- α treatment after 4 hr in K4 IM cells and after 24 hr in SW 1353 cells (Fig. 4.6 and 4.11). Previous northern blot analysis of mouse fibrosarcoma L929r2 and mouse macrophage Mf4/4 cells stimulated with TNF- α , LPS or IFN- γ revealed no change in ABIN-2 expression levels and because of this, it was thought that ABIN-2 expression is independent of NF- κ B transcriptional activity (Van Huffel *et al.* 2001; Verstrepen *et al.* 2009). However, these cells were only stimulated with the cytokine for 1 hr (Van Huffel *et al.* 2001). Longer stimulation times may be necessary for detecting the upregulation of ABIN-2 expression levels, as demonstrated in this study with the K4 IM and SW 1353 cells. Results from this chapter and chapter 3 indicate that ABIN-2 may be regulated by NF- κ B. Further experiments, for example, transfecting cells with an NF- κ B expression plasmid and analysing ABIN-2 expression levels or carrying out an EMSA, may elucidate this.

RT-PCR analysis results indicate that stimulation of K4 IM synoviocytes and SW 1353 chondrocytes with TNF- α did not alter Cezanne mRNA expression levels after 4 or 24 hr (Fig. 4.6 and 4.11). However, low constitutive levels of Cezanne were detected in both cell types. RT-PCR analysis by Evans *et al.* (2001) found that levels of Cezanne in HUVEC were similarly not affected by TNF- α treatment (time-points not given). They also state that in EaHy endothelial cells Cezanne exhibited low constitutive expression, whereas this was not the case in the human epithelial cell line HEK-293 (Evans *et al.* 2001). However, comparative real-time

PCR carried out by Enesa *et al.* (2008) revealed that transcription of Cezanne is, in fact, upregulated by TNF- α in both HUVEC and HEK 293 cells after 2 hr. Perhaps the induction of Cezanne expression by TNF- α in these cells is mediated by the NF- κ B transcriptional site identified in Chapter 3.

RT-PCR analysis of ABIN-2 in both cell types consistently resulted in an additional band at approximately 600 bp (ABIN-2 product was 114 bp) (Fig. 4.6 and 4.11) which indicates non-specific priming by one or both of the primers (Sambrook and Russell 2001). Attempts were made to eliminate the extra band by reamplifying a 1:100 dilution of the PCR products in fresh PCR buffer and primers for 30 cycles at an annealing temperature of 55°C. Separately, the annealing time of the PCR reaction was reduced from 45 s to 30 s. However, this was unsuccessful. Further investigation is required but is beyond the scope of this project. The RT-PCR results obtained indicate that ABIN-2 transcripts are upregulated in response to TNF- α stimulation in both human synoviocyte and chondrocyte cells.

Conventional PCR measures the amount of amplified DNA at the end of the PCR reaction. PCR is extremely sensitive to small differences in reaction conditions because these variations in efficiency at every cycle can accumulate into large differences in resulting product yield. Quantitative PCR (qPCR), also known as real-time PCR, takes measurements of the amplified DNA during the exponential phase of the reaction and is a much more reliable and sensitive method of analysing changes in gene expression (Sambrook and Russell 2001). Therefore, qPCR analysis was carried out on RNA extracted from TNF- α treated SW 1353 cells after 0, 1, 4 or 24 hr to more accurately determine the time at which maximal expression of A20 and ABIN-1 was observed in response to TNF- α stimulation in these cells.

GAPDH was used as the exogenous standard and quantification was determined by comparing the amount of GAPDH and the genes of interest. The $2^{-\Delta\Delta CT}$ (Livak) method was used to calculate the mRNA expression levels. The results obtained illustrate that maximum expression of A20 mRNA in chondrocytes in response to TNF- α for the times investigated was at 1 hr, with less expression at 4 hr and the mRNA levels increasing again at 24 hr (Fig. 4.14). As stated earlier, maximum induction of A20 by TNF- α in HeLa cells has previously been found to be after 30 min using qPCR analysis. However, the only times investigated in the study were 30 min and 4 hr after TNF- α treatment (Zhou *et al.* 2003). The qPCR results obtained in this study correlate

with end-point PCR results attained for the chondrocytes cells, in which a stronger A20 product was observed after treatment with TNF- α for 24 hr compared to after 4 hr. The RT-qPCR results in this study suggest that A20 may have a similar effect in chondrocytes in response to TNF- α stimulation. Using co-transfection experiments in Jurkat T cells, Krikos *et al.* (1992) demonstrated that overexpression of A20 inhibited activation of an A20 promoter CAT construct following TNF- α treatment for 12 hr, indicating that A20 exerted an inhibitory effect on its own promoter. The pattern of A20 expression observed in this study indicates that it may be negatively regulating its own expression after 4 hr TNF- α stimulation in SW 1353 cells.

According to the qPCR analysis, maximum ABIN-1 mRNA induction by TNF- α treatment in chondrocytes for the times investigated was found to be after 24 hr (Fig. 4.16). ABIN-1 expression levels were unchanged after 1 hr, but increased significantly ($p < 0.01$) after 4 hr. These qPCR results again correlate with end-point PCR results obtained for these cells in which ABIN-1 mRNA expression appeared to be slightly higher after TNF- α stimulation for 24 hr compared to 4 hr. ABIN-1 mRNA has been detected in high levels in the synovium of patients suffering from inflammatory arthritis compared to those with non-inflammatory arthritis (Gallagher *et al.* 2003). The analysis of ABIN-1 or A20 expression levels in response to TNF- α in human chondrocyte cells has not previously been determined and these results will add to the knowledge already gained in the pathogenesis of inflammatory arthritis.

In the chondrocyte cells, the induction of A20 mRNA levels in response to TNF- α stimulation appear to be much higher compared to ABIN-1 mRNA expression levels (Fig. 5.14 and 5.16). A20 expression may be induced more strongly than ABIN-1 expression after treatment with TNF- α in the SW 1353 cells. The qPCR results suggest a different temporal expression response for A20 and ABIN-1 in chondrocyte cells.

The Thermo Scientific Solaris qPCR gene expression assays used detect all known splice variants of the gene of interest by designing the primers and probes to anneal within a region common to all of them. Therefore, only one primer/probe set (assay) is required for each gene of interest. Furthermore, the Solaris qPCR assays and master mixes are designed so that every assay performs optimally under the same cycling conditions, meaning that little optimization was required. The volume of template cDNA was varied (1, 1.5 and 2 μ l) in order to obtain acceptable Ct values. Two microlitres of cDNA was found to be optimal for the qPCR assays.

The RT-PCR and qPCR results obtained in this study indicate that A20, ABIN-1 and ABIN-2 are upregulated in human synoviocyte and chondrocyte cells in the inflammatory environment of the RA joint, where high levels of the inflammatory cytokine TNF- α are found. Therefore, these results suggest that A20, ABIN-1 and ABIN-2 have important roles in inflammatory disease. Results indicate that Cezanne mRNA expression levels were not altered by TNF- α stimulation in K4 IM or SW 1353 cells.

While RT-(q)PCR analyses demonstrate a change in mRNA expression levels, western blotting or enzyme-linked immunosorbent assays (ELIZAs) would reveal whether the upregulated mRNA detected was paralleled by increases in protein levels.

4.6 Conclusions

Differential gene expression was observed in both K4 IM and SW 1353 cell types in response to stimulation with the inflammatory cytokine TNF- α . RT-PCR analyses indicate that A20, ABIN-1 and ABIN-2 mRNA levels were upregulated after TNF- α treatment in both cell types. The changes in gene expression observed appear to be displayed in a cell specific temporal pattern, while Cezanne mRNA expression levels were unchanged following stimulation with TNF- α in these cells in the time period examined.

Chapter 5

Investigating A20 as a means of modulating the NR4A subfamily of nuclear receptors

lyit | Institiúid Teicneolaíochta Éilictríonannalinn
Letterkenny Institute of Technology

5. Investigating A20 as a means of modulating the NR4A subfamily of nuclear receptors

5.1 Introduction

In macrophage cells, it has been demonstrated that NR4A subfamily overexpression upregulates the expression of A20, among several other genes associated with inflammation, indicating the potential role of this subfamily in the regulation of A20 and A20-interacting proteins (Pei *et al.* 2006). One of the aims of this study was to examine the potential of A20 as a means of modulating the NR4A subfamily in the pathogenesis of RA. In order to elucidate this, transient transfection experiments were carried out in which an NBRE-luciferase reporter construct was co-transfected into cellular models of inflammatory arthritis, with and without a constitutively active NURR1 expression vector. In addition, an A20 expression plasmid was co-transfected into these cells. The luciferase activity was then measured in these cells using the Dual Luciferase Reporter (DLR) Assay System (Promega) and compared to controls transfected in a similar manner without the presence of A20. Further transfection experiments were carried out to investigate the effects of A20 on the transcriptional activation of the NR4A target gene IL-8 by NURR1. It has previously been established that NURR1 induces expression of the proinflammatory chemokine IL-8, and in addition, NURR1 enhances NF- κ B p65 induction of IL-8 independently of the NBRE binding site (Aherne *et al.* 2009). Cells were co-transfected with an IL-8 human promoter luciferase reporter construct, a NURR1 expression vector and an A20 expression construct with and without a p65 expression vector. The luciferase assay results were compared to those obtained without the presence of A20 overexpression. In this manner, the effects of A20 on the transcriptional activity of NURR1 were elucidated.

5.2 Verification of Plasmids used for Transfection Experiments

Prior to use, the quality and composition of the plasmids were verified by digesting with restriction enzymes and gel electrophoresis as described in sections 2.3.6 and 2.3.7. Expected banding patterns were obtained following digestion, thus confirming the composition of the plasmids.

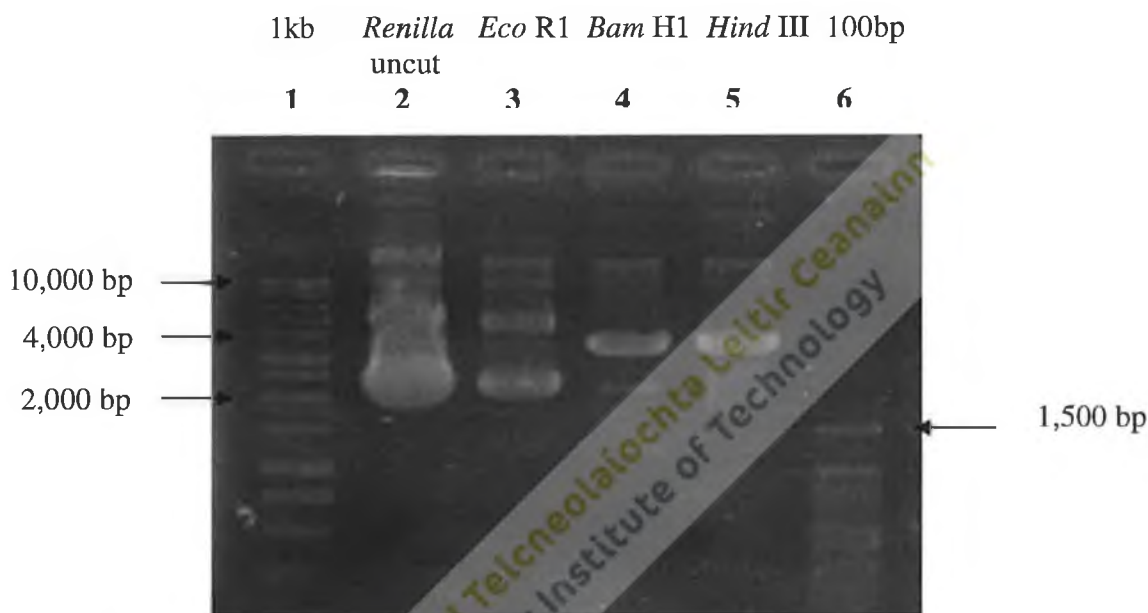


Fig. 5.1 Restriction enzyme digests of Qiagen purified *Renilla* luciferase pRL-SV40 vector (3,705 bp) electrophoresed on 0.8 % agarose gel and visualised by staining with ethidium bromide.

Lane	Sample
1	1 kb DNA ladder
2	<i>Renilla</i> luciferase vector undigested
3	<i>Renilla</i> luciferase vector digested with <i>Eco</i> R1
4	<i>Renilla</i> luciferase vector digested with <i>Bam</i> H1
5	<i>Renilla</i> luciferase vector digested with <i>Hind</i> III
6	100 bp DNA ladder

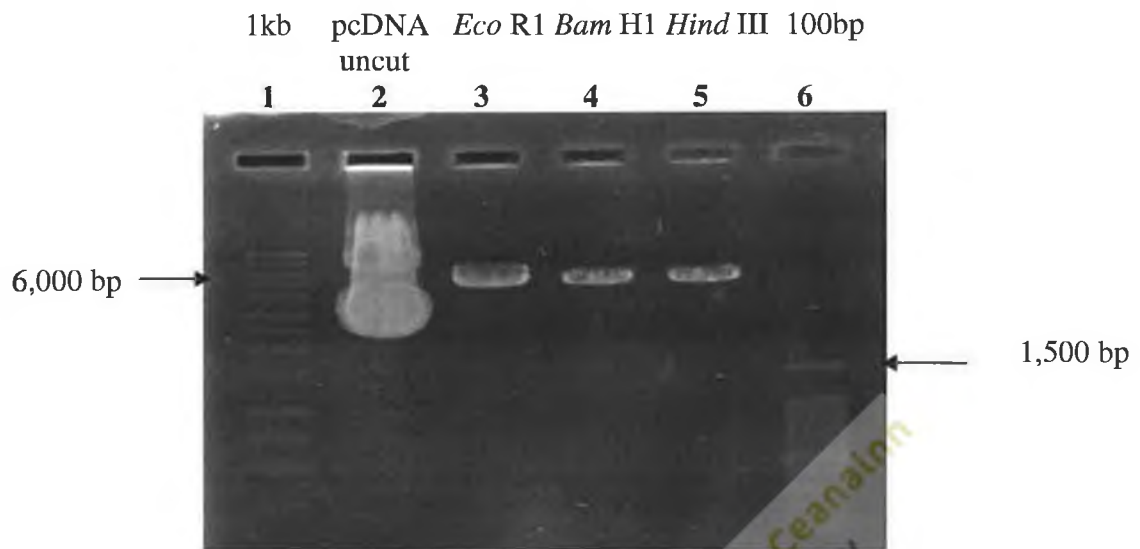


Fig. 5.2 Restriction enzyme digests of Qiagen purified pcDNA6/*myc*-His C plasmid (5,100 bp) electrophoresed on 0.8 % agarose gel and visualised by staining with ethidium bromide.

Lane	Sample
1	1 kb DNA ladder
2	pcDNA plasmid undigested
3	pcDNA digested with <i>Eco</i> R1
4	pcDNA digested with <i>Bam</i> H1
5	pcDNA digested with <i>Hind</i> III
6	100 bp DNA ladder

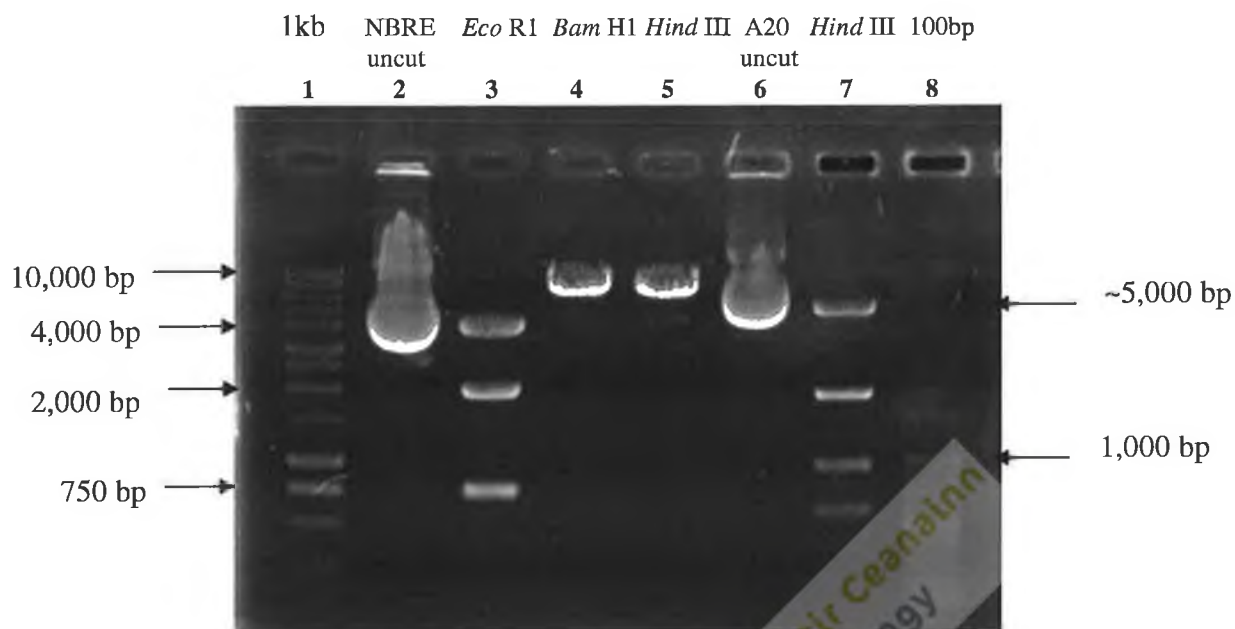


Fig. 5.3 Restriction enzyme digests of Qiagen purified pNBRE₃-tk-luciferase reporter construct (~ 5,600 bp) and pCAGGS-GFP/A20 (8,372 bp) electrophoresed on 0.8 % agarose gel and visualised by staining with ethidium bromide.

Lane	Sample
1	1 kb DNA ladder
2	pNBRE ₃ -tk-luciferase reporter construct undigested
3	pNBRE ₃ -tk-luciferase construct digested with <i>Eco</i> R1
4	pNBRE ₃ -tk-luciferase construct digested with <i>Bam</i> H1
5	pNBRE ₃ -tk-luciferase construct digested with <i>Hind</i> III
6	A20 expression vector undigested
7	A20 vector digested with <i>Hind</i> III
8	100 bp DNA ladder

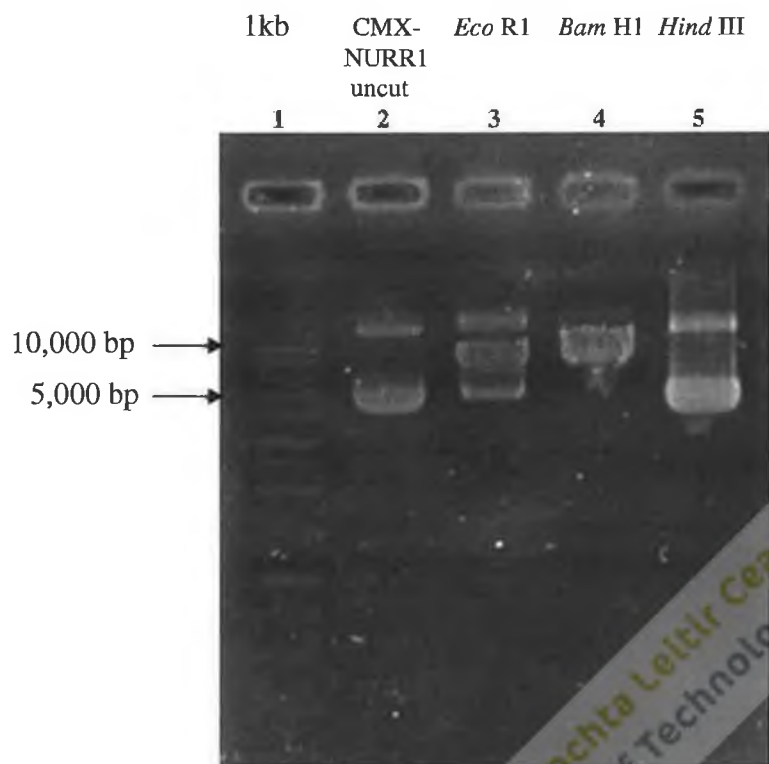


Fig. 5.4 Restriction enzyme digests of Qiagen purified CMX-NURR1 plasmid (7,200 bp) electrophoresed on 0.8 % agarose gel and visualised by staining with ethidium bromide.

Lane	Sample
1	1 kb DNA ladder
2	CMX-NURR1 expression plasmid undigested
3	CMX-NURR1 plasmid digested with <i>Eco</i> R1
4	CMX-NURR1 plasmid digested with <i>Bam</i> H1
5	CMX-NURR1 plasmid digested with <i>Hind</i> III
6	100 bp DNA ladder

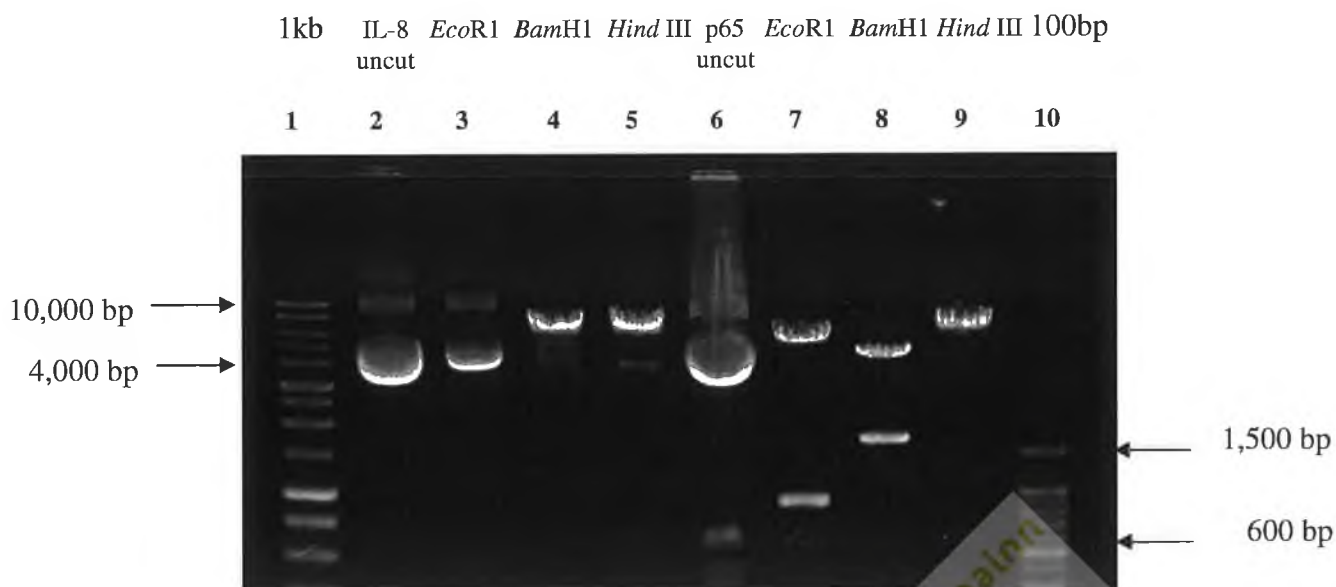


Fig. 5.5 Restriction enzyme digests of Qiagen purified IL-8-luciferase reporter construct (11508 bp) and p65 expression vector electrophoresed on 0.8 % agarose gel and visualised by staining with ethidium bromide.

Lane	Sample
1	1 kb DNA ladder
2	IL-8-luciferase construct undigested
3	IL-8-luciferase construct digested with <i>Eco</i> R1
4	IL-8-luciferase construct digested with <i>Bam</i> H1
5	IL-8-luciferase construct digested with <i>Hind</i> III
6	p65 expression vector undigested
7	p65 digested with <i>Eco</i> R1
8	p65 digested with <i>Bam</i> H1
9	p65 digested with <i>Hind</i> III
10	100 bp DNA ladder

5.3 Transfection Efficiencies

Green Fluorescent Protein (GFP) assays were carried out as described in section 2.5.9 in order to determine the transfection efficiency of the transfection reagent Turbofect for each of the two cell lines used in this study - K4 IM synoviocytes and SW 1353 chondrocytes. From these assays, the transfection efficiency of Turbofect for the synoviocytes was an average of approximately 40 % and for the chondrocytes was an average of approximately approximately 70 %.



Fig. 5.6 K4 IM synoviocytes transfected with a GFP expression vector viewed using the Olympus 1X51 inverted fluorescent microscope with mercury lamp under 100X magnification. A: normal view of cells transfected with GFP, B: cells transfected with GFP viewed under mercury lamp showing expression of GFP, C: normal view of cells not transfected with GFP (control), D: control cells viewed under mercury lamp.

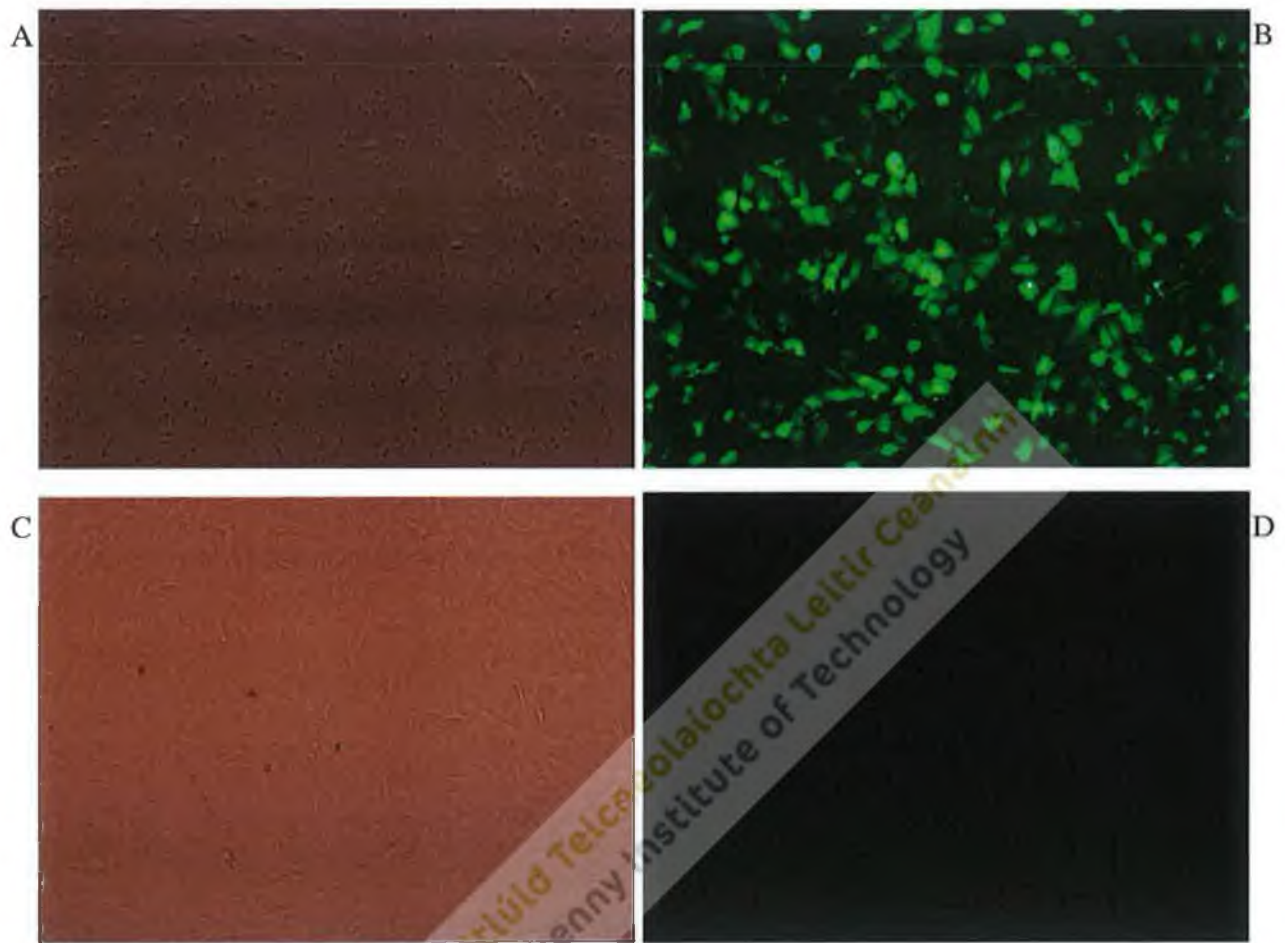


Fig. 5.7 SW 1353 chondrocytes transfected with a GFP expression vector viewed using the Olympus 1X51 inverted fluorescent microscope with mercury lamp under 100X magnification. A: normal view of cells transfected with GFP, B: cells transfected with GFP viewed under mercury lamp showing expression of GFP, C: normal view of cells not transfected with GFP (control), D: control cells viewed under mercury lamp.

5.4 NBRE-luciferase Assays

Human immortalized K4 IM synovial fibroblasts and human immortalized SW 1353 chondrocytes were grown in 75 cm³ cell culture flasks to 70-80 % confluency. The cells were then trypsinized, counted and seeded into 24-well culture plates at a concentration of 1.4 x 10⁴ cells/well as described in section 2.5.5. Twenty-four hours later, the cells were serum-starved and transfected as described in section 2.5.7. Luciferase assays were performed 24 hr after transfection, as described in section 2.5.9. The results obtained are illustrated below.

5.4.1 NBRE- Luciferase Assay Results – K4 IM Synoviocytes

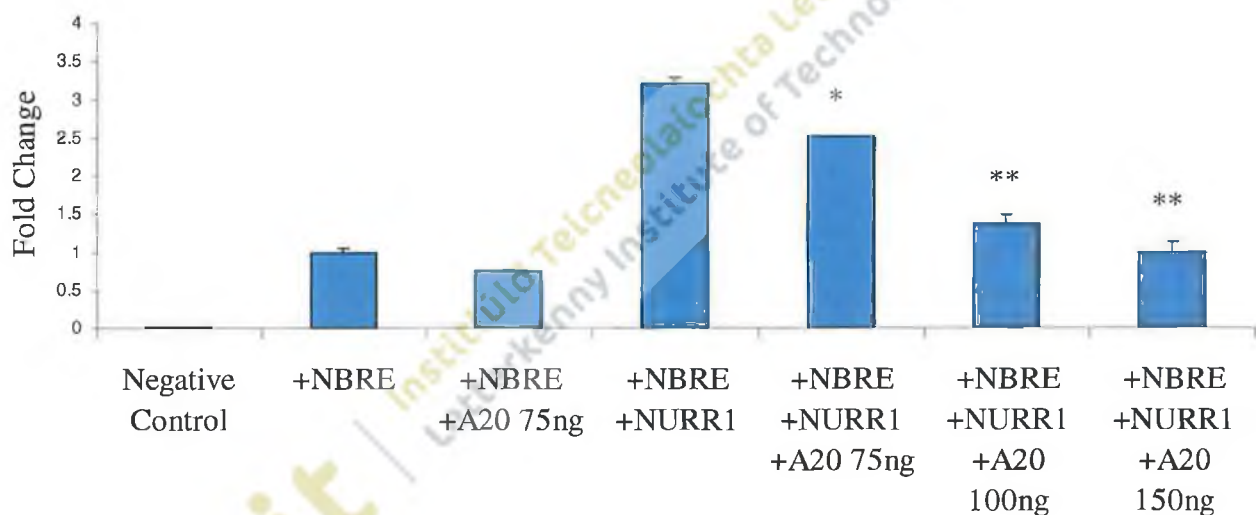


Fig. 5.8 NBRE-luciferase assay results for K4 IM cells demonstrating a dose-dependant inhibitory effect of A20 on the activation of the pNBRE₃-tk-luciferase reporter construct by NURR1. The cells were not serum-starved in this experiment and transfected in triplicate in supplemented medium using GeneJuice. Cells were assayed 24 hr post-transfection. Results represent the mean fold change plus standard error of the mean (SEM) compared to the NBRE reporter construct alone. * p < 0.01, ** p < 0.001 compared with NBRE-luciferase construct + CMX-NURR1 vector.

**Table 5.1 Composition of DNA Transfected into K4 IM cells using GeneJuice for
NBRE-Luciferase Assay**

Sample	Contents
Negative control	puB6 empty vector (325 ng)
+NBRE	puB6 (250 ng), NBRE reporter construct (75 ng)
+NBRE +A20 (75ng)	puB6 (175 ng), NBRE (75 ng), A20 expression plasmid (75 ng)
+NBRE +NURR1	puB6 (150 ng), NBRE (75 ng), CMX-NURR1 expression plasmid (100 ng)
+NBRE +NURR1 +A20 (75 ng)	puB6 (75 ng), NBRE (75 ng), CMX-NURR1 (100 ng), A20 (75 ng)
+NBRE +NURR1 +A20 (100 ng)	puB6 (50 ng), NBRE (75 ng), CMX-NURR1 (100 ng), A20 (100 ng)
+NBRE +NURR1 +A20 (150 ng)	NBRE (75 ng), CMX-NURR1 (100 ng), A20 (150 ng)

5.4.1 NBRE- Luciferase Assay Results – K4 IM Synoviocytes continued

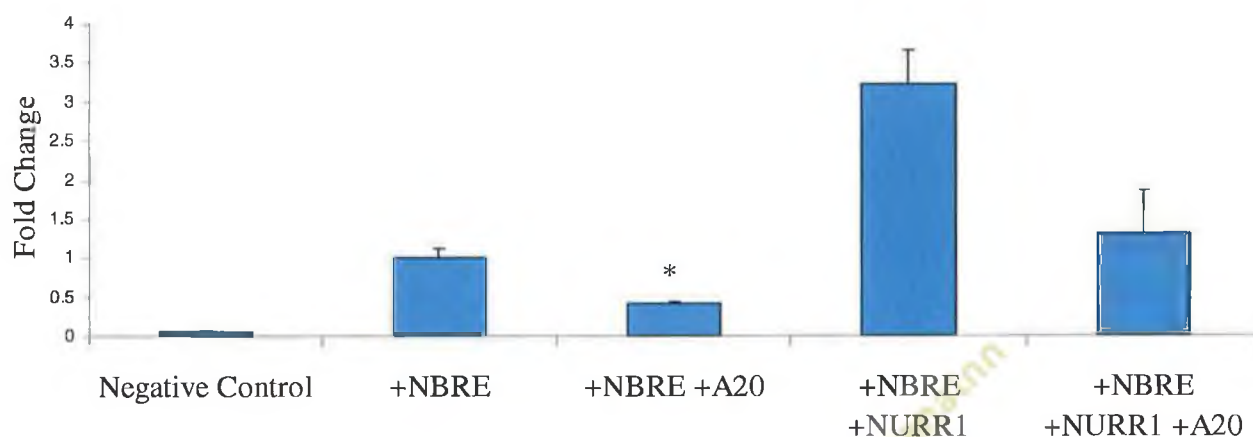


Fig. 5.9 NBRE-luciferase assay results for K4 IM cell line illustrating an inhibitory effect of A20 on the activation of the pNBRE₃-tk-luciferase reporter construct. Cells were serum-starved 24 hr prior to transfection and transfected in triplicate using the transfection reagent Turbofect. Cells were assayed 24 hr post-transfection. NBRE-luciferase values obtained were normalized to *Renilla* luciferase activity. These results represent the mean fold change plus SEM compared to the NBRE reporter construct alone. Identical trends were obtained in at least two further independent experiments. * $p < 0.05$ compared to NBRE-luciferase construct in each of three separate experiments.

Table 5.2 Composition of DNA Transfected into K4 IM cells using Turbofect for NBRE-Luciferase Assays

Sample	Contents
Negative control	<i>Renilla</i> luciferase construct (0.362 ng), pcDNA empty vector (900 ng)
+NBRE	<i>Renilla</i> (0.362 ng), pcDNA (650 ng), NBRE reporter construct(250 ng)
+NBRE +A20	<i>Renilla</i> (0.362 ng), pcDNA (400 ng), (250 ng), A20 expression plasmid (250 ng)
+NBRE +NURR1	<i>Renilla</i> (0.362 ng), pcDNA (250 ng), NBRE (250 ng), CMX-NURR1 expression plasmid (400 ng)
+NBRE +NURR1 +A20	<i>Renilla</i> (0.362 ng), NBRE (250 ng), CMX-NURR1 (400 ng), A20 (250 ng)

5.4.2 NBRE-Luciferase Assay Results – SW 1353 Chondrocytes

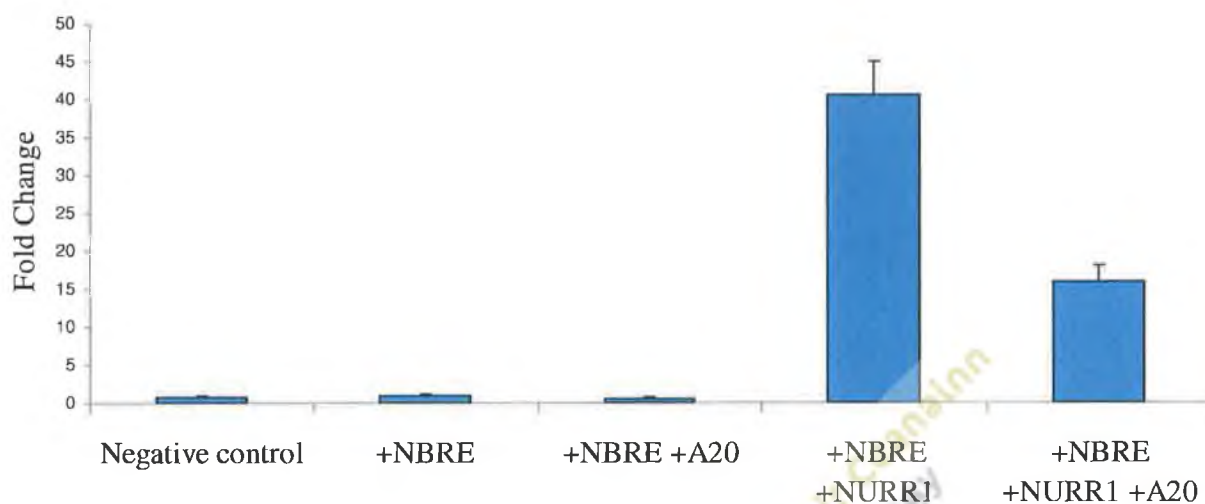


Fig. 5.10 NBRE-luciferase assay results for SW 1353 cell line illustrating the inhibitory effect of A20 on the activation of the pNBRE₃-tk-luciferase reporter construct. Cells were serum-starved 24 hr prior to transfection and transfected in triplicate using the transfection reagent Turbofect. Cells were assayed 24 hr post-transfection. NBRE-luciferase values obtained were normalized to *Renilla* luciferase activity. These results represent the mean fold change plus SEM compared to the NBRE reporter construct alone. Whilst p values were not always significant at the 5 % level, identical trends were obtained in at least two further independent experiments.

Table 5.3 Composition of DNA transfected into SW 1353 cells using Turbofect for NBRE-Luciferase Assays

Sample	Contents
Negative control	<i>Renilla</i> luciferase construct (0.362 ng), pcDNA empty vector (900 ng)
+NBRE	<i>Renilla</i> (0.362 ng), pcDNA (650 ng), NBRE reporter construct(250 ng)
+NBRE +A20	<i>Renilla</i> (0.362 ng), pcDNA (400 ng), (250 ng), A20 expression plasmid (250 ng)
+NBRE +NURR1	<i>Renilla</i> (0.362 ng), pcDNA (250 ng), NBRE (250 ng), CMX-NURR1 expression plasmid (400 ng)
+NBRE +NURR1 +A20	<i>Renilla</i> (0.362 ng), NBRE (250 ng), CMX-NURR1 (400 ng), A20 (250 ng)

5.5 IL-8 Luciferase Assays

Previous studies have demonstrated that NURR1 induces transcription of the proinflammatory chemokine IL-8 in K4 IM cells. Furthermore, co-expression of the NF- κ B subunit p65 and NURR1 led to a synergistic increase in IL-8 transcription (Davies *et al.* 2005, Aherne *et al.* 2009). Therefore, transient transfection experiments were carried out in which an IL-8 human promoter luciferase reporter construct was co-transfected into cells along with CMX-NURR1, a p65 expression vector and the A20 expression plasmid. The luciferase activity measured was compared to that obtained without the A20 plasmid. Hence, the effect of A20 on the transcriptional activity of NURR1 on a known target gene was determined in order to establish the relationship between A20 and an inflammatory gene.

Synoviocytes and chondrocytes were seeded into 24-well culture plates at a concentration of 2.5×10^4 cells/well as described in section 2.5.5. The cells were transfected 24 hr later as described in section 2.5.7. Luciferase assays were carried out 24 hr post-transfection, as described in section 2.5.9.

5.5.1 IL-8 Luciferase Assay Results – K4 IM Synoviocytes

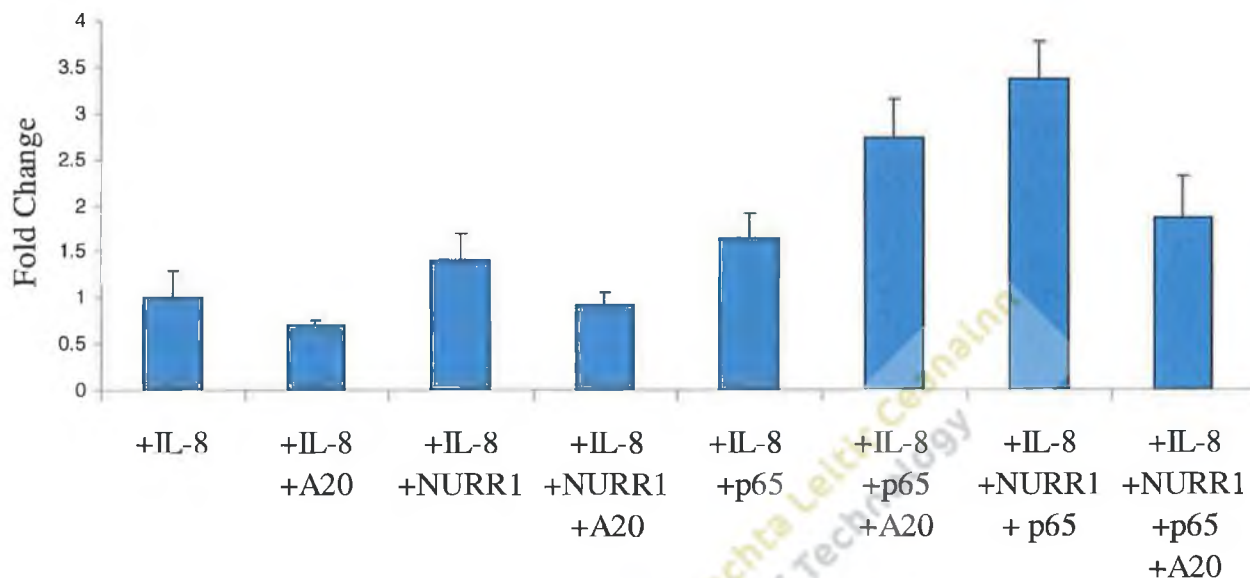


Fig. 5.11 IL-8-luciferase assay results for the K4 IM cell line illustrating an inhibitory effect by A20 on the transactivation of the IL-8 reporter construct by endogenous NURR1, overexpressed NURR1 and overexpressed NURR1 in combination with the NF- κ B subunit p65. Cells were seeded in 24 well plates and transfected 24 hr later in triplicate. Cells were assayed 24 hr post-transfection. IL-8-luciferase values obtained were normalized to *Renilla* luciferase activity. Results represent the mean fold change plus SEM compared to the IL-8 reporter construct alone.

Similar trends were obtained for the effects of A20 on the transactivation of the IL-8 reporter construct by endogenous and overexpressed NURR1 in at least two further independent experiments. However, variable trends were obtained for the effects of A20 overexpression on the transcriptional activity of p65 and p65 in combination with NURR1.

The composition of DNA which was transfected into K4 IM cells for this experiment is given in Table 5.4.

**Table 5.4 Composition of DNA transfected into cells using Turbofect
for IL-8-Luciferase Assays**

Sample	Contents
+IL-8	<i>Renilla</i> luciferase reporter construct (0.362 ng), pcDNA empty vector (310 ng), IL-8 reporter construct (100 ng)
+IL-8 +A20	<i>Renilla</i> (0.362 ng), pcDNA (210 ng), IL-8 (100 ng), A20 expression plasmid (100 ng)
+IL-8 +NURR1	<i>Renilla</i> (0.362 ng), pcDNA (110 ng), IL-8 (100 ng), CMX-NURR1 expression plasmid (200 ng)
+IL-8 +NURR1 +A20	<i>Renilla</i> (0.362 ng), IL-8 (100 ng), CMX-NURR1 (200 ng), A20 (100 ng)
+IL-8 +p65	<i>Renilla</i> (0.362 ng), pcDNA (300 ng), IL-8 (100 ng), p65 expression vector (10 ng)
+IL-8 +p65 +A20	<i>Renilla</i> (0.362 ng), pcDNA (200 ng), IL-8 (100 ng), p65 (10 ng), A20 (100 ng)
+IL-8 +NURR1 +p65	<i>Renilla</i> (0.362 ng), pcDNA (100 ng), IL-8 (100 ng), CMX-NURR1 (200 ng), p65 (10 ng)
+IL-8 +NURR1 +p65 +A20	<i>Renilla</i> (0.362 ng), IL-8 (100 ng), CMX-NURR1 (200 ng), p65 (10 ng), A20 (100 ng)

5.5.2 IL-8 Luciferase Assay Results – SW 1353 Chondrocytes

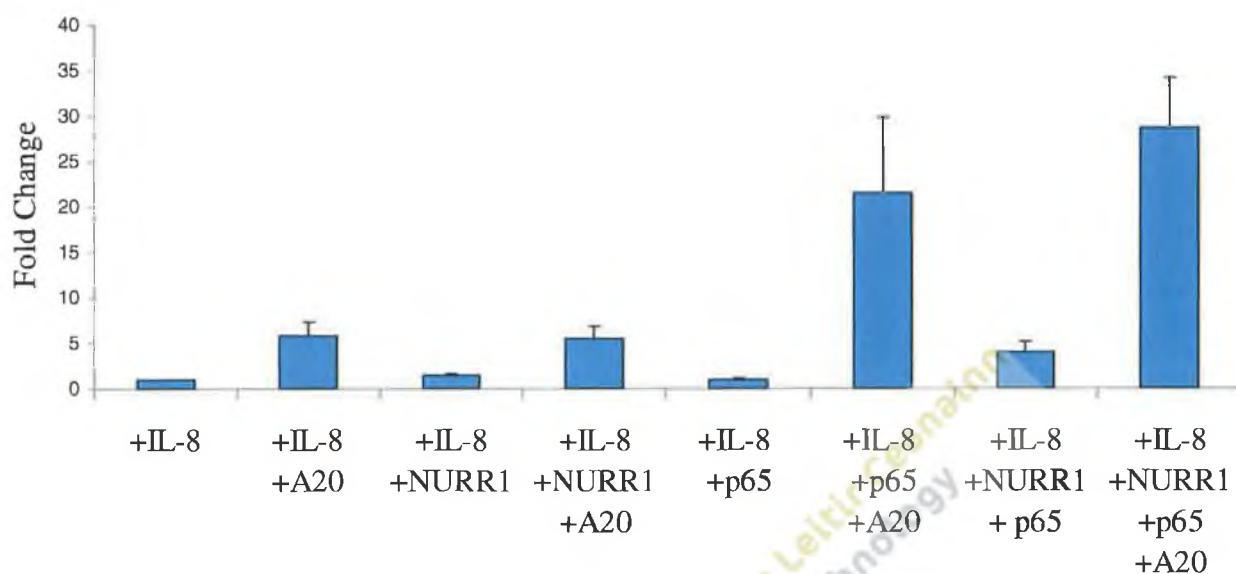


Fig. 5.12 IL-8-luciferase assay results for SW 1353 cells showing an enhancing effect by A20 on the transcriptional activity of endogenous NURR1, overexpressed NURR1 and overexpressed p65 on the IL-8-luciferase reporter construct. Cells were transfected using the transfection reagent Turbofect in triplicate and assayed 24 hr post-transfection. IL-8-luciferase values obtained were normalized to *Renilla* luciferase activity. These results represent the mean fold change plus SEM compared to the NBRE reporter construct alone. While p values were not always significant, similar trends were obtained for at least two further independent experiments.

The composition of DNA which was transfected into SW 1353 cells for each of the samples in this experiment is given in Table 5.4.

5.6 Discussion

Many studies have demonstrated the anti-inflammatory effects of the zinc-finger protein A20. It is a potent NF- κ B inhibitory protein and also has the ability to down-regulate AP-1, another pro-inflammatory transcription factor (O'Reilly and Moynagh 2003). A20-deficient mice develop severe multi-organ inflammation and die prematurely (Lee *et al.* 2000). Overexpression of the NR4A subfamily member NURR1 leads to the induction of inflammatory genes including IL-8 and increasing levels of NURR1 are found in synovial tissue of RA patients compared to normal

synovial tissue (Aherne *et al.* 2009; Davies *et al.* 2005; McEvoy *et al.* 2002; Pei *et al.* 2006). Therefore, the potential modulation of NURR1 by A20 was investigated in this study. NR4A subfamily members bind to the NBRE DNA binding site in order to regulate target gene expression (Wilson *et al.* 1991). The effect of A20 on the transcriptional activity of NURR1 was determined by carrying out co-transfection experiments of an NBRE-luciferase reporter construct and an A20 expression plasmid, with and without a NURR1 expression vector. Luciferase assays were then carried out to determine the amount of luciferase expressed in these cells, and therefore, the ability of NURR1 to transactivate the NBRE binding site.

NURR1 is the most upregulated member of the NR4A family in response to PGE₂, IL-1 β and TNF- α in primary RA and normal synoviocytes and NURR1 expression is notably higher in synovial tissue of RA patients compared to healthy subjects. Furthermore, NURR1 is the major subfamily member expressed in K4 IM and SW 1353 cells (McEvoy *et al.* 2002; Murphy *et al.* 2001). Therefore, studies focused on this NR4A subfamily member for analysis of modulation by A20 in the context of human inflammatory arthritis.

NBRE-luciferase transfection experiments illustrated a dose-dependent inhibitory effect of A20 on the transcriptional activity of NURR1 (Fig. 5.8). Increasing concentrations of A20 (75 – 150 ng) led to decreasing levels of NBRE-luciferase activation by NURR1 (from 3.2 – 0.99 fold induction). At 150 ng, A20 sufficiently suppressed CMX-NURR1 activation of the NBRE-luciferase construct to a level equal to the transcriptional activity of endogenous NURR1. Each concentration of A20 investigated resulted in a significant ($p < 0.01$) or highly significant ($p < 0.001$) reduction in the ability of NURR1 to transactivate the NBRE-luciferase construct. Further K4 IM synoviocyte transfection data (Fig. 5.9) predominantly demonstrated a similar inhibitory effect by A20 on the transactivation activity of both endogenous and overexpressed NURR1. A20 significantly ($p < 0.05$) suppressed endogenous NURR1-induced NBRE-luciferase activation and markedly diminished CMX-NURR1 activation of the NBRE-luciferase reporter construct in each of three independent experiments.

The SW 1353 chondrocyte results (Fig. 5.10) demonstrate that A20 had a consistent inhibitory effect on endogenous NURR1, with diminished activation of the NBRE-luciferase reporter construct in the presence of A20 overexpression compared to the NBRE-luciferase construct alone. The addition of CMX-NURR1 to the NBRE-luciferase reporter construct in chondrocyte

cells resulted in a marked (30 fold average) induction of NBRE-luciferase activation. Overexpression of A20 consistently attenuated this induction of NBRE-luciferase activity by CMX-NURR1 in these cells, demonstrating a novel inhibitory effect of A20 on this NR4A subfamily member. While identical trends were observed in all experiments, not all resulted in a significant ($p < 0.05$) reduction of NURR1 transcriptional activity by A20.

The NBRE-luciferase assays in the K4 IM synoviocytes did produce some variable results (data not shown). This may be due to the lower transfection efficiency of the transfection reagent Turbofect for the K4 IM cells (approximately 40 %) compared to the SW 1353 cells (approximately 70 %) as demonstrated by the GFP assay results (Fig. 5.6 and 5.7). The variable results obtained may, however, be due to differences in the stages of the cell cycle between experiments, although both cell types were serum-starved to synchronise the cells.

Transfection of equal concentrations of CMX-NURR1 into both cell types resulted in less NBRE-luciferase activation in K4 IM cells compared to SW 1353 cells (an average of 3 fold for K4 cells compared to 30 fold for SW cells). This may be due to the variable transfection efficiency as described above. However, since the NBRE-luciferase activity was normalised to *Renilla* luciferase activity in both cell types, it may be that NURR1's ability to activate the NBRE transcriptional site depends on the cell context.

Cells which had not been serum-starved and transfected in supplemented medium produced similar values and trends to those which had been serum-starved and transfected in SFM (data not shown). This was the case for both cell types used in this study. This demonstrated that the presence of serum in the supplemented medium did not affect the results obtained.

The results in this study indicate a novel function of A20 in its ability to suppress activity of the transcription factor NURR1. To date, few inhibitors of the NR4A nuclear receptor subfamily have been identified. Ralph *et al.* (2005) demonstrated that the disease-modifying anti-rheumatic drug methotrexate can directly attenuate NURR1 expression in response to inflammatory stimuli and growth factors. Dexamethasone, a glucocorticosteroid, has been found to inhibit cytokine-induced NURR1 expression levels in primary synoviocytes (Murphy *et al.* 2001). In addition, a study by Ohkura *et al.* (1999) indicated that a C-terminal truncated isoform of NURR1, termed NURR2, negatively regulates each of the NR4A2 subfamily members. The NR3B subfamily of

estrogen-related receptors has also been shown to repress the transcriptional activity of NR4A subfamily members (Lammi *et al.* 2007). Further studies may confirm A20 as being among these repressors of NURR1 activity and, if so, reveal the mechanism by which NURR1 is inhibited. In addition, the effect of A20 on the other members of the NR4A subfamily, NUR77 and NOR-1, remains to be elucidated.

The inhibitory effect of A20 on endogenous NURR1 transcriptional activity may reflect the situation in a normal joint, where NURR1 levels are not raised. Transfection of CMX-NURR1 into the cells is equivalent to introducing ectopic NURR1, which is reflective of the inflammatory state (McEvoy *et al.* 2002). Therefore, the ability of A20 to dampen overexpressed NURR1 transactivation reveals a possible means by which NURR1 may be modulated in an inflamed situation, such as an RA joint.

Studies have found that overexpression of NURR1 induces transactivation of the proinflammatory chemokine IL-8. Co-expression of NURR1 and the NF- κ B subunit p65 lead to increased IL-8 induction. NURR1 co-operates with p65 to induce IL-8 transactivation in a mechanism which is independent of NURR1 binding to DNA (Aherne *et al.* 2009). Therefore, the effect of A20 on NURR1's ability to induce IL-8 expression on its own and in the presence of p65 was investigated. This was carried out by co-transfecting an IL-8 human promoter luciferase reporter construct and a NURR1 expression vector with and without p65 and assessing the effect of A20 overexpression on IL-8 reporter transactivation.

IL-8 is a proinflammatory chemokine that has been identified as being significantly upregulated in RA joints. It attracts polymorphonuclear neutrophils into the joint, heightening the immune response. IL-8 also induces angiogenesis, enabling further inflammatory mediators to enter the joint (Slavic *et al.* 2005). In the K4 IM synoviocytes, there was a consistent inhibitory effect by A20 on the ability of overexpressed and endogenous NURR1 to transactivate the IL-8 promoter in the absence of p65 (Fig. 5.11). The ability of A20 to suppress NURR1 activation of the IL-8 promoter was not always significant ($p < 0.05$), however. Co-expression of NURR1 and p65 did display a slight synergistic effect on IL-8 promoter activity. Aherne *et al.* (2009) obtained strong synergistic increases in IL-8 promoter transactivation by NURR1 and p65 in the same cell type. Aherne *et al.* (2009) used 400-800 ng of CMX-NURR1 plasmid in their experiments compared to 200 ng of CMX-NURR1 in this study, however. Nonetheless, the same pattern of NURR1 and

p65-induced activation of the IL-8 promoter was observed. Variable results were obtained for the K4 IM cells in assessing the effect of A20 on p65 transactivation of the IL-8 promoter and on A20's effect on the combined transcriptional activity of NURR1 and p65 (data not shown). Again, this may be due to the lower transfection efficiency of the transfection reagent Turbofect for this cell type or due to differences in the cell cycle between experiments. Alternatively, the effects of A20 on the transcriptional activity of NURR1 and p65 may be variable in the K4 IM cells. It may be that A20-interacting proteins such as ABIN-1/ABIN-2 or others are affecting the ability of A20 to modulate the transcriptional activity of NURR1 in K4 IM cells. This may explain why some variable results were obtained for the NBRE-luciferase assay for this cell type also.

A consistent enhancing effect was observed by A20 on the ability of NURR1 to transactivate the IL-8 promoter in the SW 1353 chondrocyte cells. Similarly, A20 had an enhancing effect on the ability of p65 to induce IL-8-luciferase activity. In addition, A20 expression appeared to increase the combined transcriptional activity of NURR1 and p65 on the IL-8 promoter (Fig. 5.12). It appears that A20 positively modulates NURR1's transcriptional activation of the human IL-8 promoter in human chondrocyte cells. However, there was not always a statistically significant ($p < 0.05$) increase in NURR1 activation of the IL-8 promoter by A20. A stronger synergistic effect by the co-expression of NURR1 and p65 on IL-8 transcriptional activity was observed in the SW 1353 cells compared to the K4 IM cell line.

Previous studies carried out by Aherne *et al.* (2009) found that upregulation of IL-8 by NURR1 was independent of NURR1 binding to the IL-8 promoter and did not involve interaction with the RXR receptor. The IL-8 promoter does not contain the NBRE binding site (Aherne *et al.* 2009). Therefore, it appears that modulation of NURR1 by A20 is NBRE independent. In order to control the transcriptional activity of NURR1, A20 may not interact with the NBRE site, blocking or enhancing transcription of IL-8, depending on the cell context. Instead, it appears that A20 may directly modulate the actions of NURR1 through protein-protein interactions or indirectly, via intermediate proteins.

The results from the IL-8-luciferase assays indicate that A20 may have a functional effect on the ability of NURR1 to transactivate target genes and that this effect may be cell type specific. The results also suggest that A20 may positively modulate NF- κ B target genes, a role not previously

identified with this protein. Furthermore, results suggest that A20 may be involved in the regulation of NR4A target genes such as IL-8, in addition to those activated by NF- κ B. This indicates a novel role of A20 in the regulation of inflammation.

5.7 Conclusions

Transient transfection experiments and luciferase assays have revealed that A20 may play a role in modulating the transcriptional activity of the NR4A member NURR1 in the context of inflammatory arthritis. In K4 IM synoviocytes and SW 1353 cells, A20 inhibited transactivation of the NR4A transcription factor binding site. Results indicate that transcriptional activation of the NR4A target gene IL-8 by NURR1 may be influenced by A20 and that the type of modulation may be cell type specific.

Chapter 6

Summary

lyit | Institiúid Teicneolaíochta Lethr Ceannainn
Letterkenny Institute of Technology

6. Summary

The aims of this investigation were to elucidate the potential interaction between A20 and the NR4A subfamily of nuclear receptors in the context of RA and to determine the effects of the inflammatory cytokine TNF- α on the expression of A20, ABIN-1, ABIN-2 and Cezanne in the multicellular environment of RA. Bioinformatic analysis of A20 and the A20-related genes ABIN-1, ABIN-2 and Cezanne identified the NR4A transcriptional binding site, the NBRE site, within the promoter region of these genes. Further bioinformatic analysis indicates that the NBRE sites found in ABIN-1 and Cezanne may be functionally significant, suggesting that the NR4A subfamily members may regulate expression of these A20-related genes.

Human K4 IM synoviocytes and SW 1353 chondrocytes were stimulated with the inflammatory cytokine TNF- α . RT-PCR analyses of the resulting RNA indicate that A20, ABIN-1 and ABIN-2 were upregulated in response to TNF- α treatment in both cell models of RA. Differential expression of Cezanne was not detected following stimulation with TNF- α in these cell types. qPCR analyses of chondrocytes treated with this cytokine over a 24 hr period confirmed the end-point PCR results obtained for this cell type and illustrated that, in the timeframe investigated, maximum A20 mRNA expression was after stimulation with TNF- α for 1 hr, while maximum ABIN-1 mRNA expression was after 24 hr stimulation.

Co-transfection experiments and luciferase assays were carried out on synoviocyte and chondrocyte cells to investigate the effect of A20 on the transcriptional activity of NURR1. The results obtained imply that A20 may inhibit the ability of NURR1 to transactivate the NBRE binding site in both cell types. Further results suggest that A20 may regulate the transcriptional activity of NURR1 independent of the NBRE site, since A20 overexpression modulated the ability of this nuclear receptor to induce the NR4A target gene IL-8, a gene which does not contain the NBRE site. Results indicate that modulation of NURR1 by A20 may be cell context dependent.

From the results of this study, it appears that A20 may play a previously unknown role in regulating the transcriptional activity of the NR4A nuclear receptor NURR1.

Chapter 7

Bibliography

lyit | Institiúid Teicneolaíochta Lelitr Ceannainn
Letterkenny Institute of Technology

7. Bibliography

Aherne, C.M., McMorrow, J., Kane, D., FitzGerald, O., Mix, K.S., Murphy, E.P., 2009. Identification of NR4A2 as a transcriptional activator of IL-8 expression in human inflammatory arthritis. *Molecular Immunology* **46**(16), 3345-3357.

Ah-Kim, H., Zhang, X., Islam, S., Sofi, J.I., Glickberg, Y., Malemud, C.J., Moskowitz, R.W., Haqqi, T.M., 2000. Tumor necrosis factor alpha enhances the expression of hydroxyl lyase, cytoplasmic antiproteinase-2 and a dual specificity kinase TTK in human chondrocyte-like cells. *Cytokine* **12**(2), 142-150.

Aletaha, D., Neogi, T., Silman, A.J., Funovits, J., Felson, D.T., Bingham III, C.O., Birnbaum, N.S., Burmester, G.R., Bykerk, V.P., Cohen, M.D., Combe, B., Costenbader, K.H., Dougados, M., Emery, P., Ferraccioli, G., Hazes, J.M.W., Hobbs, K., Huizinga, T.W.J., Kavanaugh, A., Kay, J., Kvien, T.K., Laing, T., Mease, P., Ménard, H.A., Moreland, L.W., Naden, R.L., Pincus, T., Smolen, J.S., Stanislawska-Biernat, E., Symmons, D., Tak, P.P., Upchurch, K.S., Vencovský, Wolfe, F., Hawker, G., 2010. 2010 Rheumatoid arthritis classification criteria. *Arthritis & Rheumatism* **62**(9), 2569-2581.

Arthritis Ireland, 2006. *Rheumatoid Arthritis Survey*. Retrieved from http://www.arthritisireland.ie/research/downloads/Research_RA%20survey.pdf on 22nd June 2009.

Atzeni, F., Antivalle, M., Pallavicini, F.B., Caporali, R., Bazzani, C., Gorla, R., Favalli, E.G., Marchesoni, A., Sarzi-Puttini, P., 2009. Predicting response to anti-TNF treatment in rheumatoid arthritis patients. *Autoimmunity Reviews* **8**(5), 431-437.

Beyaert, R., Heyninck, K., Van Huffel, S., 2000. A20 and A20-binding proteins as cellular inhibitors of nuclear factor- κ B-dependant gene expression and apoptosis. *Biochemical Pharmacology* **60**, 1143-1151.

Bio-Rad Laboratories Inc., 2011 *Fluorescent Primer- and Probe-Based Chemistries*. Retrieved from http://www3.bio-rad.com/B2B/vanity/gexp/content.do?BV_SessionID=@@@@1994672812.1314102906@@@@&BV_EngineID=ccccadfehdlgeedcfngcfkmdhkkdfll.0&root=/Product%20Family/GX/Home&pcatoid=-35468&ccatoid=-36527&country=US&language=English&BV_SessionID=@@@@1994672812.1314102906@@@@&BV_EngineID=ccccadfehdlgeedcfngcfkmdhkkdfll.0#eclipse on 23rd August 2011.

Bonta, P.I., Pols, T.W.H., de Vries, C.J.M., 2007. NR4A Nuclear receptors in atherosclerosis and vein-graft disease. *Trends in Cardiovascular Medicine* **17**(3), 105-111.

Bonta, P.I., van Tiel, C.M., Vos, M., Pols, T.W.H., van Thienen, J.V., Ferreira, V., Arkerbout, K., Seppen, J., Spek, C.A., van der Poll, T., Pannekoek, H., de Vries, C.J.M., 2006. Nuclear receptors NUR77, NURR1, and NOR-1 expressed in atherosclerotic lesion macrophages reduce lipid loading and inflammatory responses. *Arteriosclerosis, Thrombosis, and Vascular Biology* **26**, 2288-2294.

Buch, M., Emery, P., 2002. The aetiology and pathogenesis of rheumatoid arthritis. *Hospital Pharmacist* **9**, 5-10.

Carlos, T.M., Harlan, J.M., 1994. Leukocyte-endothelial adhesion molecules. *Blood* **84**, 2068-2101.

Chein, C.-Y., Liu, W.-K., Chou, C.-K., Su, J.-Y., 2003. The A20-binding protein ABIN-2 exerts unexpected function in mediating transcriptional coactivation. *FEBS Letters* **543**, 55-60.

Chou, C. T., Liao, H.T., Chen, C.H., Chen, W.S., Wang, H.P., Su, K.Y., 2007. The clinical application of anti-CCP in rheumatoid arthritis and other rheumatic diseases. *Biomarker Insights* **2**, 165-171.

Coghlan, M.J., Jacobson, P.B., Lane, B., Nakane, M., Wei Lin, C., Elmore, S.W., Kym, P.R., Luly, J.R., Carter, G.W., Turner, R., Tyree, C.M., Hu, J., Elgort, M., Rosen, J., Miner, J.N., 2003. A novel anti-inflammatory maintains glucocorticoid efficacy with reduced side effects. *Molecular Endocrinology* **17**(5), 860-869.

Cohen, C.D., Klingenhoff, A., Boucherot, A., Nitsche, A., Henger, A., Brunner, B., Schmid, H., Merkle, M., Saleem, M.A., Koller, K.P., Werner, T., Gröne, H. J., Nelson, P.J., Kretzler, M., 2006. Comparative promoter analysis allows de novo identification of specialized cell junction-associated proteins. *Proceedings of the National Academy of Sciences* **103**(15), 5682-5687.

Cohen, S.B., Dore, R.K., Lane, N.E., Ory, P.A., Peterfy, C.G., Sharp, J.T., van der Heijde, D., Zhou, L., Tsuji, W., Newmark, R., 2008. Denosumab treatment effects on structural damage, bone mineral density, and bone turnover in rheumatoid arthritis: a twelve-month, multicenter, randomized, double-blind, placebo-controlled, phase II clinical trial. *Arthritis & Rheumatism* **58**(5), 1299-1309.

Combe, B., 2009. Progression in early rheumatoid arthritis. *Best Practice & Research Clinical Rheumatology* **23**, 59-69.

Corper, A.L., Sohi, M.K., Bonagura, V.R., Steinitz, M., Jefferis, R., Feinstein, A., Beale, D., Taussig, M.J., Sutton, B.J., 1997. Structure of human IgM rheumatoid factor Fab bound to its autoantigen IgG Fc reveals a novel topology of antibody-antigen interaction. *Nature Structural Biology* **4**, 374 – 381.

Cronstein, B.N., 2007. Interleukin-6 A key mediator of systemic and local symptoms in rheumatoid arthritis. *Bulletin of the NYU Hospital for Joint Diseases* **65**(Suppl 1), S11-S15.

d'Abusco, A.S., Politi, L., Giordano, C., Scandurra, R., (2010) A peptidyl-glucosamine derivative affects IKK α kinase activity in human chondrocytes. *Arthritis Research and Therapy* **12**:R8. Retrieved from <http://arthritis-research.com/content/12/1/R18> on 18th July 2011.

Dale, J.W., von Schantz, M., 2002. *From Genes to Genomes*. John Wiley & Sons Ltd., Chicester.

Davies, M.R., Harding, C.J., Raines, S. Tolley, K., Parker, A.E., Downey-Jones, M., Needham, M.R.C., 2005. NURR1 dependent regulation of pro-inflammatory mediators in immortalized synovial fibroblasts. *Journal of Inflammation (Lond)* **2**, 15.

Davis, L.S., 2003. A Question of Transformation. The synovial fibroblast in rheumatoid arthritis. *American Journal of Pathology* **162**(5), 1399-1402.

Den Broeder, A.A., de Jong, E., Franssen, M.J.A.M., Jeurissen, M.E.C., Flendrie, M., van den Hoogen, F.H.J., 2006. Observational study on efficacy, safety, and drug survival of anakinra in rheumatoid arthritis patients in clinical practice. *Annals of the Rheumatic Diseases* **65**(6), 760-762.

Deng, G.-M., Lenardo M., 2006. The role of immune cells and cytokines in the pathogenesis of rheumatoid arthritis. *Drug Discovery Today: Disease Mechanisms* **3**(2), 163-168.

De Waard, V., Arkenbout, E.K., Vos, M., Mocking, A.I.M., Niessen, H.W.M., Stooker, W., de Mol, B. A.J.M., Quax, P.H.A., Bakker, E.N.T.P., VanBavel, E., Pannekoek, H., de Vries, C.J.M., 2006. TR3 nuclear receptor prevents cyclic stretch-induced proliferation of venous smooth muscle cells. *American Journal of Pathology* **168**(6), 2027-2035.

Dixit, V.M., Green, S., Sarma, V., Holzman, L.B., Wolf, F.W., O' Rourke, K., Ward, P.A., Prochownik, E.V., Marks, R.M., 1990. Tumor necrosis factor- α induction of novel gene products in human endothelial cells including a macrophage-specific chemotaxin. *Journal of Biological Chemistry* **265**(5), 2973-2978.

Enesa, K., Zakkar, M., Chaudhury, H., Luong, L.A., Rawlinson, L., Mason, J.C., Haskard, D.O., Dean, J.L.E., Evans, P.C., 2008. NF- κ B suppression by the deubiquitinating enzyme cezanne. *Journal of Biological Chemistry* **283**(11), 7036-7045.

European Medicines Agency, 2005. *European Medicines Agency concludes action on COX-2 inhibitors*. European Medicines Agency Document Reference EMEA/207766/2005. Retrieved from http://www.ema.europa.eu/docs/en_GB/document_library/Press_release/2010/01/WC500059088.pdf on 9th August 2011.

Evans, P.C., 2005. Regulation of pro-inflammatory signaling networks by ubiquitin: identification of novel targets for anti-inflammatory drugs. *Expert Reviews in Molecular Medicine* **7**(12), 1-19.

Evans, P.C., Taylor, E.R., Coadwell, J., Heyninck, K., Beyaert, R., Kilshaw, R.J., 2001. Isolation and characterization of two novel A20-like proteins. *Biochemical Journal* **357**, 617-623.

Firestein, G.S., 2003. Evolving concepts of rheumatoid arthritis. *Nature* **423**, 356-361.

Fries, K.L., Miller, W.E., Raab-Traub, N., 1996. Epstein-Barr virus latent membrane protein 1 blocks p53-mediated apoptosis through the induction of the A20 gene. *Journal of Virology* **70**(12), 8653-8659.

Gallagher, J., Howlin, J., McCarthy, C., Murphy, E.P., Bresnihan, B., FitzGerald, O., Godson, C., Brady, H. R., Martin, F. (2003). Identification of Naf1/ABIN-1 among TNF- α -induced expressed genes in human synoviocytes using oligonucleotide microarrays. *FEBS Letters* **551**, 8-12.

Gao, L., Coope, H., Grant, S., Ma, A., Ley, S.C., Harhaj, E.W., 2011. ABIN1 cooperates with TAX1BP1 and A20 to inhibit antiviral signaling. *Journal of Biological Chemistry* M111.283762. Retrieved from <http://www.jbc.org/content/early/2011/09/01/jbc.M111.283762.long> on 9th September 2011.

Gartehner, G., Thieda, P., Morgan, L.C., Thaler, K., Hansen, R.A., Jonas, B., 2009. *Drug class review: targeted immune modulators*. Oregon Health and Science University, Portland, Oregon. Retrieved from <http://www.ncbi.nlm.nih.gov/books/NBK47225/> on 10th October 2009.

Gebauer, M., Saas, J., Sohler, F., Haag, J., Soder, S., Pieper, M., Bartnik, E., Beninga, J., Zimmer, R., Aigner, T., 2005. Comparison of the chondrosarcoma cell line SW 1353 with primary human adult articular chondrocytes with regard to their gene expression profile and reactivity to IL-1beta. *Osteoarthritis Cartilage* **13**(8), 697-708.

Genomatix Software GmbH, 2009. Retrieved from <http://www.genomatix.de> on 17th November 2008.

Glick, B.R., Pasternak, J.J., 2003. *Molecular Biotechnology* 3rd edn. ASM Press, Washington.

Gomez, G., Sitkovsky, M.V., 2003. Targeting G protein-coupled A2a adenosine receptors to engineer inflammation *in vivo*. *International Journal of Biochemistry and Cell Biology* **35**, 410-414.

Gronemeyer, H., Gustafsson, J.A., Laudet, V., 2004. Principles for modulation of the nuclear receptor superfamily. *Nature Reviews Drug Discovery* **3**, 950-964.

Haas, C., Aicher, W.K., Dinkel, A., Peter, H.H., Eibel, H., 1997. Characterization of SV40T antigen immortalized human synovial fibroblasts: maintained expression patterns of EGR-1, HLA-DR and some surface receptors. *Rheumatol International* **16**, 241-247.

Hames, B.D., Hooper, N.W., 2000. *Instant Notes on Biochemistry* 2nd edn. Bios Scientific Publishers Ltd., Oxford.

Hancock, W.W., Buelow, R., Sayegh, M.H., Turka, L.A., 1998. Antibody-induced transplant arteriosclerosis is prevented by graft expression of anti-oxidant and anti-apoptotic genes. *Nature Medicine* **4**, 1392-1396.

Harant, H., Lindley, I.J., 2004. Negative cross-talk between the human orphan nuclear receptor Nur77/Nak-1/TR3 and nuclear factor- κ B. *Nucleic Acids Research* **32**(17), 5280-5290.

Harhaj, E.W., Dixit, V.M., 2011. Deubiquitinases in the regulation of NF- κ B signaling. *Cell Research* **21**(1). 22-39.

Hartz, P.A., 2009. National Center for Biotechnology Information Online Mendelian Inheritance in Man. *Podoplanin; PDPN*. Johns Hopkins University. Retrieved from <http://www.ncbi.nlm.nih.gov/omim/608863> on 14th April 2010.

Hayden, M.S., Ghosh, S., 2004. Signaling to NF- κ B. *Genes & Development* **18**, 2195-2224.

He, K.-L., Ting, A.T., 2002. A20 inhibits tumour necrosis factor (TNF) alpha-induced apoptosis by disrupting recruitment of TRADD and RIP to the TNF receptor 1 complex in Jurkat T cells. *Molecular and Cellular Biology* **22**(17), 6034-6045.

Heyninck, K., Beyaert, R., 1999. The cytokine-inducible zinc finger protein A20 inhibits IL-1-induced NF- κ B activation at the level of TRAF6. *FEBS Letters* **442**, 147-150.

Heyninck, K., Beyaert, R., 2005. A20 inhibits NF- κ B activation by dual ubiquitin-editing functions. *TRENDS in Biochemical Sciences* **30**(1), 1-4.

Heyninck, K., Kreike, M.M., Beyaert, R., 2003. Structure-function analysis of the A20-binding inhibitor of NF- κ B activation, ABIN-1. *FEBS Letters* **536**, 135-140.

Hinata, K., Gervin, A.M., Zhang, Y.J., Khavari, P.A., 2003. Divergent gene regulation and growth effects by NF- κ B in epithelial and mesenchymal cells of human skin. *Oncogene* **22**, 1955-1964.

Hinz, M., Lemke, P., Anagnostopoulos, I., Hacker, C., Krappmann, D., Mathas, S., Dörken, B., Zenke, M., Stein, H., Scheidereit, C., 2002. Nuclear factor kappa B-dependent gene expression profiling of Hodgkin's disease tumor cells, pathogenetic significance, and link to constitutive signal transducer and activator of transcription 5a activity. *Journal of Experimental Medicine* **196**(5), 605-617.

Iha, H., Peloponese, J.M., Verstrepen, L., Zapart, G., Ikeda, F., Smith, C.D., Starost, M.F., Yedavalli, V., Heyninck, K., Dikic, I., Beyaert, R., Jeang, K.T., 2008. Inflammatory cardiac valvulitis in TAX1BP1-deficient mice through selective NF- κ B activation. *The EMBO Journal* **27**, 629-641.

Islander, U., Jochems, C., Lagerquist, M.K., Forsbald-d'Elia, H., Carlsten, H., 2010. Estrogens in rheumatoid arthritis; the immune system and bone. *Molecular and Cellular Endocrinology* **335**(1), 14-29.

Jaattela, M., Mouritzen, H., Elling, F., Bastholm, L., 1996. A20 zinc finger protein inhibits TNF and IL-1 signaling. *Journal of Immunology* **156**(3), 1166-1173.

Jacque, E., Ley, S.C., 2009. RNF11, a new piece in the A20 puzzle. *The EMBO Journal* **28**, 455-456.

Ju, J.W., Kim, S.J., Jun, C.D., Chun, S.J., 2002. p38 kinase and c-Jun N-terminal kinase oppositely regulates tumor necrosis factor α -induced vascular cell adhesion molecule-1 expression and cell adhesion in chondrosarcoma cells. *IUBMB Life* **54**, 293-299.

Karouzakis, E., Neidhart, M., Gay, R.E., Gay, S., 2006. Molecular and cellular basis of rheumatoid joint destruction. *Immunology Letters* **106**, 8-13.

Kast, R.E., 2005. Evidence of a mechanism by which etanercept increased TNF- α in multiple myeloma: New insights into the biology of TNF- α giving new treatment opportunities- the role of bupropion. *Leukemia Research* **29**(12), 1459-1463.

Kimby, E., 2005. Tolerability and safety of rituximab (MabThera®) *Cancer Treatment Reviews* **31**(6), 456-473.

Klareskog, L., Catrina, A.I., Paget, S., Rheumatoid Arthritis. *Lancet* **373**(9664), 659-672.

Krikos, A., Laherty, C.D., Dixit, V.M., 1992. Transcriptional activation of the tumour necrosis factor α -inducible zinc finger protein, A20, is mediated by κ B elements. *The Journal of Biological Chemistry* **267**(25), 17971-17976.

Lammi, J., Rajalin, A.-M., Huppunen, J., Aarnisalo, P., 2007. Cross-talk between the NR3B and NR4A families of orphan nuclear receptors. *Biochemical and Biophysical Research Communications* **359**(2), 391-397.

Le, W.D., Xu, P., Jankovic, J., Jiang, H., Appel, S.H., Smith, R.G., Vassilatis, D.K., 2003. Mutations in NR4A2 associated with familial Parkinson disease. *Nature Genetics* **33**, 85-89.

Lee, C.H., Jeon, Y.T., Kim, S.H., Song, Y.S., 2007. NF- κ B as a potential molecular target for cancer therapy. *BioFactors* **29**, 19-35.

Lee, E.G., Boone, D.L., Chai, S., Libby, S.L., Chien, M., Lodolce, J.P., Ma, A., 2000. Failure to regulate TNF-induced NF- κ B and cell death responses in A20-deficient mice. *Science* **289**(5488), 2350-2354.

LeRoith, D., Taylor, S.I., Olefsky, J.M., 2004. *Diabetes Mellitus: A Fundamental and Clinical Text* 3rd edn. Lippincott Williams and Wilkins, Philadelphia.

Lin, J, Ziring, D., Desai, S., Kim, S., Wong, M., Korin, Y., Braun, J., Reed, E., Gjertson, D., Singh, R.R., 2008. TNF α blockade in human diseases: an overview of efficacy and safety. *Clinical Immunology* **126**(1), 13-30.

Liu, D., Jia, H., Holmes, D.I., Stannard, A., Zachary, I., 2003. Vascular endothelial growth factor-regulated gene expression in endothelial cells. *Arteriosclerosis, Thrombosis, and Vascular Biology* **23**, 2002-2007.

Liu, J.W., Dunoyer-Geindre, S., Blot-Chabaud, M., Sabatier, F., Fish, R.J., Bounameaux, H., Dignat-George, F., Druithof, E.K.O., 2010. Generation of human inflammation-resistant endothelial progenitor cells by A20 gene transfer. *Journal of Vascular Research* **47**, 157-167.

Liu, W.K., Chien, C.-Y., Chou, C.K., Su, J.-Y., 2003. An LKB1-interacting protein negatively regulates TNF α -induced NF- κ B activation. *Journal of Biomedical Science* **10**(2), 242-252.

Liu, W.K., Yen, P.-F., Chien, C.-Y., Fann, M.-J., Su, J.-Y., Chou, C.-K., 2004. The inhibitor ABIN-2 disrupts the interaction of receptor-interacting protein with the kinase subunit IKK λ to block activation of the transcription factor NF- κ B and potentiate apoptosis. *Biochemical Journal* **378**, 867-876.

Livak, K.J., Schmittgen, T.D., 2001. Analysis of relative gene expression data using real-time quantitative PCR and the 2^{-Delta Delta C(T)} method. *Methods* **25**(4), 402-408.

Lundy, S.K., Sarkar, S., Tesmer, L.A., Fox, D.A., 2007. Cells of the synovium in rheumatoid arthritis T lymphocytes. *Arthritis Research & Therapy* **9**(1), 202.

Makarov, S.S., 2001. NF- κ B in rheumatoid arthritis: a pivotal regulator of inflammation, hyperplasia, and tissue destruction. *Arthritis Research* **3**, 200-206.

Marlor, C.W., Webb, D.L., Bombara, M.P., Greve, J.M., Blue, M.L., 1992. Expression of vascular cell adhesion molecule-1 in fibroblast-like synoviocytes after stimulation with tumor necrosis factor. *American Journal of Pathology* **140**(5), 1055-1060.

Marone, M., Mozzetti, S., De Ritis, D., Pierelli, L., Scambia, G., 2001. Semiquantitative RT-PCR analysis to assess the expression levels of multiple transcripts from the same sample. *Biological Procedures Online* **3**(1), 19-25.

Mauro, C., Pacifico, F., Lavorgna, A., Mellone, S., Iannetti, A., Acquaviva, R., Formisano, S., Vito, P., Leonardi, A., 2006. ABIN-1 Binds to NEMO/IKK γ and co-operates with A20 in inhibiting NF- κ B. *Journal of Biological Chemistry* **281**(27), 18482-18488.

Maxwell, M.A., Muscat, G.E.O., 2005. The NR4A subgroup: immediate early response genes with pleiotropic physiological roles. *Nuclear Receptor Signaling* **4**, e002. Retrieved from <http://www.ncbi.nlm.nih.gov/pmc/articles/PMC1402209/pdf/nrs04002000.pdf> on 12th November 2009.

McEvoy, A.N., Murphy, E.A., Ponnio, T., Conneely, O.M., Bresnihan, B., FitzGerald, O., Murphy, E.P., 2002. Activation of nuclear orphan receptor NURR1 transcription by NF- κ B and cyclic adenosine 5'-monophosphate response element-binding protein in rheumatoid arthritis synovial tissue. *Journal of Immunology* **168**, 2979-2987.

McNally, R.S., Davis, B.K., Clements, C.M., 2011. DJ-1 enhances cell survival through the binding of Cezanne, a negative regulator of NF- κ B. *Journal of Biological Chemistry* **286**(6), 4098-4106.

Meusch, U., Rossol, M., Baerwald, C., Hauschildt, S., Wagner U., 2009. Outside-to-inside signaling through transmembrane tumor necrosis factor reverses pathologic interleukin-1 β production and deficient apoptosis of rheumatoid arthritis monocytes. *Arthritis & Rheumatism* **60**(9), 2612-21.

Miagkov, A.V., Kovalenko, D.V., Brown, C.E., Didsbury, J.R., Cogswell, J.P., Stimpson, S.A., Baldwin, A.S., Makarov, S., 1998. NF- κ B activation provides the potential link between inflammation and hyperplasia in the arthritic joint. *Proceedings of the National Academy of Sciences* **95**, 13859-13864.

Mix, K.S., Attur, M.G., Al-Mussawir, H., Abramson, S.B., Brinckerhoff, C.E., Murphy, E.P., 2007. Transcriptional repression of matrix metalloproteinase gene expression by the orphan nuclear receptor NURR1 in cartilage. *Journal of Biological Chemistry* **282**(13), 9492-9504.

Müller-Ladner, U., Gay, R.E., Gay, S., 2000. Activation of synoviocytes. *Current Opinion in Rheumatology* **12**, 186-194.

Murphy, E.P., Conneely, O.M., 1997. Neuroendocrine regulation of the hypothalamic pituitary adrenal axis by the NURR1/NUR77 subfamily of nuclear receptors. *Molecular Endocrinology* **11**(1), 39-47.

Murphy, E.P., Dobson, A.D.W., Keller, C.H., Conneely, O.M., 1996. Differential regulation of transcription by the NURR1/NUR77 subfamily of nuclear transcription factors. *Gene Expression* **5**, 169-179.

Mycek, M.J., Harvey, R.A., Champe, P.C., 2000. *Lippincott's Illustrated Reviews: Pharmacology*. Lippincott Williams & Wilkins, Philadelphia.

National Center for Biotechnology Information, 2011. Gene *ACTB actin, beta [Homo sapiens]* US National Library of Medicine. Retrieved from <http://www.ncbi.nlm.nih.gov/sites/entrez?Db=gene&Cmd=ShowDetailView&TermToSearch=60> on 16th July 2011.

Ning, S., Pagano, J.S., 2010. The A20 deubiquitinase negatively regulates LMP1 activation of IRF7. *Journal of Virology* **84**(12), 6130-6138.

Nogid, A., Pham, D.Q., 2006. Role of abatacept in the management of rheumatoid arthritis. *Clinical Therapeutics* **28**(11), 1764-1778.

Nomiyama, T., Nakamachi, T., Gizard, F., Heywood, E.B., Jones, K.L., Ohkura, N., Kawamori, R., Conneely, O.M., Bruemmer, D., 2006. The NR4A orphan nuclear receptor NOR1 is induced by platelet-derived growth factor and mediates vascular smooth muscle cell proliferation. *Journal of Biological Chemistry* **281**(44), 33467-33476.

Nurmohamed, M.T., Dijkmans, B.A.C., 2008. Are biologics more effective than classical disease-modifying antirheumatic drugs? *Arthritis Research & Therapy* **10**(5), 118.

Ohkura, N., Hosono, T., Maruyama, K., Tsukada, T., Yamaguchi, K., 1999. An isoform of NURR1 functions as a negative inhibitor of the NGFI-B family signaling. *Biochimica et Biophysica Acta* **1444**, 69-79.

Ohkura, N., Maruyama, K., Tsukada, T., Hosono, T., Yamaguchi, K., 1998. The NGFI-B family: orphan nuclear receptors of the steroid/thyroid receptor superfamily. *Journal of Reproduction and Development* **44**(4), 321-335.

O'Kane, M., Markham, T., McEvoy, A.N., Fearon, U., Veale, D.J., FitzGerald, O., Kirby, B., Murphy, E.P., 2008. Increased expression of the orphan nuclear receptor NURR1 in psoriasis and modulation following TNF- α inhibition. *Journal of Investigative Dermatology* **128**, 300-310.

Oldfield, V., Dhillon, S., Plosker, G.L., 2009. Tocilizumab: a review of its use in the management of rheumatoid arthritis. *Drugs* **69**(5), 609-32.

Ordentlich, P., Yan, Y., Zhou, S., Heyman, R.A., 2003. Identification of the antineoplastic agent 6-mercaptopurine as an activator of the orphan nuclear hormone receptor NURR1. *Journal of Biological Chemistry* **278**(27), 24791-24799.

O'Reilly, S.M., Moynagh, P.N., 2003. Regulation of Toll-like receptor 4 signaling by A20 zinc finger protein. *Biochemical and Biophysical Research Communications* **303**, 586-593.

Otero, M., Goldring, M.B., 2007. Cells of the synovium in rheumatoid arthritis Chondrocytes. *Arthritis Research & Therapy* **9**(5), 220.

Papoutsopoulou, S., Symons, A., Tharmalingham, T., Belich, M.P., Kaiser, F., Kioussis, D., O'Garra, A., Tybulewicz, V., Ley, S.C., 2006. ABIN-2 is required for optimal activation of Erk MAP kinase in innate immune responses. *Nature Immunology* **7**(6), 606-15.

Pei, L., Castrillo, A., Chen, M., Hoffmann, A., Tontonoz, P., 2005. Induction of NR4A orphan nuclear receptor expression in macrophages in response to inflammatory stimuli. *Journal of Biological Chemistry* **280**, 29256-29262.

Pei, L., Castrillo, A., Tontonoz, P., 2006. Regulation of macrophage gene expression by the orphan nuclear receptor NUR77. *Molecular Endocrinology* **20**(4), 786-794.

Perlmann, T., Jansson, L., 1995. A novel pathway for vitamin A signaling mediated by RXR heterodimerization with NGFI-B and NURR1. *Genes and Development* **9**, 769-782.

Phelan, M.C., 1998. *Current Protocols in Cell Biology*. John Wiley and Sons, Inc. Retrieved from <http://georgelab.eng.uci.edu/Resources/Cell%20culture%20technique%20-%20Methods/Basic%20Technique%20for%20Tissue%20Culture.pdf> on 20th July 2011.

Piecyk, M., Anderson, P., 2001. Signal transduction in rheumatoid arthritis. *Best Practice & Research Clinical Rheumatology* **15**(5), 789-803.

Plushner, S.L., 2008. Tocilizumab: an interleukin-6 receptor inhibitor for the treatment of rheumatoid arthritis. *The Annals of Pharmacotherapy* **2**(11), 1660-1668.

Pratt, A.G., Isaacs, J.D., Matthey, D.L., 2009. Current concepts in the pathogenesis of early rheumatoid arthritis. *Best Practice & Research Clinical Rheumatology* **23**, 37-48.

Ralph, J.A., McEvoy, A.N., Kane, D., Bresnihan, B., FitzGerald, O., Murphy, E.P., 2005. Modulation of orphan nuclear receptor NURR1 expression by methotrexate in human inflammatory joint disease involves adenosine A2A receptor-mediated responses. *Journal of Immunology* **175**, 555-565.

Rang, H.P., Dale, M.M., Ritter, J.M., Flower, R.J., 2007. *Pharmacology* 7th edn. Elsevier Churchill Livingstone, London.

Rannou, F., François, M., Corvol, M.-T., Berenbaum, F., 2006. Cartilage breakdown in rheumatoid arthritis. *Joint Bone Spine* **73**, 29-36.

Rubbert-Roth, A., Finckh, A., 2009. Treatment options in patients with rheumatoid arthritis failing initial TNF inhibitor therapy: a critical review. *Arthritis Research & Therapy* **11**(Suppl 1) S1.

Sacchetti, P., Mitchell, T.R., Granneman, J.G., Bannon, M.J., 2001. NURR1 enhances transcription of the human dopamine transporter gene through a novel mechanism. *Journal of Neurochemistry* **76**, 1565-1572.

Sambrook, S., Russell, D.W., 2001. *Molecular Cloning, a Laboratory Manual* Volume 2 3rd edn. Cold Spring Harbor Laboratory Press, New York.

Schaefer, J.F., Millham, M.L., de Crombrughe, B., Buchbinder, L., 2003. FGF signaling antagonizes cytokine-mediated repression of Sox9 in SW1353 chondrosarcoma cells. *Osteoarthritis and Cartilage* **11**(4), 233-241.

Schoemaker, M.H., Ros, J.E., Homan, M., Trautwein, C., Liston, P., Poelstra, K., van Goor, H., Jansen, P.L.M., Moshage H., 2002. Cytokine regulation of pro- and anti-apoptotic genes in rat hepatocytes: NF- κ B-regulated inhibitor of apoptosis protein 2 (cIAP2) prevents apoptosis. *Journal of Hepatology* **36**, 742-750.

Seymour, H.E., Worsley, A., Smith, J.M., Thomas, S.H.L., 2001. Anti-TNF agents for rheumatoid arthritis. *British Journal of Clinical Pharmacology* **51**, 201-208.

Shembade, N., Harhaj, N.S., Liegl, D.J., Harhaj, E.W., 2007. Essential role for TAX1BP1 in the termination of TNF- α -, IL-1- and LPS-mediated NF κ B and JNK signaling. *The EMBO Journal* **26**, 3910-3922.

Shembade, N., Parvatiyar, K., Harhaj, N.S., Harhaj, E.W., 2009. The ubiquitin-editing enzyme A20 requires RNF11 to downregulate NF- κ B signaling. *The EMBO Journal* **28**, 513-522.

Silverman, G.J., Carson, D.A., 2003. Roles of B cells in rheumatoid arthritis. *Arthritis Research & Therapy* **5** (Suppl 4) S1-6. Retrieved from <http://www.ncbi.nlm.nih.gov/pmc/articles/PMC2833442/?tool=pubmed> on 29th July 2009.

Slavic, V., Stankovic, A., Kamenov, B., 2005. The role of interleukin-8 and monocyte chemotactic protein-1 in rheumatoid arthritis. *Medicine and Biology* **12**(1), 19-22.

Smolen, J.S., Landewé, R., Breedveld, F.C., Dougados, M., Emery, P., Gaujoux-Viala, C., Gorter, S., Knevel, R., Nam, J., Schoels, M., Aletaha, D., Buch, M., Gossec, L., Huizinga, T., Bijlsma, J.W., Burmester, G., Combe, B., Cutolo, M., Gabay, C., Gomez-Reino, J., Kouloumas, M., Kvien, T.K., Martin-Mola, E., McInnes, I., Pavelka, K., van Riel, P., Scholte, M., Scott, D.L., Sokka, T., Valesini, G., van Vollenhoven, R., Winthrop, K.L., Wong, J., Zink, A., van der Heijde, D., 2010. EULAR recommendations for the management of rheumatoid arthritis with synthetic and biological disease-modifying antirheumatic drugs. *Annals of the Rheumatic Diseases* **69**, 964-975.

Song, Y.H., Rothe, M., Goeddel, D.V., 1996. The tumour necrosis factor-inducible zinc finger protein A20 interacts with TRAF1/TRAF2 and inhibits NF- κ B activation. *Proceedings of the National Academy of Sciences* **93**, 6721-6725

Srivastava, S.K., Ramana, K.V., 2009. Focus on molecules: nuclear factor-kappaB. *Experimental Eye Research* **88**(1), 2-3.

Szekanecz, Z., Koch, A.E., 2000. Cell-cell interactions in synovitis. Endothelial cells and immune cell migration. *Arthritis Research* **2**, 368-373.

Tak, P.P., Kalden, J.R., 2011. Advances in rheumatology: new targeted therapeutics. *Arthritis Research and Therapy* **13**(Suppl 1), S5.

Tessier, P., Audette, M., Cattaruzzi, P., McColl, S.R., 1993. Up-regulation by tumor necrosis factor alpha of intercellular adhesion molecule 1 expression and function in synovial fibroblasts and its inhibition by glucocorticoids. *Arthritis and Rheumatism* **3**(11), 1528-1539.

Thinda, S., Tomlinson, J.S., 2009. Mesenteric rheumatoid nodules masquerading as an intra-abdominal malignancy: a case report and review of the literature. *World Journal of Surgical Oncology* **7**, 59.

Tsavaris, N., Skopelitis, E. 2007. New research communications on cancer drug resistance. In: *Cancer Drug Resistance Research Perspectives*. (Torres, L.S., ed.). Nova Science Publishers, Inc., New York pp. 7-27.

Van Huffel, S., Delaei, F., Heyninck, K., De Valck, D., Beyaert, R., 2001. Identification of a Novel A20-binding of Nuclear Factor- κ B Activation Termed ABIN-2. *Journal of Biological Chemistry* **276**(32), 30216-30223.

Verstrepen, L., Carpentier, I., Verheist, K., Beyaert, R., 2009. ABINs: A20 binding inhibitors of NF- κ B and apoptosis signaling. *Biochemical Pharmacology* **78**(2), 105-114.

Volokhov, D.V., Graham, L.J., Brorson, K.A., Chizhikov, V.E., 2011. Mycoplasma testing of cell substrates and biologics: review of alternative non-microbiological techniques. *Molecular and Cellular Probes* **25**, 69-77.

Vincenti, M.P., Brinckerhoff, C.E., 2001. Early response genes induced in chondrocytes stimulated with the inflammatory cytokine interleukin-1 β . *Arthritis Research* **3**, 381-388.

Wakeling, A.E., 2000. Similarities and distinctions in the mode of action of different classes of antioestrogens. *Endocrine-Related Cancer* **7**, 17-28.

Walsh, 2002. *Watson's Clinical Nursing and Related Sciences* 6th edn. Elsevier Science Ltd., Edinburgh.

Wang, K., Wan, Y.-J.Y., 2008. Nuclear receptors and inflammatory diseases. *Experimental Biology and Medicine* **233**, 496-506.

Wertz, I.E., Dixit, V.M., 2008. Ubiquitin-mediated regulation of TNFR1 signaling. *Cytokine & Growth Factor Reviews* **19**, 313-324.

Weyrich, P., Staiger, H., Stancakova, A., Schafer, S. A., Kirchhoff, K., Ullrich S., Ranta, F., Gallwitz, B., Stefan, N. Machicao, F., Kuusisto, J., Laakso, M., Fritsche, A., Haring, H.U., 2009. Common polymorphisms within the NR4A3 locus, encoding the orphan nuclear receptor NOR-1, are associated with enhanced beta-cell function in non-diabetic subjects. *BMC Medical Genetics* **10**(1), 77.

Wilder, R.L., Case, J.P., Crofford, L.J., Kumkumian, G.K., Lafyatis, R., Remmers, E.F., Sano, H., Sternberg, E.M., Yocum, D.E., 1990. Endothelial cells and the pathogenesis of rheumatoid arthritis in humans and streptococcal cell wall arthritis in Lewis rats. *Journal of Cellular Biochemistry* **45**(2), 162-166.

Wilson, T.E., Fahrner, T.J., Johnston, M., Milbrandt, J., 1991. Identification of the DNA binding site for NGFI-B by genetic selection in Yeast. *Science* **25**, 1296-1300.

Wullaert, A., Heyninck, K., Janssens, S., Beyaert, R., 2006. Ubiquitin: tool and target for intracellular NF- κ B inhibitors. *TRENDS in Immunology* **27**(11), 533-540.

Wullaert, A., Verstrepen, L., Van Huffel, S., Adib-Conquy, M., Cornelis, S., Kreike, M., Haegman, M., El Bakkouri, K., Sanders, M., Verhelst, K., Carpentier, I., Cavaillon, J.M., Heyninck, K., Beyaert, R., 2007. LIND/ABIN-3 is a novel lipopolysaccharide-inducible inhibitor of NF κ B activation. *Journal of Biological Chemistry* **282**(1), 81-90.

Yamamoto, Y., Gaynor, R.B., 2001. Therapeutic potential of inhibition of the NF κ B pathway in the treatment of inflammation and cancer. *Journal of Clinical Investigations* **107**(2), 135-142.

You, B., Jiang, Y.-Y., Chen, S., Yan, G., Sun, J., 2009. The orphan nuclear receptor NUR77 suppresses endothelial cell activation through induction of I κ B α expression. *Circulation Research* **104**, 742-749.

Zeng, H., Qin, L., Zhao, D., Tan, X., Manseau, E.J., Van Hoang, M., Senger, D.R., Brown, L.F., Nagy, J.A., Dvorak, H.F., 2006. Orphan nuclear receptor TR3/NUR77 regulates VEGF-A-induced angiogenesis through its transcriptional activity. *Journal of Experimental Medicine* **203**, 719-729.

Zetoune, F.S., Murthy, A.R., Shao, Z., Hlaing, T., Zeidler, G.M., Li, Y., Vincenz, C., 2001. A20 inhibits NF- κ B activation downstream of multiple MAP3 kinases and interacts with the I κ B signalosome. *Cytokine* **15**(6), 282-298.

Zhang, X.K., 2007. Targeting NUR77 translocation. *Expert Opinion on Therapeutic Targets* **11**(1), 69-79.

Zhou, A., Scoggin, S., Gaynor, R.B., Williams, N.S., 2003. Identification of NF- κ B-regulated genes induced by TNF- α utilizing expression profiling and RNA interference. *Oncogene* **22**(13), 2054-2064.

lyit | Institute of Technology
Letterkenny Institute of Technology

APPENDIX A

lyit | Institiúid Teicneolaíochta Leitir Ceánalinn
Letterkenny Institute of Technology

Appendix A

Solutions for DNA Manipulations

50X TAE

242 g Tris
57.1 ml Acetic Acid
100 ml 0.5 M EDTA (pH 8.0)
Adjusted to 1 L with ultrapure H₂O.

Solutions for DNA Miniprep

Solution I

50 mM Glucose
25 mM Tris.Cl (pH 8.0)
10 mM EDTA (pH 8.0)

Solution II (Freshly Prepared)

0.2 M NaOH
1 % (w/v) SDS

Solution III

60 ml 5 M Potassium Acetate
11.5 ml Glacial Acetic Acid
28.5 ml Ultrapure H₂O

The resultant solution is 3 M with respect to potassium and 5 M with respect to acetate.

50% (v/v) Glycerol

25 ml Ultrapure H₂O
25 ml Glycerol

Autoclaved and stored at room temperature.

Reagents for RNA Extraction and Analysis

0.1 % DEPC-treated H₂O

One millilitre of diethylpyrocarbonate (DEPC) was added to 1 L ultrapure H₂O and mixed. This was incubated at room temperature for 16 hr with a loose cap and autoclaved.

1 % Formaldehyde Gel

Zero point five grams of agarose were added to 43.5 ml DEPC-treated H₂O and melted in the microwave. The following reagents were added in the fume hood:

5.0 ml	10X MOPS Running Buffer
1.5 ml	Formaldehyde (50%)

The gel was poured in the fume hood and allowed to set for 30 min. After electrophoresis, the RNA was visualised by staining in a solution of approximately 400 ml of ultrapure H₂O containing 0.03 mg ethidium bromide for 1 hr. The gel was then destained in DEPC-treated H₂O for 10 min and viewed using a gel imaging system.

1X MOPS Running Buffer

The 10X MOPS running buffer was diluted one part buffer to nine parts DEPC-treated H₂O.

Bacterial Growth Media

LB Agar plus Selective Antibiotic

The selective antibiotic was added to a final concentration of 100 µg/ml to autoclaved LB agar (50°C), mixed and poured into sterile petri dishes. The agar was left to set for 30 min and stored at 4°C.

LB Broth plus Selective Antibiotic

The selective antibiotic was added to a final concentration of 100 µg/ml to autoclaved LB broth (50°C) and stored at 4°C.

Ampicillin and Kanamycin Stock Solutions (100 mg/ml)

One hundred milligrams of ampicillin or kanamycin were dissolved per ml of sterile ultrapure H₂O. The solutions were filtered using a 0.45 µm filter to sterilize and stored in sterile eppendorfs at -20°C.

Cell Culture Reagents

Supplemented RPMI Medium (500 ml)

440 ml	RPMI 1640
50 ml	Fetal Bovine Serum (Heat Inactivated)
5 ml	L-glutamine (2 mM/ml)
5 ml	Penicillin (10,000 U/ml) Streptomycin (10 mg/ml)

Phosphate Buffered Saline (PBS)

One PBS tablet (Oxoid) was dissolved in 100 ml ultrapure H₂O and autoclaved to sterilize.

Luciferase Assay Reagents

1X Passive Lysis Buffer

The 5X Passive Lysis Buffer (Promega) was diluted one part buffer to four parts ultrapure H₂O.

Stop and Glo Reagent (Freshly prepared)

The Stop and Glo substrate (Promega) was diluted one part substrate to 50 parts Stop and Glo buffer (Promega).